

ABSTRACT

ROHRBAUGH, NATHANIEL W. Improving the Performance of Semiconductor Sensor Devices Using Surface Functionalization. (Under the direction of Dr. Alben Ivanisevic.)

As production and understanding of III-nitride growth has progressed, this class of material has been used for its semiconducting properties in the fields of computer processing, microelectronics, and LEDs. As understanding of materials properties has advanced, devices were fabricated to be sensitive to environmental surroundings such as pH, gas, or ionic concentration. Simultaneously the world of pharmaceuticals and environmental science has come to the age where the use of wearable devices and active environmental sensing can not only help us learn more about our surroundings, but help save lives. At the crossroads of these two fields work has been done in marrying the high stability and electrical properties of the III-nitrides with the needs of a growing sensor field for various environments and stimuli.

Device architecture can only get one so far, and thus the need for well understood surface functionalization techniques has arisen in the field of III-nitride environmental sensing. Many existing schemes for functionalization involve chemistries that may be unfriendly to a biological environment, unstable in solution, or expensive to produce. One possible solution to these issues is the work presented here, which highlights a surface modification scheme utilizing phosphonic acid based chemistry and biomolecular attachment. This dissertation presents a set of studies and experiments quantifying and analyzing the response behaviors of AlGa_N/Ga_N field effect transistor (FET) devices via their interfacial electronic properties. Additional investigation was done on the modification of these surfaces, effects of stressful environmental conditions, and the utility of the phosphonic acid surface treatments.

Signals of AlGaIn/GaN FETs were measured as I_{Drain} values and in the earliest study an average signal increase of 96.43% was observed when surfaces were incubated in a solution of a known recognition peptide sequence (SVSVGMPKSPRP). This work showed that even without a form of surface modification the devices were capable of generating a response in the presence of a charged biomolecule. Solution exposure tests done devices showed that incubating peptides on the device surfaces produced a weak interaction and following 24 hrs of soaking no signs of peptide remained via XPS analysis.

Subsequent testing was done to incorporate the phosphonic acid functionalization techniques shown previously by other members of this lab to the AlGaIn/GaN surfaces as a remedy to this solution instability. In this second study FETs were modified using a heated phosphoric acid:ethephon etch followed by an incubation in TAT-C peptide. Resulting IV measurements done on the samples showed a shift in threshold voltage of the FETs following the etching procedure followed by a recovery of this shift from prolonged solution exposure. In total samples were given 168 hours of soaking and showed persistent peptide presence through the N 1s peak from XPS scans.

FETs modified with this phosphonic acid derivative were examined in a third study under a simulated pollutant sensing scenario by measuring varied concentrations of Hg via a phytochelatin peptide bound to FET surfaces. HNO_3 used in the Hg stock solution led to degradation of the FET signal but did not remove the phytochelatin layer. This led to a compensation effect in sensing the highest levels of Hg, lower concentrations however were successfully tested and showed varied responses from the FETs relative to the Hg content.

In a concluding study on devices work was done to understand broader effects on the AlGaIn/GaN FETs relative to a simulated biological sensing environment. Here an effect was

noted from the addition of a biological fouling solution to the FETs and an increase in this effect when the biofouling was done to a phosphonic modified FET surface. Additionally devices were modified and soaked for 5 weeks and showed no shift or degradation in signal. Lastly in controlling for gate width of the FET it was found that the shorter 50 μm gates were more susceptible to environmental interference than the 100 and 150 μm gated devices.

Thus this work has shown that modifying AlGaIn/GaN devices with phosphonic acid derivatives is a viable functionalization method that is both adaptable and stable in solution over time. In moving forward, opportunities are available for testing a larger variety of analytes in both the medical and environmental fields. The final goal for this technology would be the fabrication and design of a multi-device sensing unit leading to eventual production of these sensors on an industrial scale for the use in future personal medical devices or environmental monitoring systems.

© Copyright 2016 Nathaniel W Rohrbaugh

All Rights Reserved

Improving the Performance of Semiconductor Sensor Devices Using Surface
Functionalization

by
Nathaniel W Rohrbaugh

A dissertation submitted to the Graduate Faculty of
North Carolina State University
in partial fulfillment of the
requirements for the degree of
Doctor of Philosophy

Materials Science and Engineering

Raleigh, North Carolina

2016

APPROVED BY:

Dr. Albena Ivanisevic
Committee Chair

Dr. Ramon Collazo
Committee Member

Dr. Jan Genzer
Committee Member

Dr. Lew Reynolds
Committee Member

DEDICATION

For Mom and Dad.

BIOGRAPHY

Nathaniel Wilday Rohrbaugh was born on October 27th, 1990 in Raleigh, North Carolina to parents Richard and Susie. Nathaniel attended Green Hope High School in Cary, NC and graduated in 2009. During his time there he partook in distance running events on the cross country and track teams for four years and becoming a captain of the cross country team in his final year. In addition to these events Nathaniel was a leader of the Green Hope FCA, and worked in the tech theatre department on the set building team that won Wake County's Outstanding Set Design in 2009.

After graduating Nathaniel went on to attend North Carolina State University in the Materials Science and Engineering Department. During his time there he partook in summer undergraduate research for all years of his time there through the research group of Dr. Jerome Cuomo. He worked on several consulting projects and worked on plasma deposition projects with other graduate students, and seed germination studies on atmospheric plasma.. After completing a bachelor's degree in science from North Carolina State he began his graduate work with Albena Ivanisevic also at North Carolina State. Here he worked on III-nitride materials for biological sensors and did consulting work in a thin films related field. His work included travel to Orlando, FL for a conference, lab work at Duke University, and resident summer research at the Prague Institute of Physics, CZ. His time here allowed him to take up hobbies such as wood turning and furniture craft at the NCSU Craft Center as well. Upon fulfilling all requirements for the Ph.D program Nathaniel graduated in December of 2016 with a doctoral degree in Materials Science from North Carolina State.

ACKNOWLEDGMENTS

My biggest thanks go to out to my advisor, Dr. Albena Ivanisevic for a multitude of reasons. Her patience, support, and guidance helped keep me on track and able to graduate with a Ph.D in less than four years. Without my time in her group I don't think I would be able to leave as confident in my perspectives and understandings of designing and operating experiments in a lab setting as I am now. I would additionally like to thank my committee members: Ramon Collazo, for the access, cooperation, and support he provided to my research and the greater exposure to the world of III-nitrides and growth I gained from it; Dr. Lew Reynolds, who brought insight and a more critical look at my findings, and for consistently having some of the most interesting and engaging classes in our department; and Dr. Jan Genzer, for also providing a non-MSE perspective on the science I have been learning, and thus making me learn about a field of interface science I would not normally have been exposed to. Another thank you to Dr. Yara Yingling who in particular helped give me insight when I was starting graduate school.

More thanks to those who welcomed me into my the research group when I joined including both Stewart Wilkins and Lauren Bain. Stewart I can thank for helping to feed my motorcycle obsession and Lauren for finally having someone to relate to on the nuances of baking, food, and annoying Brady. My later group members and friends as well including Nora Berg, Brady Pearce, and Patrick Snyder. All of you I would call good friends have made my time in this group worthwhile and enjoyable both in and outside of work. Other people that I've had the pleasure of sharing an office or time with at work like Dr. Christer Akoula, Chris Ledford, Weston Straka, Dr. Jacob Majikes, Brian Wells, and Nicole Estrich.

To the GSA folk and all the times I got to serve the department in a more social and fun sense like buying beer or organizing dinners and chili cook-offs. The folks in RB1 including Dr. Ronnie Kirste, Felix Kaess, and most of all the Bryan twins Isaac, and Zach. The twins in particular deserve so much more credit than they received for the work they did for me and their coworkers, and both are wonderful individuals who I am glad I was able to share a camping trip with. All of these people helped make my time in the MSE department more enjoyable, enlightening, and supportive and I am thankful for all of you.

Special thanks to Dr. Jerome Cuomo for all the support, conversations, and opportunities to expose me to a laboratory environment very early on in my college career. These years truly helped shape me into the more curious engineer that I am today, in addition to getting to work with such a passionate and knowledgeable professor as Dr. Cuomo.

Lastly, I'd like to thank my family and friends for their support over the years, and especially my parents Richard and Susie for their love and role in shaping me to who I am today.

TABLE OF CONTENTS

LIST OF TABLES	viii
LIST OF FIGURES	ix
Chapter 1 Stability and Reliability of III-Nitride Based Biosensor	1
1.1 III-Nitride Materials.....	1
1.2 Doping of nitrides.....	4
1.3 Water stability resistance to etching and degradation.....	9
1.4 Toxicity.....	12
1.5 Biocompatibility.....	16
1.6 Chemical functionalization.....	19
1.6.1 Aluminum Nitride.....	19
1.6.2 Gallium Nitride.....	20
1.6.3 Aluminum Gallium Nitride.....	24
1.7 Sensing devices.....	24
1.8 FET Behavior.....	30
1.9 Analytes/receptors.....	33
1.10 III-nitride FET biosensor stability.....	36
1.11 Unmet Needs.....	41
Chapter 2 AlGaIn/GaN Field Effect Transistors Functionalized with Recognition Peptides	44
2.1 Summary.....	44
2.2 Introduction.....	44
2.3 Experimental.....	46
2.4 Sensing response to incubated biomolecules.....	48
2.5 Aqueous stability.....	51
2.6 Particulate interference.....	53
Chapter 3 Longer term stability assessment of AlGaIn/GaN field effect transistors modified with peptides; a comparison of device characteristics versus surface properties	56
3.1 Summary.....	56
3.2 Introduction.....	56
3.3 Experimental and chemical functionalization.....	58
3.4 Functionalized AlGaIn/GaN topography.....	60
3.5 Conductivity response.....	61
3.6 Surface peptide stability.....	64
Chapter 4 HgNO₃ Sensitivity of AlGaIn/GaN Field Effect Transistors Functionalized with Phytochelating Peptides	67
4.1 Summary.....	67
4.2 Introduction.....	67
4.3 Experimental.....	69
4.4 XPS Surface confirmation.....	70
4.5 HNO ₃ degradation effects.....	71

4.6 Concentration sensing of Hg.....	75
Chapter 5 Biofouling and long-term solution exposure stability of phosphonic acid derivative modified AlGa_N/Ga_N Field Effect Transistors.....	76
5.1 Summary.....	76
5.2 Introduction.....	76
5.3 Experimental and biofouling procedures.....	78
5.4 Long term solution exposure.....	82
5.5 Biofouling and phosphonic acid derivative effects.....	82
5.6 Gate width dependency of response.....	84
Chapter 6 Conclusions and Future Outlook.....	85
6.1 Conclusions.....	85
6.1.1 Chapter 2.....	85
6.1.2 Chapter 3.....	85
6.1.3 Chapter 4.....	87
6.1.4 Chapter 5.....	89
6.2 Future directions and outlooks.....	90

LIST OF TABLES

Table Number and Caption

- 1.1 Example analyte and receptor pairings shown for III-nitride compounds used in biological or non-biological sensing devices. Beneath the receptor information indicates the molecule or compound that acts as a receiving component of a sensing scheme, and the analyte represents the aqueous or environmental stimuli that interact with the III-nitride surface groups.
- 2.1 List of adsorbates utilized in this study
- 3.1 Mean peak area ratios for N 1s and N-Ga peaks.

LIST OF FIGURES

Figure Number and Caption

- 1.1 Example diagrams of both Zinc Blende and Wurtzite structures seen in III-nitride compounds.
- 1.2 Figure 1. Cell growth on various GaN surfaces; A) and B) fibroblast growth on GaN using SAM modified surfaces, adapted with permissions from Faucheux et al.¹, C) and D) neuron growth on GaN using modified surface topographies, adapted with permission from Bain et al.², E) and F) neuron cell growth using IKVAV binding proteins on GaN, adapted with permissions from Jewett et al.³
- 1.3 A) Basic chemisorption functionalization with aniline following ion bombardment of GaN surfaces under UHV conditions.⁴ B) Example of organosilane surface attachment following hydroxide termination to the surface, using the forementioned TUBTS molecule.⁵ C) Example of a Grignard reagent attachment to GaN using a chlorine terminated surface.⁶
- 1.4 Schematic of biomolecule functionalized AlGaN/GaN FET. Adapted with the permission from Rohrbaugh et al.⁵⁴
- 1.5 Top down view of an FET used in the studies described in this work. Shown are the source, drain and gate regions. Additional dimensions shown are the gate length and gate width. Gate length being held at a constant 15 μm across all samples, and gate width being either 50, 100, or 150 (shown above) μm .
- 1.6 Testing methods and objectives of the different properties that make up the stability of a biological sensor.
- 2.1 (A) Device schematic and dimensions. (B) Optical image of the diced chip layout shown an example of the 13 FET sites probed for the current measurements. (C) SEM micrograph of a clean FET used for this study; highlighted regions indicate areas where XPS and AFM analysis was performed. (D) SEM micrograph of an FET device after exposure to GaN powder.

- 2.2 (a) X-ray photoelectron spectroscopy analysis of clean devices, RP modified and RP modified devices after soaking in solution. (b) Drain current changes of devices modified with all adsorbates. (c) Drain current changes of devices modified with all adsorbates after soaking in solution.
- 2.3 Full sample set of percent changes observed for the RP modified FET groups. Three samples were removed for XPS analysis.
- 2.4 Change in drain current of devices modified with RP and exposed to GaN powder slurry.
- 3.1 Functionalization scheme of AlGaIn/GaN FET surfaces through an in-situ functionalization with phosphoric acid and ethephon followed by incubation in a cysteine terminated peptide.
- 3.2 Representative AFM images of peptide surfaces at different stages in the solution exposure process. a) peptide terminated device surface prior to soaking in water; peptide agglomerates can be seen as white spots along surface; RMS Roughness of 1.41 ± 0.3 nm, and a maximum surface feature height of 39.3 nm. b) Device surface after 24 hrs of water soaking; fewer particulates and an increase in small defects count are observed; RMS Roughness of 1.89 ± 0.4 nm, and a maximum surface height of 71.2 nm. c) Poly lysine device surfaces demonstrating an excessively thick and relatively smooth biofilm; RMS Roughness of 3.2 ± 0.4 nm, and a maximum surface feature height of 16.9 nm.
- 3.3 a) Gate voltage sweep data for control groups including the etched, pristine, ethephon functionalized and poly lysine sample sets. b) Gate voltage sweep data for soaking stages starting at 24 hrs and going up to 168 hrs. Lines on both parts of the figure represent average value over an entire sample group, and shaded regions represent ± 1 standard deviation.
- 3.4 Representative high resolution N 1s XPS scans of device surfaces from each soaking group. Data for a peptide terminated device prior to soaking as well as a clean (control) device is also shown.

- 4.1 a) Ethephon and phosphoric acid surface functionalization, b) Peptide incubation resulting in covalent binding between peptide chains and AlGa_N/Ga_N FET surfaces, c) Hg standard solution exposure to Hg-sensitive peptide functionalized AlGa_N/Ga_N FETs.
- 4.2 XPS spectra of cleaned surfaces, peptide functionalized, 1, 10, 100 and 1000 ppm Hg confirming lack of amide and Hg peaks prior to the functionalization steps and affirming the diminishing Hg peaks as concentration was stepped down.
- 4.3 a) Three control groups testing the effects of the different solution treatments performed in this experiment including a water control, full ethephon functionalization, and then full functionalization plus the undiluted Hg stock solution. b) Comparison of water, 1000 ppm, and 10 ppm effects on functionalized samples and the negative peptide control using TAT-C.
- 4.4 I_D response of phytochelatin modified AlGa_N/Ga_N FETs exposed to varying concentrations of Hg in nitric acid solution. Each bar represents a single chip containing a maximum of 13 individual FETs. Significant differences exist between these groups indicating a sensitivity to varying Hg concentration within the solution.
- 5.1 Scheme outlining the functionalization and treatment of the AlGa_N/Ga_N FETs throughout the experimentation. a) groups of FETs are functionalized in either PP or PFB. b) FETs are soaked in either a long term DI water solution or biofouling solution. c) FETs are removed, dried, and tested for ID signal response.
- 5.2 Comparison of ID response at peak transconductance of each sample group. a) Shows shifting ID signal from the initial untreated phase of the study up to the etched and functionalized phase including a 5 week soak test and a BSA fluid soak test. b) Shows the shift in ID from the functionalization phase of the study until the final soaking and testing of each sample group, BSA control was tested again from the same setup in part a) for comparison.
- 5.3 Comparison of ID response at peak transconductance of each sample group. a) Shows shifting ID signal from the initial untreated phase of the study up to the etched and

functionalized phase including a 5 week soak test and a BSA fluid soak test. b) Shows the shift in ID from the functionalization phase of the study until the final soaking and testing of each sample group, BSA control was tested again from the same setup in part a) for comparison.

Stability and Reliability of III-Nitride Based Biosensors

1.1. III-Nitride Materials

Two particular materials of significant interest within recent years have been AlGa_N and Ga_N. These two materials are commonly combined in a heterojunction structure for high electron mobility transistors (HEMT). From a biological compatibility stand point the AlGa_N/Ga_N system has been shown to be non-toxic when put under physiological conditions as well as maintaining a chemically stable surface.⁷ Furthermore cellular growth studies have revealed that AlGa_N/Ga_N is a suitable surface for cell growth and tissue interfacing.⁸ These devices are fabricated such that layered AlGa_N/Ga_N produces a conductive channel at their interface, close to the sensing surface. It is this interface that gives this material its characteristic properties as a biosensing platform, and allows for quantification of dissolved or airborne compounds. Interactions between the surface of the AlGa_N/Ga_N device and its environment generate changes in along the surface that influence the conductive channel.⁹ The electrical fields of these interactions produce conductance changes in the channel, thus these devices fall under the category of field effect transistors (FETs). One of the largest benefits of the AlGa_N/Ga_N system is the adaptability of the surface to different modification and functionalization schemes. This is made possible by the availability of surface bonding sites and the innate chemical inactivity in the presence of both acidic and basic solutions.¹⁰ Thus, combining the benefits of physiological stability, sensitivity to surface interactions, and wide range of surface modifications the AlGa_N/Ga_N system is one of the most widely used III-nitride currently being used in biosensor research and development. While the AlGa_N/Ga_N system provides an excellent example of applied III-nitrides to biosensors it represents only one area in the larger research field that is III-

nitrides. AlN, GaN, InN all share similar surface properties and have been examined as possible base materials for novel biosensing platforms.

In this chapter we will be discussing III-nitrides for biosensing as a wider field of study. Although there will be a large amount of focus given to AlGaIn/GaN as the most prominent III-nitride of study in literature for biosensing, other less commonly used III-nitrides will be explored as well. Specific biosensor device functionality, specificity, selectivity and operation will be discussed on a material by material basis. Additionally, a background into the materials themselves will be provided from a stability perspective with regard to solution exposure, doping, and interactions with biological systems.

The group III-Nitrides can be defined as the class of materials that encompasses all compounds formed between a III group element binding with nitrogen. This includes AlN, GaN, InN, InGaIn, and AlGaIn; as well as all other binary, tertiary, and quaternary combinations. Interest has greatly increased in the past decades as the need for light emitting diodes (LEDs) and other optoelectronics has risen. III-Nitrides offer both wide bandgap semiconductor materials like GaN and AlN, as well as narrow bandgap materials like InN.^{11,12,13} It is due to this wide bandgap character that these materials have taken such an interest for optoelectronics.¹⁴ The bandgap can be tuned depending on the alloy compositions, or other factors induced during processing such as strain.^{15,16} All of these materials have a direct bandgap making them attractive for light emission and detector applications.¹⁷

III-nitride materials may crystallize into two structures: wurtzite (hexagonal) and zinc blende (cubic). Example diagrams of both wurtzite and zinc blende can be seen in Figure 1. Wurtzite is the most common solid phase of the two, and is a form of the hexagonal crystal system with primary axes

in the a and c directions.¹⁸ Anisotropic behavior exists between the a and c directions.¹⁹ Polarization is inherent to the wurtzite structure of the III-nitrides and can be categorized as either spontaneous and piezoelectric. Spontaneous polarization comes from electric fields generated between alternating layers of N and III group metal in the material and the non-centro symmetry of the hexagonal crystal structure.²⁰ Zinc blende structures have similar alternating layers to wurtzite but lacks this spontaneous polarization due to the lack of non-centro symmetry. Piezoelectric polarization arises from stresses on the III-nitride material.²⁰ Typical heteroepitaxy used for these materials results in strain; therefore both polarization effects will always be present in III-nitride deposited layers.

III-nitrides films are typically grown in the $+c$ orientation of the crystal with the surface being the (0001) plane. Due to the non-centrosymmetric nature of the hexagonal structure, two different orientations of the crystal lattice are possible along the c -axis. Thus the crystal can be grown in the $+c$ orientation (0001) referred to as the III (either Ga, In or Al)-polar and the $-c$ orientation (000-1) referred to as the N-polar.²¹ This orientation also determines the direction of the spontaneous polarization of the crystal, thus referring to its polarity orientation. The corresponding polarity determines the possible surface reconstructions available for the c -planes, or simply the number of dangling bonds available on the surface.²² In the III-polar case, a negative polarization charge at the surface induces a positively charged depletion region near the surface, while for the N-polar surface a positive polarization charge induces a negatively charge region. This negative charge region arises from accumulation of free carrier or a change in the occupation of the surface states. Polarization differences across interfaces between III-nitride layers determine the induce charge at that interface. Such an example is the polarization discontinuity found between the AlGa_N/Ga_N interfaces where electron accumulation forms a 2 dimensional electron gas with resulting high electron mobility. This

is the basis for the formation of the conductive channel in the field effect transistors previously described and as such they are typically described as high electron mobility transistors (HEMT).

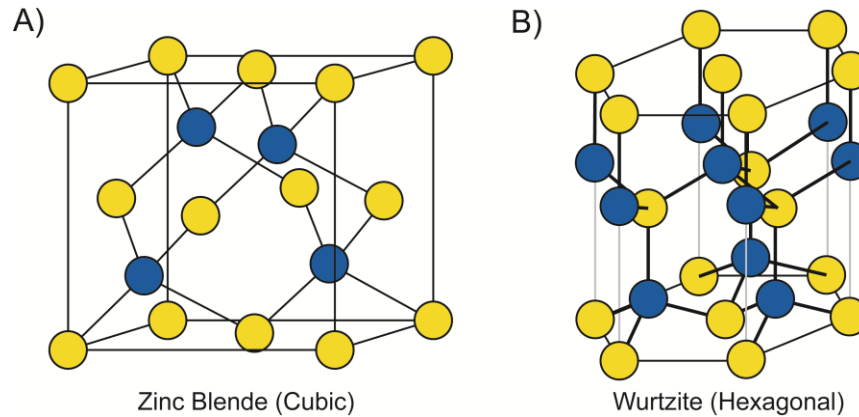


Figure 1.1. Example diagrams of both Zinc Blende and Wurtzite structures seen in III-nitride compounds.

1.2. Doping of nitrides

Doping of III-nitride materials has become more common practice in recent years and can be incorporated into the MOCVD growth processes.¹⁶ The addition of dopants to these films allows for tunable conductivity characteristics and selection of the charge carrier type that will be dominant in the film.²³ When defining doping charge carriers, n-type refers to electrons dominating, and p-type being hole dominated conduction. Dopants of a higher valence than the base material, in this case group IV, are added to generate n-type behavior. In contrast, for hole dominated films a lower valence dopant is added, such as a group II material. Depending on the charge carrier type, either donor or acceptor states will be created within the bandgap of a semiconducting material.²⁴ However, effective doping is only possible if the activation energy of the charge carriers is low enough to provide free electrons or holes with sufficient amounts at room temperature. Here, the activation energy is defined as the energy that is needed to detach a carrier from its dopant. Since this energy is typically provided by the temperature of the material (thermal activation) the activation energy should be $< kT$ which is

around 27 meV at room temperature. Furthermore, compensation of dopants due to incorporation of unwanted charged point defects needs to be controlled. This highlights the need to find shallow dopant and control compensation in III-Nitrides.

Most common dopants in GaN and its ternary materials are Si for n-type behavior and Mg for p-type. These provide good representation for doping in this material system as both are widely used and well researched for III-nitride materials. Si is a shallow donor in GaN with an activation energy of 12 meV. For Si doped GaN a good controllability has been found and free carrier concentrations ranging from $1 \times 10^{16} \text{ cm}^{-3}$ to $5 \times 10^{19} \text{ cm}^{-3}$ have been demonstrated. Higher free carrier concentrations can be targeted with Ge if needed. However, p-type doping with Mg is found to be more difficult.^{24,25} This can be related to the higher activation energy of the Mg-acceptor of 160 meV, the formation of Mg-H complexes and passivation after growth, and limitations in the doping capabilities due to self-compensation for $\text{Mg} > 3 \times 10^{19} \text{ cm}^{-3}$.^{24,26} While the Mg-H complex can be activated following fabrication with an additional annealing step in an H free atmosphere and compensation can be controlled using advanced point defect control mechanisms, the activation energy stays the main limiting factor.²⁷ Consequently, typical free carrier concentrations of MOCVD grown GaN:Mg are in the range of $3\text{-}6 \times 10^{17} \text{ cm}^{-3}$ for $3 \times 10^{19} \text{ cm}^{-3}$ acceptors. Thus, the conductivity of Mg p-type doping as a whole is relatively low given the above factors when compared to the capabilities of Si n-type doping.^{28,23}

Doping in the other binary III-nitride systems is based on the results and experience from GaN. N-type behavior in AlN has been shown with Si but doping capabilities are limited due the formation of a DX-center and increase of the activation energy to $>200 \text{ meV}$.²⁹ P-doping using Mg has been tried in AlN as well, but no free holes or p-conductivity has been demonstrated as of today. InN possesses native n-type behavior in many cases due to its surface high electron affinity.^{30,31} Some reports suggest this is in part to impurity formation within the InN.^{32,33,34} BN is

more accessible to dopants due to its smaller atomic radii as shown in work involving Si and Mg.^{35,36,37} Nuances of doping for each of these binary compounds are beyond the scope of this work and is still a field where new up and coming research is being done. As such for more information on doping effects on stability of biosensors readers are encouraged to investigate further with some of the references provided here.

III-nitride ternary compounds are unique from a doping perspective in that both Group III elements in the ternary compound can be treated as dopants of each other depending on desired characteristics and tuning of the desired final structure. Similar to literature mentioned previously on binary III-nitrides research within this field is broad and as such only n-type AlGaN will be discussed in a briefly as an example. N-type doping of low Al-content AlGaN has been shown using Si and provides a good example of the balancing that must be done with the two III-group elements in the final product. In work done by Collazo et al, AlGaN with varying ratios of Al to Ga are explored relative to their Si doped n-type behavior.³⁸ The activation energies of Si impurity formation within GaN and AlN are approximately 17 meV and 200 meV respectively.³⁹ Thus, as Al content increases in AlGaN a drop off in n-type behavior is observed resulting in almost complete removal of the behavior at $\text{Al}_{0.8}\text{Ga}_{0.2}\text{N}$.³⁸ This decrease in n-type behavior can be further explained by DX center formation and vacancy-complex compensation within the AlGaN. More information into AlGaN's conductive properties and performance relative to growth processes and doping can be found in the extensive review on the subject in Jones et al.¹⁶

In discussing the environmental stability that doped III-nitride materials possess a definition of shallow and deep dopants needs to be established. Shallow dopants like that of Si donors in GaN have relatively small activation energies which can be filled from thermal energy within the compound.⁴⁰ These dopants once activated create available charge carriers for the n/p type behavior designed for the material. Here, the majority of shallow dopants will be active or intended to be active

once the III-nitride compound is in a conducting mode. Deep dopants however, require a much greater energy to ionize and in many cases will not provide free charge carriers to aid in conduction.¹⁶ Dopants such as these provide compensating centers that can act as recombination sites for electrons and holes, and are commonly referred to as charge carrier traps.⁴¹

Doped GaN, both n-type and p-type, experiences a carrier removal or relocation when exposed to neutron radiation that varies on the type of charge carrier.⁴² The methodology of quantifying radiation damage takes into account the number of carriers that no longer contribute to the overall n-type or p-type behavior. This is typically because the carrier or dopant has been moved to a dislocation site within the lattice. In this study by Pearton et al. carrier removal rates were 20 times higher for p-type doping than in n-type doping, however both methods had removal rates $>10^3$ cm^{-1} under proton radiation doses of 10^{14} cm^2 .⁴² Under the same testing neutron and electron radiation were examined with neutron radiation having a weaker removal rate. The rate of removal for neutron radiation was $<10^2 - 10^0$ cm^{-1} however, electron radiation yielded a weaker removal at $<10^1 - 10^{-1}$ cm^{-1} over a wider range of dosages. The generation of electron traps within the GaN layers leads to a Fermi level pinning effect (reported at a conduction band energy of -0.95 eV) which can lead to self-compensating effects for conductivity.⁴³ In general under radiation dosing n-GaN has been observed to become semi-insulating as carriers are displaced. The problem presents itself with $\text{Al}_x\text{Ga}_{1-x}\text{N}$ heterojunction layers at various levels of Al doping. The self-compensating effects of radiation damage manifested itself here as an overall increase in resistivity of the GaN layers in AlGaN/GaN heterostructures.⁴⁴ This increase in resistivity resulted in degradation of the 2DEG in both AlGaN/GaN interfaces and AlN/GaN interfaces, and is largely attributed to the increase in defect density causing a drop in mobility. Cited values for the drop in conductance were as high as 50% for elevated levels of electron dosing.⁴⁴ Further work by Polyakov et al. into neutron effects on the same series of AlGaN/GaN and AlN/GaN (additionally InAlN/GaN) showed cause for concern for stability

of 2DEG layers under such conditions.⁴² It was observed that with increasing Al content in AlGaN/GaN heterostructures (up to Al_{0.5}Ga_{0.5}N) an increase in trap concentration was observed which in turn lead to decreases in the carrier mobility and conductance of the device.⁴⁵ Similar effects were observed in proton irradiated samples of AlGaN/GaN as well.⁴⁶ Thus it can be said that radiation effects are of significant concern for GaN based devices and heterostructures if the intended end use requires reliable performance under prolonged and elevated radiation exposure. In context of electrical stability these effects stand out and may present problems over time, but there are ways to mitigate these effects by lowering initial dislocation densities in GaN based materials.⁴³ There is also evidence for recovery and relaxation of radiation induced carrier migration over time after following a strong radiation exposure.⁴⁷

Despite these findings, III-nitrides when compared to other materials have shown evidence of significantly higher radiation hardness.⁴⁸ In terms of overall resilience both AlGaN and GaN shown radiation hardness values less than but comparable to diamond.^{49,48} AlN has been further investigated for creating resistant layers from UV up to gamma radiation.^{50,51,52} In this work done by Tittmann et al. AlN showed high resilience when exposed to 5.8×10^{18} neutrons cm⁻² and 26.8 MGy gamma radiation, this was quantified by the lack of change in AlN's piezoelectric properties.⁵¹ InN has not been as widely studied for radiation hardness but has shown interesting responses in relation to charge carrier removal. N-type InN demonstrates an opposite effect to GaN and other III-nitride compounds in that it shows an increase in carrier concentration once exposed to high levels of radiation. This can be explained by the high electron accumulation that occurs in InN and the innate n-type behavior that comes from higher defect densities.⁵³ Highly crystalline InN nanowires exhibit minimal electron accumulation, thus defects brought on by radiation damage increase this accumulation and undermining deliberate processing to remove electron accumulation along the surface.⁵⁴ It is worth noting that heat treating of radiation damaged III-nitrides allows for some recovery of conductive

properties. In this same study by Emtsev et al. annealing of InN and GaN allowed for a recovery of properties to values similar to previous measurements done before the radiation treatments.⁵³ Annealing GaN required temperatures greater than 600°C before substantial electron mobility and charge carrier concentrations recovered. InN showed opposite effects as a reduction in mobility was observed at temperatures between 400° and 500°C. Once temperatures exceeded 500°C electron mobility began to return to that of pre-radiation treatment levels.⁵³

1.3. Water stability resistance to etching and degradation

Solution based measurements for biosensors require an understanding of a material's behavior when exposed to a variety of liquid environments. Leeching of material into solution or defect exacerbation are examples of mechanisms that can degrade surfaces of biosensing devices. Fortunately, III-nitride materials have been shown to possess a high tolerance for wet etching conditions and have high chemical stability.^{55,56} Two types of etching are discussed here in the context of III-nitrides; electrochemical etching and conventional etching. The use of chemical etchants such as hot acids is an example of conventional etching and are used in cleaning and processing of III-nitride materials for biosensors.⁵⁷ Electrochemical etching relies on potential differences between the III-nitride and the charged species interacting with the surface, examples include anodic etching or electroless etching. The primary difference for these two mechanisms is the necessity of charge carriers for electrochemical etching and the absence of them in chemical etching.⁵⁸ As such electrochemical processes are more likely to take place in physiological environments encountered by biosensors where a highly diverse and dense concentration of electrolyte species could be found.

The high bond energy of III-nitrides is what allows for this resistance to most etching methods. Bond energies of III-nitrides range between 2.88 eV, 2.2 eV, and 1.93 eV for AlN, GaN, and InN respectively.⁵⁹ A benefit of this tolerance for chemical etching relative to biological applications is the ability to remove surface organic compounds and oxide layers without damaging or heavily altering the III-nitride material beneath.⁶⁰ HCl etching on GaN for removal of surface contaminants and preparing the surface for functionalization is such an example.⁶¹ Surface stability of GaN under exposure to etchants is affected by the quality of the grown film and its corresponding dislocation density. In the fabrication of III-nitride materials substrates such as Si or sapphire are commonly used and can produce a substantial lattice mismatch at the interface of the film. This interface produces threading dislocations with a density determined by the growth parameters typically in the range of 10^7 - 10^{11} cm⁻² for GaN.^{62,55} Wet etching can still be realized on III-nitrides both to show dislocations and to remove layers of the surface despite an overall resistance to common etchants. AlN and GaN have been well documented as being susceptible to H₃PO₄, KOH-NaOH, and HF/H₂O₂.^{62,63,64,65} Some examples of GaN and AlN etching rates in common chemical etchants can be seen further in Zhuang et al.⁵⁵

Stability in aqueous conditions is observable by measuring the concentration of the dissolved group III element or compound into the surrounding solution. GaN for example exhibits very low concentrations in pure DI water at reported values of 3.68 ± 0.54 ppb after 7 days.³ This demonstrates a high degree of aqueous stability in GaN for possible biosensor applications. Aluminum nitride exhibits similar behavior when bulk samples are placed into solutions. Bulk samples themselves are virtually insoluble in water, however AlN powders exhibit corrosion and hydrolysis in the presence of aqueous environments.^{66,67} This suggests a correlation between exposed surface area to solution and stability of the AlN material. Work has shown that AlN powders can be passivated to their aqueous surroundings to prolong lifetime in solution. Research on this is still dependent on a phosphoric or

phosphonic acid complex or etch to encapsulate the surface due to AlN showing high resistance to traditional etchants even as a powder.⁶⁸

BN also demonstrates highly stable surface properties under exposure to aqueous environments. Oxidation of boron nitride is generally seen as a high temperature process taking place at upwards of 1500°C, with minimal oxidation taking place at room temperature or within feasible temperatures for a biological setting.⁶⁹ When under aqueous conditions the primary reaction scheme for BN degradation via hydrolysis is the formation of metaboric acid (HBO_2) and orthoboric acid (H_3BO_3).⁷⁰ However, even these processes were shown to not become substantial until temperatures greater than 700°C, which is far beyond the bounds of what a biological sensor material would encounter. In recent work BN was shown to be a strong candidate for ultra-hydrophobic surfaces due to its chemical inertness and lack of reactivity in water at < 100°C.⁷¹ The growth morphologies given in this study show that even in vertically grown nanosheet conformations water reactivity was negligible. Nanosheet surface morphologies have a much higher amount of exposed surface area than epitaxially grown BN, further illustrating BN's aqueous stability and lack of reactivity. BN's high aqueous stability allows it to be used in applications of perpetual water contact, like those proposed for the use of nano-porous structures of BN in water filtration. Here it was demonstrated that due to BN high resistance to oxidation it is an excellent candidate for use in removal of oils and solvents from water systems.⁷² Although it is worth noting that BN stability is dependent on crystal structure. At higher temperatures (1200°C) a hexagonal orientation of BN is more stable while closer to ambient temperatures cubic orientations are preferred.⁷³ This temperature dependence of BN and other III-nitride is not a focus of this work as operational stability for GaN and III-nitride sensors is seen well past temperatures one would find under biological conditions.

While not the dominant III-nitride of interest in aqueous environments, multiple studies on InN in aqueous environments have exhibited similar characteristics to that of other III-nitrides. InN

hydrolysis is detectable by the presence of NH_3 in solution or by surface presence of $\text{In}(\text{OH})_3$, both of which are the reaction products of hydrolysis on InN.⁷⁴ These are difficult to observe except through XPS as the hydrolysis process does not produce a noticeable amount of material loss from the surface. The effect of hydrolysis in aqueous solutions seems to be negligible as research into InN as an anion sensing platform deemed the material an excellent candidate for such a role and did not observe any degradation effects of the InN surfaces while exposed to various ionic solutions.^{75,76} Etching of InN surfaces is expectedly difficult and similar to AlN and GaN. Acidic solutions typically do not have any effect on InN, but basic solutions such as KOH and NaOH are capable of etching the surfaces.⁷⁷ However, etching of the surface is a relatively slow process with etching rates from this study ranging from $\sim 5 \text{ \AA}/\text{min}$ at ambient temperature to $\sim 400 \text{ \AA}/\text{min}$ at elevated (60°C) temperatures. In general InN is very stable and not easily etched by any common etchant with the exception of highly basic solutions, and even such at a markedly slow rate.

1.4. Toxicity

Toxicity can be seen as the amount of a material that is needed initiate damage or harm instead of a helpful or neutral response within an organism or cellular system.⁷⁸ In contrast, biocompatibility relates the interfacing of tissues and cellular structures with a given biomaterial. In general concentrations of III-nitride materials are very low in natural settings as they are not naturally occurring compounds. III-nitrides are largely chemically inert under biological conditions and in water solutions. The possible concern then from III-nitrides in the environment comes from the leeching of the III group element (Ga, Al, In, B) into surrounding environments. Industrial pollution would be an example of a point source for this type of contamination. Al is well known to be toxic and having detrimental effects to biological systems, which is one reason why many biosensors are

focused on Ga-based systems.⁷⁹ Ga has yet to show any toxic effects on biological systems and exists in nature at very low concentrations within materials with daily contact. Toxicity of some III group materials such as InN are not well known as they are not naturally occurring in large quantities.

One study examined the accumulation of Ga in 1300 food samples and revealed that Ga concentrations in most (84% of those tested) common foods was beneath the limit of quantification of 0.002 mg kg^{-1} and 83% of foods tested concentrations were beneath the limit of detection of the instrument at 0.001 mg kg^{-1} .⁸⁰ The only substantial findings from this study relative to Ga were an increased level of Ga in fats and oil products with an average level of over 0.005 mg kg^{-1} .⁸⁰ Shellfish and chocolate were the only other substantial sources at 0.008 and 0.010 mg kg^{-1} , respectively. Indium dosing for humans is also not considered substantial from foods that occur naturally, and is instead linked almost entirely to industry related pollutants and water contamination.⁸¹ In this study done by Ayadi et al. indium was given to mice via injection to gain some insight into effects on mammalian tissues from indium.⁸¹ Results from this work showed highly toxic effects from indium nitrate given at dosages of 28 mg kg^{-1} . Monitoring prolactin concentrations from mouse mammary glands showed a drop to 23% that of levels seen in control mice. This coupled with decreasing body weight and food intake provides evidence that indium is indeed toxic when leached into biological systems. Similar studies have been done on male rats and found similar results that indium deposits accumulating in cellular lysosomes lead to necrosis of the tissue and loss of weight in the rats.^{82,83} Indium's toxic effects have been known for some time despite newer studies highlighting the issues of ingesting large quantities. Work dating back to the early 1970s has shown that indium once dissolved into solution has the same nephrotoxic effects as Al and less so Ga.⁸⁴ This study examined both ionic indium and hydrated indium oxide. For ionic indium it was found that almost all damage occurred in the kidneys with some accumulation in the liver when tested in mice. This accumulation was seen as 17.83% of the administered dose per gram persisting in the kidneys after three days for

the LD₅₀ of 12.5 mg/kg. This increased to 33.14% for an LD₁₀₀ level of dosage at 16.5 mg/kg indium. In both instances necrosis was observed in localized areas near injection sites for both liver and kidney after three days. When not injected directly into organs the accumulation led to the loss of cell structure in both the cytoplasm and nuclei and was observed at LD₅₀ levels. Epithelial swelling was also observed. In more recent studies indium containing compounds have been examined for pulmonary effects on both humans and animals as technology has shifted to producing indium compounds such as InN, ITO, and InP. Results in this case were similar to the injected indium studies. These again indicated that the intake of fine powders from indium processing led to accumulation of indium within tissues.⁸⁵ Here indium compounds were shown to cause severe damage to pulmonary tissues and possibly demonstrate carcinogenic effects as well depending on the degree of In accumulation within cellular structures. Based off of findings such as these, standards in countries like Japan have instituted a 3 µg/L concentration of indium in biological serum as the upper limit for safe dosage for humans.⁸⁶

GaN has been shown to be nontoxic and is thus one of the more promising III-nitrides. This lack of toxicity in GaN extends to some of its other compounds such as gallium nitrate which has been shown to be useful for cancer treatments.⁸⁷ In this study done by Kelsen, a continuous supply of gallium nitrate supplied intravenously to patients only showed toxic effects when doses reached 700 mg/M².⁸⁷ The units used in such toxicity measurements are commonly expressed in terms of body weight or body surface area (BSA) as used in Kelsen et al, an explanation of these units is provided here.⁸⁸ Under such levels nephrotoxic effects were seen as kidneys of the patients were inundated with gallium nitrate. Otherwise the study showed that the kidney remove gallium nitrate from the body dropping gallium levels in the body from 1.9 µg/ml during infusion periods to 0.4 µg/ml several days after.⁸⁷ This work done on blood plasma concentrations is dated back to the 1980s, but more recent work has shown similar results and still shows gallium nitrate suitable for metal-based cancer

therapies.⁸⁹ This work is consistent with the previous findings that gallium nitrate has no strong toxicity to bone marrow and when given through manageable infusions show no overall toxic effects in the body. This is not to say that gallium within the body is inert on its own. It has been shown that gallium at certain concentrations will begin to replace iron in cellular processes, more notably by binding to transferrin proteins which are typically used for iron transport.⁹⁰ Gallium nitrate and the subsequent release of Ga into cellular structures have mostly been examined for treatment of lymphoma cells (both Hodgkin's and non-Hodgkin's). One reason for this is the level of radioactive Ga-67 provides a means to measure the metabolic processes that are characteristic of lymphoma cells again by replacing iron in cellular activity.⁹¹ For a more in-depth look into Ga compounds pharmacokinetic behaviors and applications readers are directed toward a review on subject by Chitambar et al.⁷⁸

AlN is largely inert in both biological fluids and most etchants, the exception to this rule however is when AlN comes in contact with fluids while in a dispersive powder form. In these circumstances the increased surface area was enough to overcome the inherent chemical inertness of the AlN and allow for some dissolution into the environment. From a toxicity perspective the concentration of AlN is relevant as Al accumulation in kidneys and lysosomes of cells is toxic. One study investigated the degree of dissolution of AlN when in contact with various biological solutions.⁹² Here simulated blood serum, gastric juice, and physiological solution were tested relative to the size of AlN particulate. The findings indicate that the finer the powder the greater the degree at which it dissolves into solution up to 95% in gastric and intestinal fluids for nanopowders. Fiber crystals showed only ~10% dissolution in ionic and gastric solutions and almost no dissolution within blood. This is consistent with previously mentioned work that larger AlN substrates and surfaces are markedly more stable in solution.

1.5. Biocompatibility

Biological compatibility refers to the ability of the III-nitride to exist in a biological system without disrupting regular cell activity or harming the host organism. In a broad sense materials used in biosensing applications must be conducive to cell growth by either not causing cell death (apoptosis) or being a surface that cells are willing to grow upon.⁹³ Within the scope of III-nitrides as biosensing platforms cells are either in contact with the native III-nitride surface or a modified surface layer such as a SAM.¹ Studies quantify this biocompatibility through cell density counts and cell population over time. Methods of doing this involve sterilized surfaces populated with cell lines (PC12 or HeLa for example) which are then monitored over time for removal of cells into solution or apoptosis. This provides information as to how well cells adhere to the surfaces, cell growth relative to surface topology, and cell damage incurred by the III-nitride surface. Examples of cell growth studies can be found in Figure studying both topography and surface functionalization. GaN provides an example of the III-nitrides that has demonstrated a high degree of biocompatibility both as a stand-alone surface and as one modified with biological molecules.^{3,93} GaN surfaces did not significantly affect or impede cell growth, and once etched showed a better cell adhesion than etched silicon. Further work has been done on examining bare GaN surfaces with varied topographies and surface adherence of cells.⁹⁴ In general it has been shown that cells prefer rougher surfaces to smoother ones for adhesive ability.⁹⁵ Mimicking surface roughness of tissue is possible using adlayers of polymer molecules, but similar effects have been shown using bare surfaces put through both etching and polishing. One study in particular found that the effects of polishing and etching GaN were sufficient to create a surface roughness suitable for cell growth and prorogation. This same study additionally tested RF assisted growth of GaN nanowires along the surface and found similar results.² Here an increase in cell adhesion on unmodified GaN was observed when surfaces were roughened via

polishing. Subsequent increases were again observed with etching, and then finally sharply increasing when nanowires were introduced. The cell phenotypes were dependent upon the surface of the GaN following these treatments.² Cells grew with significantly more branching when placed upon polished surfaces (high degree of parallel surface features) than the nanowire arrangement. These findings are in agreement with research that examined modified-nanotextured GaN surfaces with similar values of high cell adhesion capabilities for GaN.⁹⁶ Both of these studies conclude that GaN is a suitable surface for biosensing uses and can be fabricated to encourage cell adhesion further. Surface modification was used in both of these cases to create a more favorable surface for cell adhesion.

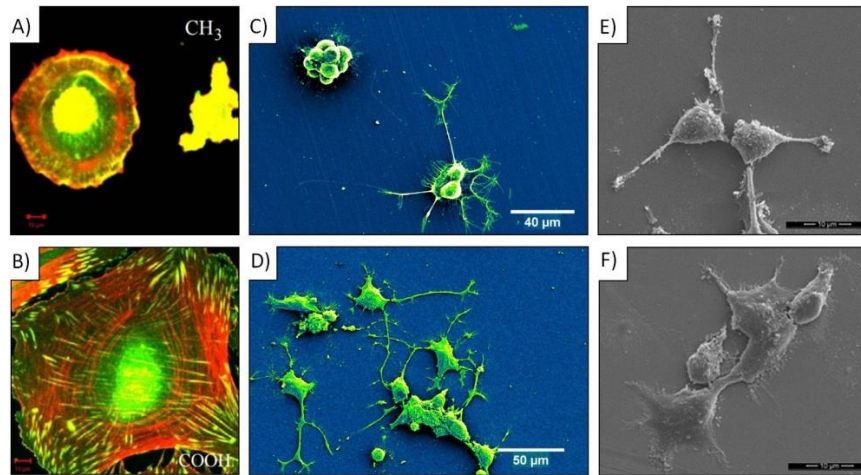


Figure 1.2. Cell growth on various GaN surfaces; A) and B) fibroblast growth on GaN using SAM modified surfaces, adapted with permissions from Faucheux et al.¹, C) and D) neuron growth on GaN using modified surface topographies, adapted with permission from Bain et al.², E) and F) neuron cell growth using IKVAV binding proteins on GaN, adapted with permissions from Jewett et al.³

The inherent biocompatibility of other III-nitride materials is not as well understood or as studied as GaN. What has been done however, does not yield as promising of results as modified GaN surfaces. Research into AlN provided poor results which align with literature regarding aluminum nitride's toxic effects on different organ systems in mammals.⁹² Examination of AlN surfaces for

cellular level studies along the AlN surface showed axonal degeneration and damage to glial cells within a 10 day time frame.⁹⁷ AlN is remarkably stable in biological media, but leeching of AlN occurs into solution and is dependent on the surface topography.⁹² Although damage may not be wide spread this would directly affect the stability of any cellular matrix that is being brought into contact with an AlN device or sensor. Thus AlN seems a poor choice for biological sensing apparatuses.

A similar effect of AlN can be observed in $\text{Al}_x\text{Ga}_{1-x}\text{N}$ systems for biocompatible interfacing, although to a lessened and more controllable degree. Examination of this effect revealed a relation between cell death rate and increasing percent Al content within the $\text{Al}_x\text{Ga}_{1-x}\text{N}$ matrix.⁹⁸ In this work Al content was measured from 0% up to 35% and throughout all examined concentrations of Al within the $\text{Al}_x\text{Ga}_{1-x}\text{N}$ matrix there was evidence of cellular activity.⁹⁸ Growth rates of cells did suffer with increasing Al, indicating that some of the toxic effects of AlN appear to carry over to AlGaN. The conclusion to be drawn from this is that AlGaN (at least documented up to Al content of 35%) does not directly mirror pure AlN for its lack of biocompatibility. Instead, previous work by Podolska et al. highlighted AlGaN as a promising surface for biological sensor interfacing as well, although noted some cell counts were suboptimal.⁹⁹ This also helps support the use of AlGaN/GaN type heterostructures for biosensing devices where cell interfacing or interactions may be a possibility.

InN and InGaN have been shown in literature to have a similar behavior to AlN/AlGaN. Regarding their cellular interfacing, some evidence suggests that the ternary InGaN may behave in similar fashion to AlGaN as described.⁸¹ While InN has shown some promise as a biosensing platform fewer experiments have explored InN behavior with cellular structures. InN has been tested in biological media for the stability of InN surfaces and surface components, but less focus on directly binding cells for tissue interfaces. InN has similar behavior to AlN when placed in a biological system in that increasing In content in mammalian tissue can lead to cellular damage and kidney

malfunction.⁸¹ Thus interfacing directly with InN may be unfavorable for cellular systems. One study of InGaN however, revealed that these surfaces may provide a biocompatible intermediate between InN and GaN.¹⁰⁰ Here, lymphocytes were grown on flexible LED devices including Si, AlInGaPAs, and InGaN. This may prove similar to AlGaIn that when In is the lesser component of a GaN ternary system the toxic effects can be mediated. In turn allowing for a biologically compatible surface to be made from an In based III-nitride compound. Until this is done AlGaIn/GaN and GaN systems will likely remain the III-nitride of choice for biocompatible material systems.

1.6. Chemical functionalization

The surfaces of III-nitride materials have available bonding sites depending on the polarity of the surface from its growth procedure.⁹ These dangling bonds are what give III-nitride materials their broad range of functionality for various analytes or chemical acceptors. Here we will cover some III-nitride compounds and selected functionalization methods and schemes.

1.6.1. Aluminum nitride

The applications of AlN are more limited in biosensor applications due to concerns of aluminum toxicity in biological environments. However, many chemical modification methods have been explored to create a selectively sensitive surface upon AlN. One such surface modification with broader application can be seen with a benzenethiosulfonate (BTS) crosslinker capped organosilane coating.⁵ This work highlights the ability of organosilane adlayers to act as a platform for immobilization of relevant compounds such as biotin-thiol. These organosilane surface coatings form what is known as a self-assembled monolayer (SAM) and have been well documented as surface modifiers in other semiconductor materials as well.¹⁰¹ Chemically modifying AlN and other surfaces

for such organosilane SAMs typically require etchants such as H_2SO_4 or piranha to remove surface contaminants and organics.¹ Pentafluorophenyl ester and β -propiolactone were among several other chemical silanization methods studied alongside BTS, all of which serve to immobilize a specific functional group onto the surface.¹⁰² Silanization of these surfaces has also been shown using dip coating techniques and subsequent heat treatments for adlayers of polysilazane to generate ceramic coatings atop AlN.¹⁰³ These techniques demonstrate the versatility of these surfaces under more precise surface bond modifications and using higher throughput processing techniques such as the dip coat. For processing of AlN with silanization the surfaces are often terminated with hydroxyl groups at available bonding sites. Exposure of surfaces after etching or during etching with an H_2O_2 solution allows for hydroxylation to take place, thus making uniform SAM possible along AlN surfaces.⁷ This could eventually open up other chemical means of functionalization by immobilizing non SAM molecules or compounds to these hydroxyl group sites.

1.6.2. Gallium Nitride

With regards to biosensing and functional surface regions, GaN has been more widely researched and explored than AlN. As mentioned in the discussion of AlN, organosilanes and SAMs play an important role in GaN chemical functionalization as well. The use of monolayers like aminopropyltriethoxysilane (APTES) or thioglycolic acid (TGA) have been shown to successfully immobilize surface biomolecules for sensing schemes.^{104,105,106} A schematic of some of the different chemical functionalization methods discussed here can be found in Figure .

Further work has been done into exploring chemical termination methods without the use of a silane adlayer for GaN based sensors. Etching techniques on GaN surfaces can be done to terminate a surface with hydroxyl groups, but with additional steps aid in incorporating another molecule onto these hydroxyl terminated binding groups.¹⁰⁷ This has been shown in work done by our laboratory

using a phosphoric acid and phosphonic acid mix to create ethephon binding sites for future biomolecule attachment.^{21,61} Additional surface functionalization work via organophosphonic acids have been shown to be an alternative to common silanization methodology.¹⁰⁸ Phosphonic acid functionalization methods do not rely on surface hydroxide group concentration, and can bind to both oxide groups and hydrogen terminated sites.¹⁰⁹ Thus functionalization of GaN surfaces using phosphonic acids as a vehicle for other biologically relevant groups is a viable option for future surface modification schemes. As mentioned previously, phosphonic and phosphoric acids are capable of etching III-nitrides where other more common etchants cannot. This slower etching process creates new binding sites for other phosphonic acid derivatives to occupy as the etching takes place.¹⁰⁷

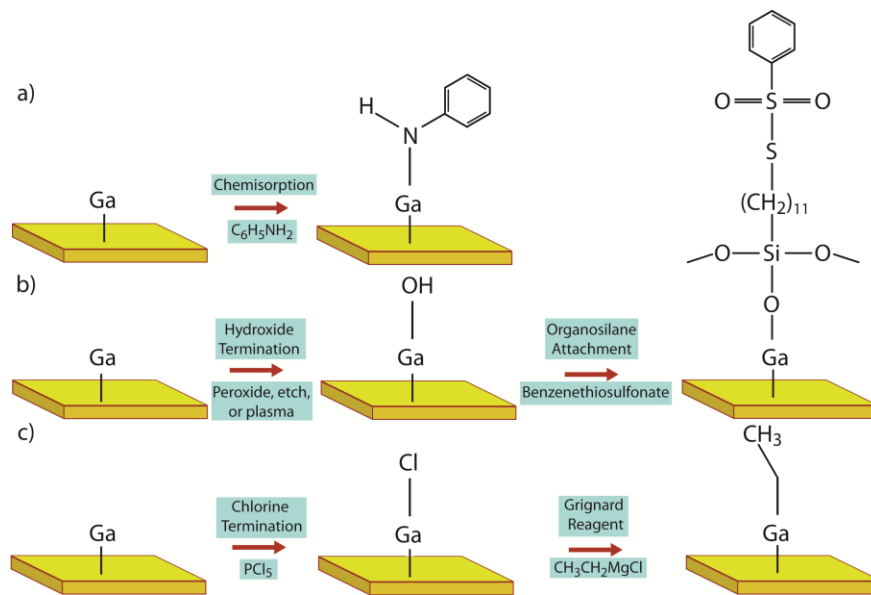


Figure 1.3. a) Basic chemisorption functionalization with aniline following ion bombardment of GaN surfaces under UHV conditions.⁴ b) Example of organosilane surface attachment following hydroxide termination to the surface, using the forementioned TUBTS molecule.⁵ c) Example of a Grignard reagent attachment to GaN using a chlorine terminated surface.⁶

Other methods of binding 1-alkene groups to GaN surfaces have been explored to generate similar layered structures to those seen by silanization and covalent attachment with phosphonic groups. Photochemical assisted binding of alkenes has been performed using ultraviolet (UV) light at a wavelength of 254 nm.¹¹⁰ Surfaces in this work were hydrogen terminated via inductively coupled hydrogen plasma and then exposed to 254 nm UV once placed in a solution of an alkene-amine molecule (10-trifluoro-acetamide-1-decene, abbreviated TFAAD).¹¹⁰ This generates a highly stable surface but lacks the adaptability of phosphonic groups while adding a plasma treatment step.¹⁰⁸ Additionally, UV treatments on biological molecules can lead to degradation of the newly bound molecules or functional groups on the surface. Thermal methods of 1-alkene binding have thus been explored to provide other options for this type of surface chemical functionalization. It was found that heat treating surfaces coated in the same TFAAD solution at 180°C was successful in binding the alkene group of the decene molecule to both hydroxyl groups and oxide groups on GaN surfaces.¹¹¹ This shows the ability to attach 1-alkenes to GaN when UV degradation is a concern, and vice versa if thermal degradation is an issue the UV method operates on the same chemical mechanism. Aside from photopatterning and thermal treatments another method of 1-alkene surface termination to GaN has been done using olefin metathesis. Here a first generation Grubbs catalyst (ruthenium chloride complex) was used following alkene surface termination to create an olefin cross-metathesis reaction to bind a 7-bromo-1-heptene marker to the GaN surface.⁶ Resultant surfaces proved resistant to oxidation and stable enough to move to attachment of a peptide monolayer to the GaN surfaces.¹¹² Here a 6-heptenoic acid was bound to the alkene terminated surfaces using the same olefin metathesis method. Peptide was successfully added to these alkene surfaces thus showing this scheme as a functional platform for sensing with a larger variety of peptides or biomolecules.¹¹²

Another method of wet chemical functionalization using the Grignard reaction has been demonstrated for GaN surfaces. Grignard reagents in a broader sense are alkyl halides introduced to magnesium in solution to generate a RMgX molecule, with R representing the alkyl group and X representing the halide.¹¹³ This method is typically used for generating carbon-carbon bonding in organic molecules. However, here it was presented as a means to cap GaP, GaAs, and GaN surfaces for superior surface stability in solution.¹¹⁴ The termination of the surface in alkyl chains prevented the degradation of GaN surface via oxidation and was able to maintain the electrical properties of the GaN film. Few experiments have been done on this methodology in regard to other crystalline III-nitride surfaces and their functionalization for biosensing or otherwise. Other work has been done using the Grignard reagents as a step within a larger chemical functionalization method, but it was not presented as the primary focus of the study itself.⁶ Thus, the full breadth of applications of Grignard reagents on III-nitrides is promising as more focus is given to these materials for tailorable biofunctional surfaces. Additionally there are research opportunities in examining the Grignard reactions on other III-nitride surfaces to explore their functionalization capabilities as well.

Earlier modification techniques utilized vacuum approaches to GaN functionalization and it is worthy of discussion as these processes are still viable options. Chemical functionalization of GaN under such conditions can be seen in the chemisorption of aniline and halogenated anilines under pressures of approximately 5×10^{-11} Torr.^{4,115} Aniline and aniline compounds were introduced to GaN surfaces following ion bombardment to remove surface contaminants and vacate surface dangling bonds. This method is successful for depositing high purity compounds onto the surface, but is not suitable for compounds and biomolecules mentioned in the previous chemical functionalization methods for GaN. Thus, research into high vacuum processing for GaN biosensors has not been fully explored, and instead focus has shifted towards wet chemical methods.

The departure from ultra-high vacuum processing for functionalization follows the trend for GaN in that functionalization methods are becoming progressively more accessible to simpler bench top chemistry procedures. Current methodology stated here has removed much of the time and resource intensive processing and replaced it with schemes and techniques which allow for a wider range of surface chemistries.

1.6.3. Aluminum gallium nitride (AlGaN)

As one of the most commonly used ternary alloys from the III-nitride set of materials, AlGaN is used heavily in biosensing research. However, the functionalization of AlGaN is not well explored as it is most commonly used in combination with GaN to form a heterojunction type device. Under these circumstances surface functionalization is similar to GaN in its response to surface bond termination schemes.

1.7. Sensing devices

Selectivity can be defined as a biosensor's ability to ignore outside interference when taking a measurement or registering an electrochemical interaction between surface bound receptors and analytes present in solution.¹¹⁶ This interference can be noise or other processes that cause some minor or major surface charge changes to the biosensor. Specificity in similar fashion refers to the actual ability of the biosensor to single out target compounds, biomolecules or ions within solution.¹¹⁷ One could view this as analyte bycatch, or unwanted entities occupying receptor sites and thus blocking possible interactions that would contribute to the biosensor's total sensitivity. These two things contribute to the overall sensitivity of the biosensor which represents the net output or signal change that a sensor can detect. Higher sensitivity means that a device can detect lower concentrations of compounds in solution with higher accuracy. This also determines the strength of

the signal that can be obtained. Research in the field has progressed towards a wider range of surface modifications and improved III-nitride biosensor fabrication techniques enabling modern biosensors to be tailored to a variety of testing modalities.

When operating a given biosensing modality the response of the material or device relative to the environmental factors can be described as the sensing mechanism. In the design and use of III-nitrides for sensing applications there are several different schemes which have been well established in literature.¹¹⁸⁻¹²² Most research into III-nitride biosensors is done through microfabricated devices that are capable of being produced in large quantities. Sensors such as FETs and HEMTs rely on conductance and charging effects to sense environmental stimuli.²¹ Others such as SAWS monitor physical motion of molecules and material and are a type of microelectromechanical system (MEMS). Both of these types of sensors act as transducers for the external stimuli and the electrical signal given off by the sensor and do so by taking advantage of the piezoelectric properties of III-nitride materials. SAWS measure shifting piezoelectric properties for the III-nitride to generate an output. FETs operate as a function of the interfacial conductance effects between their heterostructure layers; examples include AlGa_N and Ga_N or InGa_N and Ga_N in terms of III-nitrides. The 2DEG discussed earlier is an example of this induced channels at the hetero-interface between AlGa_N and Ga_N.¹²³ Along with the interface layer between the ternary and binary III-nitride two other interfaces are also present; the environment with the surface layer (in this case AlGa_N in the AlGa_N/Ga_N system) and the interface of the lower layer with the substrate itself (in this case Ga_N). A schematic of this device structure can be seen in Figure 1.4.¹²⁴ Sensing along the surface interface relates the chemistry from the outer layer of AlGa_N or Ga_N to the interior 2DEG and is what determines the sensing capabilities for a biosensing device. When considering both the piezoelectric and spontaneous polarization of the AlGa_N and Ga_N they are often lumped together as a net polarization effect and are both characteristic properties of their material.¹²⁵ These different net polarization effects in AlGa_N to

GaN depend on the aluminum content in the AlGaN. The piezoelectric component of the polarization is affected by strain induced by replacing Ga with Al and causes a mismatch at the lattice interface with bulk GaN.¹²⁶ When these properties are viewed as macroscopic polarization effects for each material they can be effectively seen as fixed surface charges.¹²⁴ Since the surfaces of the GaN bulk layer are in contact with either the substrate or the AlGaN layer these will ideally remain unchanged when put into operation. AlGaN however has an exposed surface to the environment and any internal electric field caused by polarization is now subject to environmental interactions with the AlGaN surface. Conductance and electrical behaviors will change within the 2DEG present along the AlGaN/GaN interface relative to the effects that surface charging will have on the internal electric field. Thus, monitoring the current flow or potential in AlGaN/GaN FETs becomes a means to quantify environmental effects on the sensor itself. Additionally the interface structure of the AlGaN/GaN devices is highly stable and allows for a high transconductance at low potentials and often without the need for an external electrode.¹²⁷ These surfaces are typically functionalized or capped with a receptor specific to a given environment or to an analyte intended to be measured.¹²⁸ The focus here will be put upon FET type setups and gas sensors relative to III-nitrides. SAWs will not be covered in this text; readers are encouraged to start with reviews and papers such as these.^{122,121}

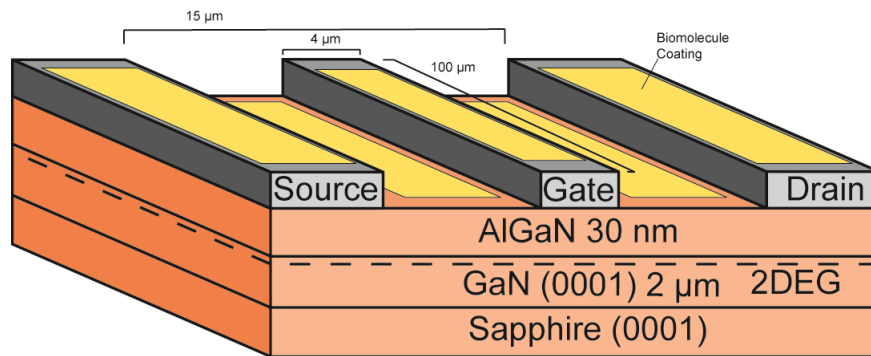


Figure 1.4. Schematic of biomolecule functionalized AlGaN/GaN FET. Adapted with the permission from Rohrbaugh et al.⁵⁴

One of the more simplistic detection schemes for these AlGaN/GaN and GaN devices is surface ion concentrations. Studies focusing on ion sensing applications rely on either capping these surfaces with an oxide layer, or capping the available GaN surface bonds with ionic elements or compounds. Chloride ion attachment along these surfaces has been performed using HCl etching of oxide layers on GaN and AlGaN.¹²⁹ In this study oxide layers were used as a medium for either Cl or OH group attachment atop the surface for pH studies. Oxide layers had to be fabricated due to the etching resistance of both AlGaN and GaN. The findings showed that GaN and AlGaN behave differently as pH sensors depending on their surface oxide layer.¹²⁹ Here, GaN has a higher propensity for Cl at lower pH levels than AlGaN, but both behave similarly under high pH conditions. This was in response to work showing that AlGaN/GaN heterostructures show stronger dependence on negative ion concentration in solution than to pH fluctuations.¹³⁰ Both of these studies showed OH and Cl affinity of the surfaces and point to these simpler immobilizations as applicable ion sensors, but suggest another modification is needed for pH sensing applications.

Other recent efforts have shown that capping GaN based ion sensors in Ga_xO_y layers using peroxide instead of chemical etching also provides a similar effect to these two previous methods and highlighting the anion affinity for the FET surface.¹²⁰ Ion sensing without altering GaN surfaces has been shown as a potentiometric sensor for various potassium and sodium salts.¹³¹ This functioned by use of the Helmholtz layer properties of each test solution, which provided potential and impedance data relating to the GaN natural affinity for anions and the potential between the GaN electrode and a Pt electrode. While an early work in the field of GaN sensing applications this highlighted the importance of the dangling bonds along the GaN surface.¹³¹ The stability of GaN was useful for these initial ion tests as it was noted that GaN potentiometric sensors were reversible due to the lack of ion binding to the actual film surfaces. The inherent dipole effects present along the surface of the (0001) configuration of GaN are what allow this to happen. More recently, modification of the GaN and

AlGaN surfaces has led to detection schemes for heavy metal ions in water sources. An example can be seen in mercury detection due to the concern of its neurotoxic behavior. AlGaN/GaN heterostructures have been used as a fast detection method for mercury when coupled with an Au metallized gate and thioglycolic acid surface layer.¹³² Time dependent I_D measurements showed response times as short as 5 s for concentrations of 10^{-5} M Hg^{2+} . When using these FET devices in the field a quick response time combined with a simple solution exposure is advantageous to off-site bench top lab testing for similar confirmations of mercury contaminants. Using thioglycolic acid as a receptor additionally allowed for a very high selectivity for Hg over other control ions; a behavior that was reexamined in a follow up study for even lower concentrations of Hg^{2+} ions in solution.¹³³ Other examples of AlGaN/GaN heterostructure devices providing a malleable ion sensing platform can be seen in the detection of dissolved nitrate. AlGaN/GaN structures were coated in a 2-nitrophenyloctyl ether and high molecular weight polyvinyl chloride solution to generate a nitrate ionophore membrane.¹²⁷ This sensing mechanism relied on the concentration of nitrate adsorbed into the polymer adlayer which in turn affected surface charge and conductivity of the AlGaN/GaN device. Similar to the Hg^{2+} detection scheme the response time is rapid with AlGaN devices (in this case less than 60 s for each KNO_3 solution addition). Both of these schemes take advantage of the high transconductance of the AlGaN/GaN heterostructure near zero exterior potential. This allows for a very high degree of sensitivity when conducting ion sensing and is seen at levels of 10^{-8} M for the Hg^{2+} and $\sim 10^{-6}$ M for NO_3^- .^{133,127}

InN has its own set of ionic sensing schemes as both an additive layer and a base layer for which surface coatings can be applied. Metallization of AlGaN/GaN gate areas have already been shown using films such as Au, but InN has also been shown as a successful coating as well. InN as mentioned has a very high affinity for electrons and thus negative ions, which provides the motivation for the study. A thin layer of ~ 10 nm in this study was enough to accumulate enough Cl^- ions to

increase piezoelectric effects in the electron gas layer of the AlGaN/GaN heterostructure.¹³⁴ Previous experiments of similar nature showed AlGaN/GaN FETs response was ~20 s and was capable of detecting concentrations down to 100 nM. Further evidence was shown that cation interactions are negligible on AlGaN/GaN surfaces under such sensing schemes.¹³⁴ Ion sensing FETs have also been implemented using InN, and in particular a surface modified InN/AlN stack has been shown to provide a stable base for *in vivo* calcium ion detection. In this work a (3-aminopropyl)trimethoxysilane layer was covalently bound to InN surfaces and combined with a phospho-tyrosine end group to provide a phosphate end group for Ca²⁺ ions to bind.¹³⁵ Results indicated a stable current measurement for each increasing order of magnitude in Ca²⁺ ion concentration (from 10⁻⁶ M up to 10⁻¹ M) with variance of current at only 1.11%. These experiments yielded logarithmic relations to OH⁻ and Cl⁻ in various salt solutions similar to that seen on the bare GaN ion exposed study.^{75,131} There was a polarity and growth dependence on the InN sensors similar to the GaN in that InN films of (0001) orientation was needed. However the surface polarity of InN does not play a large role in anion accumulation due to all wurtzite orientations of InN having similar electron accumulation effects which is generally undesirable.¹³⁶ Finally, although AlGaN is typically paired with GaN for heterostructure conformations of III-nitrides InN has also been experimented with under similar circumstances. InN/GaN has been shown to be a stable platform for pH sensing especially once a surface In₂O₃ layer has been used to passivate the surface.¹³⁷ Under this study unpassivated pH sensors had an average sensitivity of 34.75 mV/pH. However, once passivated showed an increase in sensitivity to an average of 52.04 mV/pH. This use of surface oxide layers in FETs for pH sensing is similar to prior work using Ga_xO_y oxide compounds as ionophoric surface layers.¹²⁰ InN has also been paired with AlN to create a heterostructure base for a Pt electrode in gas sensing applications, and of particular interest for acetone sensing of patients with diabetes.^{138,139} Situations such as these are typically seen using a thin film of InN of approximately 5-10 nm to

negate any effects of bulk InN interfering with the characteristically high sheet densities ($\sim 1.57 \times 10^{13} \text{ cm}^{-2}$) that occur in the first 5 nm of InN films.¹⁴⁰

1.8. FET Behavior

Here FET stands for field effect transistor which denotes a type of electronic device where the conductivity of channel can be influenced or altered by local electric field changes.¹⁴¹ This presents a label free method of detection when using FETs as a basis for biological sensing, as a charge change from any source to the device surface can alter its conductivity.¹⁴²

In general these transistors operate by the flow of current from a source to a drain terminal by passing through a gate. Charge carriers in the source and drain are n-type and require a certain bias to be placed between the gate and the source for conduction to begin. Without this bias p-type charge carriers between these regions inhibit the flow of the electrons. The mode described here is indicative of doped silicon based FETs where the thin layer of mobile electrons is generated once the proper bias is applied. In the AlGa_N/Ga_N devices the flow of these electrons pass through a similar thin layer, more commonly referred to as the 2D electron gas described earlier, however this layer is present natively along the interface of the AlGa_N and Ga_N (see Figure 1.4). This layer is the result of polarization effects that are indicative of the wurtzite crystal structure of the two III-Nitrides and was discussed previously in section 1.1. As this layer is present as part of the AlGa_N/Ga_N structure this contributes to an ON state for the device when a gate voltage of 0V is applied.²¹ This behavior is indicative of depletion type transistors in contrast to the enhancement mode seen when the device is in an OFF state at 0V_G. Depletion mode transistors in general operate by an always existing conducting channel like that seen in AlGa_N/Ga_N, again referencing the schematic seen in Figure 1.4. Enhancement mode transistors instead require an induced channel to be created like through a

positive bias applied to a gate. Doing so allows for the minority charge carriers to flow over the p-carrier region.¹⁴³

In the studies presented ahead samples were all tested for threshold voltage values which were typically between -2 and -1.5 V which is characteristic of depletion mode transistors. Threshold voltage itself is an important concept when monitoring these transistors and represents the required bias for conduction to begin. As these are depletion mode devices all values were less than 0. In reality there is not a concrete value for threshold voltage as the current relation to the gate voltage is non-linear, however linear extrapolation of such values is commonly used and is widely accepted as an adequate approximation.¹⁴³ This relation is drawn between the surface potential, gate capacitance, and charge carrier density and is discussed at greater length in work from Dieter.¹⁴³ In addition to this value, the work presented here took measurements for the respective devices at each ones' peak transconductance value. This provides the V_G most sensitive to shifts in the drain current of the device, and allows for testing at the point where a future biological sensing FET may be most responsive to environmental stimuli.¹⁴⁴ It is expressed as a derivative of the ratio of drain current and gate voltage in an expanded formula seen below in Equation 1. Similarly the linear extrapolation formula for threshold voltage can be seen in Equation 2.

Equation 1. Equation for peak transconductance, relating drain current, gate voltage as a derivative of the drain voltage.

$$\frac{dI_D / dV_{GS}}{I_D} = \frac{(I_{Dn} - I_{Dn-1}) / (V_{GSn} - V_{GSn-1})}{0.5(I_{Dn} + I_{Dn-1})}$$

Equation 2. Threshold voltage equation for V_T approximatino through linear extrapolation.

$$V_T = V_{FB} + 2\phi_F + \frac{\sqrt{2qK_s\epsilon_oN_A(2\phi_F - V_{BS})}}{C_{ox}}$$

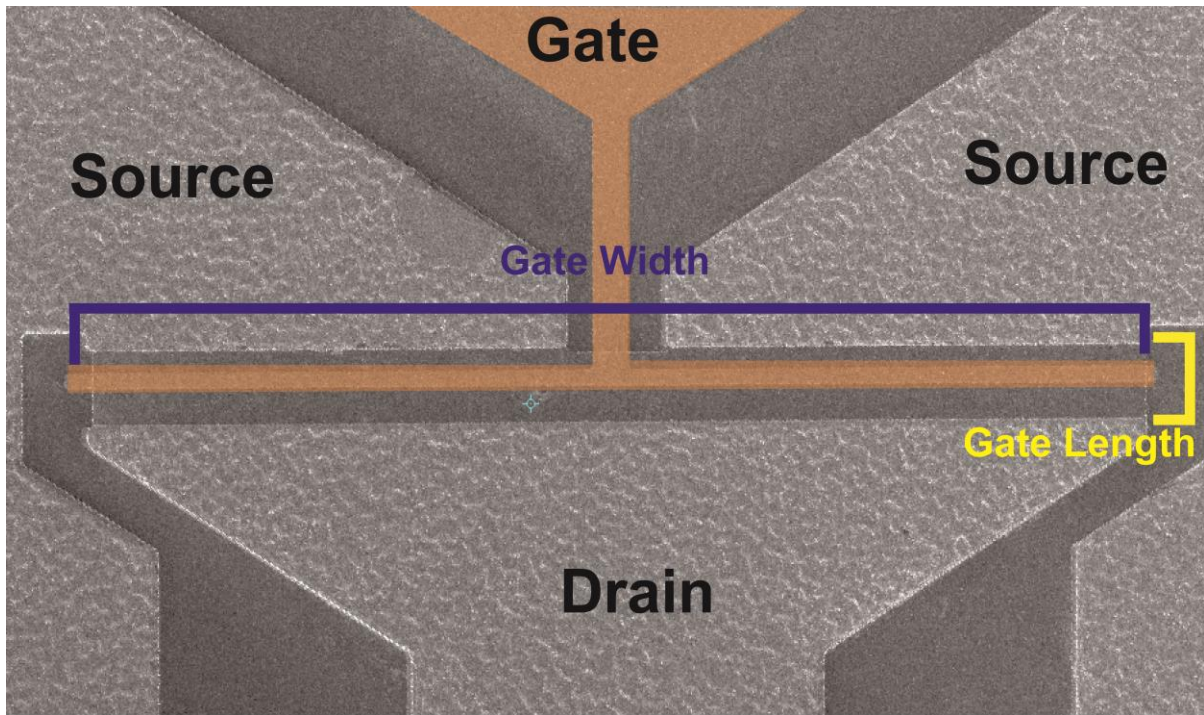


Figure 1.5 Top down view of an FET used in the studies described in this work. Shown are the source, drain and gate regions. Additional dimensions shown are the gate length and gate width. Gate length being held at a constant 15 μm across all samples, and gate width being either 50, 100, or 150 (shown above) μm .

1.9. Analytes/receptors

Biosensing devices depend upon an analyte and receptor pairing to provide a scheme for a specific sensing environmental. This pairing can be a simplistic surface response to an ion in solution, or more complicated and involve antibody binding or DNA sequences. Looking at the number of available and documented schemes, it is clear that GaN is the most common of the III-nitride as a platform for biosensor research. While we will discuss AlN, InN, and BN and their respective schemes current literature is more focused on GaN and thus will be the most represented here.

GaN has been established to have a surface that is both biocompatible and modifiable.³ Biomolecule schemes, like peptides, are a method of this modification that does well in bridging molecules and compounds in solution and the GaN or AlGaN surface. Peptides have two terminal ends and can thus be made to have one functional end adhere to GaN or a III-nitride surface and the other left free in solution. Examples of this can be seen the IKVAV peptide sequence which is derived from laminin and commonly used to support neurite growth.¹⁴⁵ IKVAV peptide was also studied and shown to improve cell adhesion and stability atop GaN surfaces.⁶

Other modes of analyte/receptor pairings have been done through functionalized nanoparticles laid atop AlGaN/GaN heterostructures. Research done here found that gold nanoparticles covered in different functional groups (thiol, carboxyl, amine, methyl) could generate changes in the electrical characteristics of the AlGaN/GaN devices.¹⁴⁶ This shows that gold nanoparticles can operate on similar principles and act as a medium between the AlGaN surface and alkanethiols on the particles. Additionally, the scheme shown here lends credence to idea that physisorption alone is capable of generating recognition properties to the biosensor surface.¹⁴⁶

InN has seen relatively little with regards to actual surface modification to create a biosensor, especially compared to GaN or AlGaN. However, research has shown InN is capable of similar

interactions with analytes or biomolecular compounds in solution. One example of this is a physisorbed peptide and phage system that examined 11 different peptides expressed by bacteriophages.¹⁴⁷ Here InN was chosen due to its high surface electron affinity as a possibility for a film that readily accepts peptides without extensive modification or chemical processes. The results of this showed one peptide sequence in particular (YPLLPESTPDAN) had remarkably high affinity for bacteriophages out of solution.¹⁴⁷

Table 1.1. Example analyte and receptor pairings shown for III-nitride compounds used in biological or non-biological sensing devices. Beneath the receptor information indicates the molecule or compound that acts as a receiving component of a sensing scheme, and the analyte represents the aqueous or environmental stimuli that interacts with the III-nitride surface groups.

Material	Type of receptor /Surface Treatment	Receptor	Analyte	Reference
GaN	Oxide adlayer	Ga _x O _y	pH	Chen ¹²⁰
	Bare Surface	Surface Ga atoms	Anionic solution activity (KOH)	Chaniotakis ¹³¹
AlN	Polyimide-Protein layer	DNA, antibody, phage selective proteins	Bacteriophage	Auner ¹²¹
	SAM, SAM/AuNP	GFP Antibodies	GFP	Chiu ¹⁰¹
InN	Bare Surface	n-polar InN	pH	Lu ⁷⁵
	Peptide	YPLLPESTPDAN	Bacteriophage	Estephan ¹⁴⁷
	Peptide	STLMTTTYHSVS	Bacteriophage	Estephan ¹⁴⁷
	Peptide	QGAHYEYSRTEL	Bacteriophage	Estephan ¹⁴⁷
	Peptide	IPGDAGKGLHMT	Bacteriophage	Estephan ¹⁴⁷
	Peptide	YDTTSSPPRLTR	Bacteriophage	Estephan ¹⁴⁷
	Peptide	GMKAAHERPLR	Bacteriophage	Estephan ¹⁴⁷
	Peptide	VLSNSLPTAIST	Bacteriophage	Estephan ¹⁴⁷

Table 1.1 Continued

AlGaIn/GaN	Peptide	GMATEATVHELTA	Bacteriophage	Estephan ¹⁴⁷
	Peptide	QNSHRVALENNT	Bacteriophage	Estephan ¹⁴⁷
	SAM	O-phospho-L-tyrosine	Dissolved calcium	Kao ¹³⁵
	Metal adlayer	Pt Catalyst	Hydrogen	Chang ¹³⁸
	Metal adlayer	Pt Catalyst	Exhaled Acetone	Kao ¹³⁹
	Bare Surface	Surface atoms	Ionic compounds	Podolska ¹³⁰
	Nanoparticle	Functional Group Terminated Au NPs	Src Kinase	Chu ¹⁴⁸
	Nanoparticle	Functionalized AuNP	DNA, proteins, metabolites	Makowski ¹⁴⁶
	ZnO nanorods	Glucose oxidase	Glucose	Pearson ¹⁰ , Review
	Biomolecule Coating	Immobilized ssDNA	Phosphorescent dye	Fahrenkopf ¹¹⁷
	Polymer Membrane	PVC with TDA Bromide and 2-nitrophenyloctyl ether	Nitrate Ions	Myers ¹²⁷
	Metal adlayer	InN Gate Coating	Chloride ions	Chu ¹³⁴
	SAM	Vitellogenin Antibody	Vitellogenin	Chu ¹⁰⁴
	SAM	Thioglycolic Acid	Dissolved mercury	Chen ¹³³
	SAM	Thioglycolic Acid	Dissolved mercury	Wang ¹³²
	SAM	Immobilized Penicillinase	Penicillin	Baur ¹⁰⁵
	SAM	Prostate Specific Antibody	Prostate Specific Antigen	Li ¹¹⁸
SAM	Anti-MIG IgG	Recombinant human MIG	Tulip ¹⁴²	
InN/GaN	Oxide adlayer	In ₂ O ₃ Passivation	pH	Lee ¹³⁷
BN	Functionalized Multiwalled BNNT	Biotin Fluorescent Ag NPs	pH	Huang ¹⁴⁹ , Golberg ¹⁵⁰

1.10. III-nitride FET biosensor stability

More recently work has been done to bring AlGaIn/GaN forward as a reliable and reproducible device that could be used for aqueous biosensing systems. Our lab has done work to determine the stability and reliability of various AlGaIn/GaN schemes within possible operational conditions. Preliminary studies done by Makowski et al. demonstrated the wide range of methods available to create a functional biosensing platform out of AlGaIn/GaN devices.^{6,112} Beyond this, multiple studies have explored the actual application of these devices with functionalized surfaces.^{144,104} However, as the technology matures research has begun to progress towards determining the viability of III-nitride sensors for sensing and less on proof of concept type scenarios. The various elements that make up biosensor stability are described and diagrammed in Figure .

GaN based surfaces offer a stable substrate when placed into aqueous environments, but the stability and reliability of a device becomes more complex as the GaN surface is tailored to specific scenarios. Questions arise as to the persistence of surface functionalization under constant use or the effectiveness of the biosensor over time once put into an operating environment. This determines whether or not the III-nitride devices would be better suited for longer term exposure to solution or if there is a currently a limitation to shorter time frames for effective detection. Storage of III-nitride devices is an example of a situation where a device may not be in operation but would be required to sit idle for an extended period of time. All of these points and concerns come back to the stability of the sensing interface that is created on the surface of the device itself.

There are numerous ways of generating a possible biosensor with a III-nitride device due to the flexibility of the surface to different modifications, see Table 1. Surface terminated ionic groups, peptide layers, and antibody systems are all possibilities. One could look at the degree of coverage as a first challenge in assessing the stability and long term utility of an FET biosensor. In a general sense, the higher the concentration of receptor material or sites present on a biosensor surface the

more sensitive and the better the response will be. This however is not always the case due to excessive functionalization on a surface. This can be thought of as an overcrowding of the surface with receptor sites such that it can become overly difficult for an analyte to bind to a surface.¹¹⁷ Receptor molecules may block one another from fully interacting with the relevant compound within the solution. This phenomenon is dependent on what is known as the Debye screening length (or Debye length) of a molecule. The Debye length represents a molecule or compound's effective distance within a solution to have an electrostatic interaction with another compound.¹⁵¹ One can think of this as the effective range around a receptor site that allows it to gather a response from the analyte in solution. When this range becomes overly crowded with receptors the bonding to the surface can become unstable and may become restricted entirely. This occurs when not enough electrostatic interactions occur with the surface to affect device conductance.¹⁵² Thus for any reliable sensing applications a series of assays would likely be required to find optimal surface densities and concentrations of receptor molecules for proper detection and sensing. An example of this can be seen in the work of Rebriev and Starodub who demonstrated several different criteria which can affect device response, one of which being concentration of the receptor enzyme in the FET coating.¹⁵³ Here a polymer mixture was dosed with urease for detection of urea within solution, and enzyme concentration was observed to best perform at a value of just 3% enzyme within the polymer adlayer.

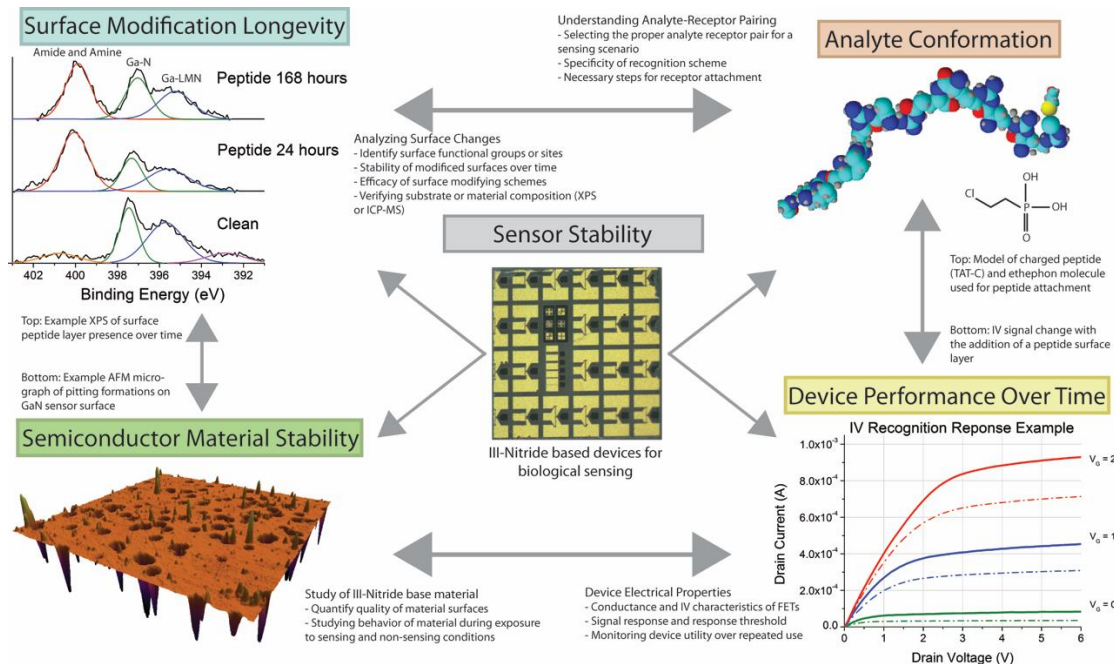


Figure 1.6. Testing methods and objectives of the different properties that make up the stability of a biological sensor.

Longevity of surface bound receptors for FETs is the next challenge that must be overcome for devices to offer stable performance over a wider range of times. It is likely devices will be placed into storage or may not see operation for some time after fabrication. These elements need to be accounted for when assessing the usable lifetime for any given FET sensor scheme or type. Much work has already been done on the subject and has shown stability of such III-nitride devices past a month of storage time.¹⁵³ In almost every case found there is a corresponding decrease in sensitivity after a given number of uses or in some cases without any operational use. Other instances documented in this study showed that storage of fabricated devices did not seem to affect the performance of the FETs.¹⁵³ In work done by this author's laboratory the strength of stability of surface bound peptide groups was examined in similar fashion. Initial work tested if a set complex chemical functionalization steps were truly necessary to create recognition on a surface and if a

recognition event could be achieved via an incubation of peptide to an AlGa_N/Ga_N FET surface.⁶⁰ For this case a solution of a recognition sequence (SVSVG_{MKPSRP}) was allowed to incubate and dry to the FET surface and then subsequently soaked for various amounts of time to determine the stability of this attachment. Results showed that drain current of the FETs increased an average of 96.43% across ~300 FETs tested. This demonstrated that incubation can successfully be used to produce recognition behavior, however longevity was a concern. Once placed in solution surface peptides appeared to dissociate back into solution within 24 hrs of soaking in water.⁶⁰ Thus revealing that the forces between incubated biomolecules and the surface are relatively weak, and some form of chemical functionalization would likely be required.

Silane chemistry and polymer adlayers have been used in other instances for longer term stability of surface receptor sites.¹⁴⁴ However, many of these use materials other than III-nitrides as a base for their sensing applications. As AlGa_N/Ga_N in particular has come out as a stronger candidate for biosensors, more work has been done on these silanization and polymer embedding methods.^{154,142,118} However, research has yet to meet the number of long term stability assessments on AlGa_N/Ga_N over other III-nitride biosensing platforms. In response, a second set of AlGa_N/Ga_N peptide binding studies done by our laboratory was performed to increase the attachment of incubated peptide to device surfaces. Additionally it provides a possible channel to further investigate the longer term stability of the AlGa_N/Ga_N devices which is currently under represented in literature.¹⁴⁴ Previous work done by our lab has shown a novel chemical functionalization technique to covalently bond functional groups to Ga_N based surfaces.^{155,107} Phosphonic acid and ethephon attachment to the AlGa_N/Ga_N device surfaces was used from these prior experiments in a one-step etch process following cleaning. This created a base to attach peptide (in this case TAT-C) and create covalently bound sites across the breadth of the FETs. Results showed a positive presence of surface bound peptide groups within solution up to 7 days of exposure.¹⁵⁶ Analysis of XPS data did not give

statistically significant evidence to a reduction in surface peptide levels over the duration of this test. Thus with regard to stability of a AlGa_N/Ga_N prepared biosensors it has been demonstrated that storage in solution appears to be viable up to a week. This helps in verifying AlGa_N/Ga_N as a platform for short term disposable type biological sensors.

There are further opportunities for research in the specificity of FET operation and response relative to other unwanted compounds or particulate present in solution. Most recognition schemes account for unwanted molecules in solution by design of the receptor choice. Antibody and enzyme immobilized on surfaces are by nature highly selective to their paired analyte, and a strong example of this can be seen in work by Ren et al.¹⁰⁴ This study and others commonly use serum or albumin based solutions to test for the reliability of FETs in detecting specific biomolecules when placed in a general biologically representative fluids. Few studies examine the effect of particulate on functionalized surfaces though. This may not be as strong a concern for sensors that will be resting in solution, but in the scenario that fluids are passing over there is the possibility of accumulation of unwanted particles on the surface. We examine this in a previous work where an excess of unmodified Ga_N powder was laid atop a recognition peptide functionalized AlGa_N/Ga_N FET to determine if additive layers of sediment or neutral compounds would prove detrimental to device operation.⁶⁰ Results of this demonstrated the robustness of the surface groups to unwanted large objects in solution. Surfaces in this study were not chemically modified and used incubated peptides, and despite this weak surface adherence, powders did not show any effect on device performance. These initial findings suggest that AlGa_N/Ga_N FETs and other III-nitride FETs in general will likely behave well within realistic biological settings where complex molecules and larger particles may build up or come in contact with the surfaces.

1.11. Unmet Needs

Growth techniques have advanced for more consistent films, functionalization techniques are better understood, their reactions within biological systems is being studied, and doping for improved properties is advancing as well. However, this research is largely centered on our basic understanding of the materials and their operation. Understanding these systems is crucial to moving forward to industrial applications, but many of these applications have yet to come to fruition. III-nitride applications in fields such as LEDs and optoelectronics are already in markets and being used in industrial processes. Sensing apparatuses, and especially biosensing applications, are where much of new research into III-nitrides is being focused. As we have covered over the course of this chapter biosensor applications have been shown repeatedly either through SAM modified devices, biological molecule modification, or surface termination. Many avenues exist for devices like FETs to become tailorable platforms for a wide range of end user applications. The remaining research to be done it seems lies within the stability of III-nitride biosensors over time and the reliability in their performance. Under laboratory conditions and short testing cycles these sensors behave well, but more intensive longer assessments need to be done. Questions of repeatability on the same sensor, loss of efficacy of surface bound sites, degrees of coverage and surface concentrations of receptor sites need to be investigated to optimize performance.

In these continued efforts to fully characterize AlGaIn/GaN devices for biosensing applications we have shown methods to covalently bond peptide groups to FET surfaces, and that this method provides a stable bond within solution for up to 7 days. Next steps are shifting focus on to the specificity and sensitivity over time using this same functionalization method. Inclusions of different peptides and biomolecules will be done to examine the specificity of peptides bound in this manner. Although likely more important is the in depth examination of device sensitivity and response over

time to actual analyte compounds. As mentioned previously device schemes involving non III-nitride materials have been widely characterized for this type of behavior and many systems have measured degradation rates from both long term storage and repeated sensing tests.¹⁴⁴ These values do not exist currently for AlGaIn/GaN for the wide range of biosensing schemes available to it. We are seeking to change this and better characterize AlGaIn/GaN solution response behavior. To do this extensive longer term stability study on the time scale of months is recommended to understand the storage capacity of these devices both in dry and wet conditions. Likewise repeated-use studies need to be done to determine the capabilities of the AlGaIn/GaN FETs to undergo multiple cycles of response. If these devices respond well to multiple sensing cycles then assessing their reliability would be the next step. The exploration of InGaIn heterojunctions and other III-nitride surfaces for biological sensing applications may be worthwhile, but currently the focus of the field is upon AlGaIn/GaN and it becoming industrially viable. Their malleability and stability in sensing environments can provide researchers with a robust platform from which to conduct medical assays, or quantification of environmental compounds. Some of the last remaining work to be done before it becomes commercially viable though is a better understanding of how the III-nitrides and in particular AlGaIn/GaN function over time under operable conditions. Stability and reliability of the signals from these devices are paramount in creating not just inexpensive disposable type in-field biosensors, but multi-use and longer term implants into biological systems.

This following thesis presents four sets of studies that investigated AlGaIn/GaN FETs based on the properties and knowledge covered in this chapter. Using this information a functionalization method using phosphonic acids coupled with incubation of biomolecules was tested on multiple different fronts and analyzed for device behavior and surface properties. Each chapter will contain respective experimental details and analysis of the data taken of the course of the work in the chapter.

In the conclusion of this thesis a summary of all important findings with further explanation and elaboration will be presented as well as recommendations for the future of the field with respect to the methodologies and devices used in these chapters.

AlGaIn/GaN Field Effect Transistors Functionalized with Recognition Peptides

Summary

Recognition peptides are used to modify AlGaIn/GaN Field Effect Transistors (FETs). The recognition sequence, SVSVGMMKPSRP, was compared to other biomolecules and subsequently the device stability was examined. Changes in the electrical characteristic were recorded using current-voltage measurements at a V_D of 1 V and V_G of -1 V. The recognition sequence coatings yielded an average increase in I_D of 96.43% compared to initial values. Exposure to solution removed the peptides from the devices indicating a weak interaction between adsorbate and the semiconductor surfaces. The peptide coatings are suitable for simple device modification for short-term recognition studies.

Gallium nitride has been shown to be a viable semiconductor material for transistor devices operating at high frequencies and high fields. Properties such as a wide bandgap and high electron mobility make this possible. These GaN based devices have been shown to operate as a customizable platform for biosensing applications.¹²⁴ This is in large part due to the high chemical stability and lack of degradation of the semiconductor material under physiological conditions.^{3,157} GaN based devices thus have the potential to provide a reliable, low cost and flexible solution for biosensing and bio-recognition platforms.^{158,159} Surface gallium bonds are available for covalent surface modification allowing for a high degree of selectivity that can be imparted onto the surface.^{160,112} GaN based biosensors provide additional electrical stability resulting in low electrical drift when exposed to ionic

solutions.¹²⁴ Broader applications in optoelectronics and catalytic processes^{161,162} have also been demonstrated where the photonic properties of GaN are used. Current methods for functionalizing these devices involve multiple steps to achieve covalent bonding of analytes to the surface,¹⁶³ physisorption of nanoparticles,¹⁶⁴ or the use of oxide layer to attach desired analyte to the biosensor. Many surface functionalization schemes use cleaning processes and solvents that can compromise the integrity of the device contacts. A simpler methodology that avoids harsh intermediary steps would thus be beneficial for GaN based biosensor devices. Such procedure should not jeopardize the device characteristics and should be based on aqueous solvents which preserve the activity of the biomolecules.

In this study, we examine the modification of GaN biosensor devices through the use of a one-step adsorption procedure that relies on peptides with recognition properties. AlGaIn/GaN field effect transistors (FETs) were selected as a sensing platform due to their stability under physiological environments as well as their proven utility for biomedical applications.^{128,165,144,166} Analyte binding along the top AlGaIn or GaN layer interacts with a two dimensional electron gas (2DEG) present at the interface between the AlGaIn and GaN layers.¹⁶⁴ This layer operates under the balance of piezoelectric and spontaneous polarization effects, and is highly susceptible to change in surface charge and binding of species with dipoles.¹⁶⁷ This interaction permits charged or bioactive molecules, such as the ones examined here, to generate a quantifiable effect on the conductance properties of the FET devices.¹⁶⁸ Affinity peptides are capable of recognizing specific materials or have a high specificity to certain surface types. Adsorbates utilized in this study are listed in Table 2.1. The first adsorbate used is designated as a Recognition Peptide (RP) with the sequence

SVSVGMPKSPRP. This sequence has been explored in other studies and has shown very good specificity^{169,170} for AlGaIn/GaN. The reverse of this peptide chain was also tested (RRP) along with a commercially available nonsensical peptide sequence (AP). Poly-l-lysine was selected as a commonly used charged bioactive molecule. Sequences such as these have been shown to have both high affinity to semiconductor surfaces along with controllable binding specificity.^{171,172}

Table 2.1. List of adsorbates utilized in this study.

Sequence	Name and abbreviation
SVSVGMPKSPRP	Recognition Peptide (RP)
PRPSPKMGVSVS	Reverse Recognition Peptide (RRP)
AQNDCEQGNILP	Arbitrary Peptide (AP)
[C ₆ H ₁₂ N ₂ O] _n	Poly-l-lysine (30,000 MW)

The III-nitride films were grown as previously described¹⁷³ using an MOCVD system. Devices were patterned with Ti/Al/Ni/Au source/drain contacts along with Ni/Au gate contacts via liftoff process.¹⁶⁴ An FET layout and schematic can be seen in Figure 2.1a,c. AlGaIn/GaN device operation is well understood, but degradation mechanisms are still not well defined particularly under solution conditions.¹⁷⁴ To ensure the device quality during production, transmission line measurements (TLM) were performed to monitor Schottky barrier and contact resistance of the metal-semiconductor interface. Wafers were then diced using a 300 μm blade into 3 mm x 3 mm chips. These diced sections contained 13

fully intact FET sites, Figure 2.1b. This configuration yielded at least 9 functional FETs present on each chip. Following cleaning, 15 μL of either 1 mM or 0.1 mM solution was placed on to chip surfaces containing one of the adsorbates listed in Table 2.1. Poly-l-lysine was used from solutions of 0.1 w/v% and 0.01 w/v%. Two different concentrations of peptide were used in order to assess if the response of the devices was dependent upon the coverage of molecules on the surface. Adsorbates were allowed to dry to the FET surfaces in the refrigerator at 4 $^{\circ}\text{C}$ for 48 hours. Chips were then allowed to equilibrate in ambient conditions in deionized water, phosphate buffered saline (PBS),¹⁷⁵ and air for two days. An unmodified control set (devices not functionalized with any analytes) was kept under the same soaking conditions and times as the four modified groups.

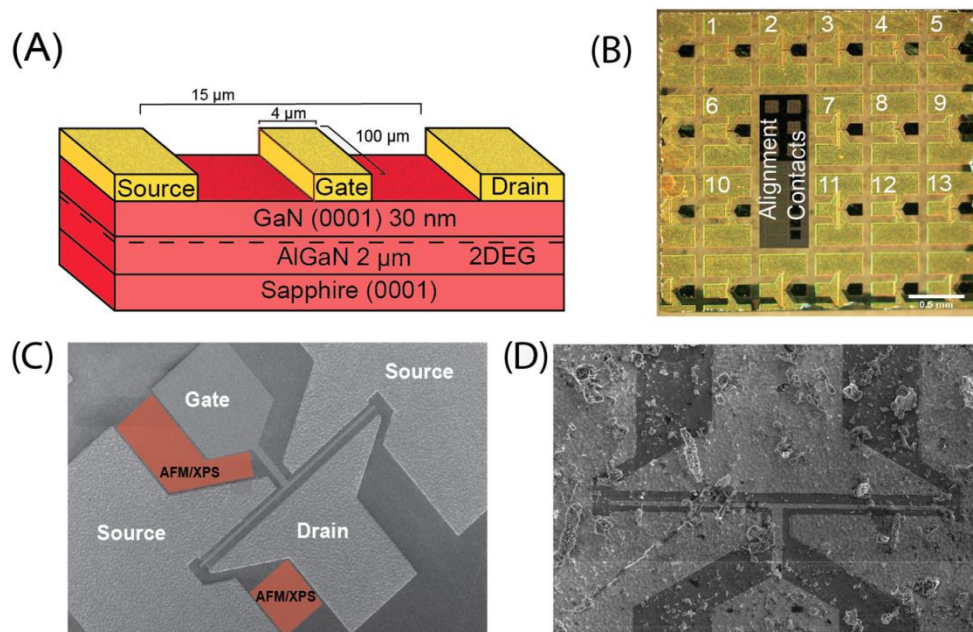


Figure 2.1. (A) Device schematic and dimensions. (B) Optical image of the diced chip layout shown an example of the 13 FET sites probed for the current measurements. (C) SEM micrograph of a clean FET used for this study; highlighted regions indicate areas where XPS and AFM analysis was performed. (D) SEM micrograph of an FET device after exposure to GaN powder.

The stability of the clean devices in solution was tested after 90 days of soaking in water. These diced chips, having undergone the same processing for surface cleaning, were soaked to examine any latent effects of long-term exposure to aqueous environments on the AlGaIn/GaN FETs. Aqueous stability and delamination effects are a possible concern for continuous monitoring systems under physiological conditions.¹⁷⁶ The initial control samples measurements averaged I_D values of 0.217 ± 0.209 mA compared to I_D values of 0.222 ± 0.216 mA for the 90- day exposure. Current voltage parameters were kept at V_D of 1 V and V_G of -1 V.¹⁶⁴ No statistically significant difference following exposure, and no difference was seen in population variance of either data set following analysis of variance (ANOVA) and Levene variance tests. This suggests that the AlGaIn/GaN devices are indeed stable following long storage periods of submersion in aqueous solutions.

Atomic force microscopy was done following surface modification with biomolecules to examine device morphology and confirm presence of adsorbates on the surface. Regions of interest for FETs can be seen in Figure 2.1c. Pristine GaN surfaces were found to have an RMS roughness of 0.8 ± 0.2 nm compared to Poly-l-lysine with an RMS roughness of 2.4 ± 0.5 nm. Both the pristine surface and Poly-l-lysine film demonstrated relatively uniform roughness across the surface. However, all peptides showed varying roughness values from the perimeter of the diced chip towards the chip center. As expected droplet evaporation proceeded more quickly along the edges causing an uneven film of peptide. The bulk chip center showed a peptide film with RMS 1.7 ± 0.1 nm. Perimeter sections of the chips showed RMS values 7.0 ± 1.6 nm indicating uneven drying versus the center where evaporation

proceeded slowly. The bigger change in roughness with the peptides is expected since they are known to cluster on surfaces.

Test groups were defined as 30-diced chips per chosen adsorbate. Individual diced chips had a minimum of 9 functioning FET locations so that each test group utilized approximately 270 individual FETs. Diced chip layout can be seen in Figure 2.1b. Combining all test groups this yields approximately 1350 FETs examined at each stage in the surface modification portion of this study. Statistical measurements done in this study were carried out using SAS v9.3, Origin v8.5, and MATLAB 2013.

Current-voltage (IV) measurements taken at each step and used to assess changes in the drain current (I_D). IV data was taken at a V_{Drain} of 1V and a V_{Gate} of -1V and contact locations can be seen in 2.1c. These values were determined by taking a representative set of V_{GS} plots. X-ray photoelectron spectroscopy (XPS) was also performed on treated FETs to confirm presence of a biomolecule adlayer. Results of XPS analysis can be seen in 2.2a and clearly show characteristic Ga-N peaks following deconvolution. Presence of both Ga-N bonding peaks and Ga auger was noted on the clean devices. An extremely pronounced amine group peak was observed on RP modified devices. This combination of both XPS and IV data confirmed a coating on the devices following solution treatments with RP.

Modification of the FET sample groups yielded an appreciable difference in only those coated in the RP solutions. All data taken was examined as a percent change from the initial measurement taken for each specific FET. No significant dispersion was found within the control group (devices not modified, but soaked in solution) from population variance. No significant difference was found amongst any of the individual test group populations

following Levene tests for homogeneity of variance. Thus, Figure 2.2b summarizes an average of 96.43% increase in I_D observed in RP modified devices. All other adsorbates tested (PL, AP, RRP) did not show any statistically significant changes in device characteristics compared to their initial values. We also recorded no significant change in the device characteristics following soaking in solution for 24 hours of devices modified with any of the adsorbates, Figure 2.2c. Additionally, the concentrations of the adsorbates yielded no significant difference in conduction characteristics. The significance of these values was compared using ANOVA with added Tukey tests against an α value of 0.05.

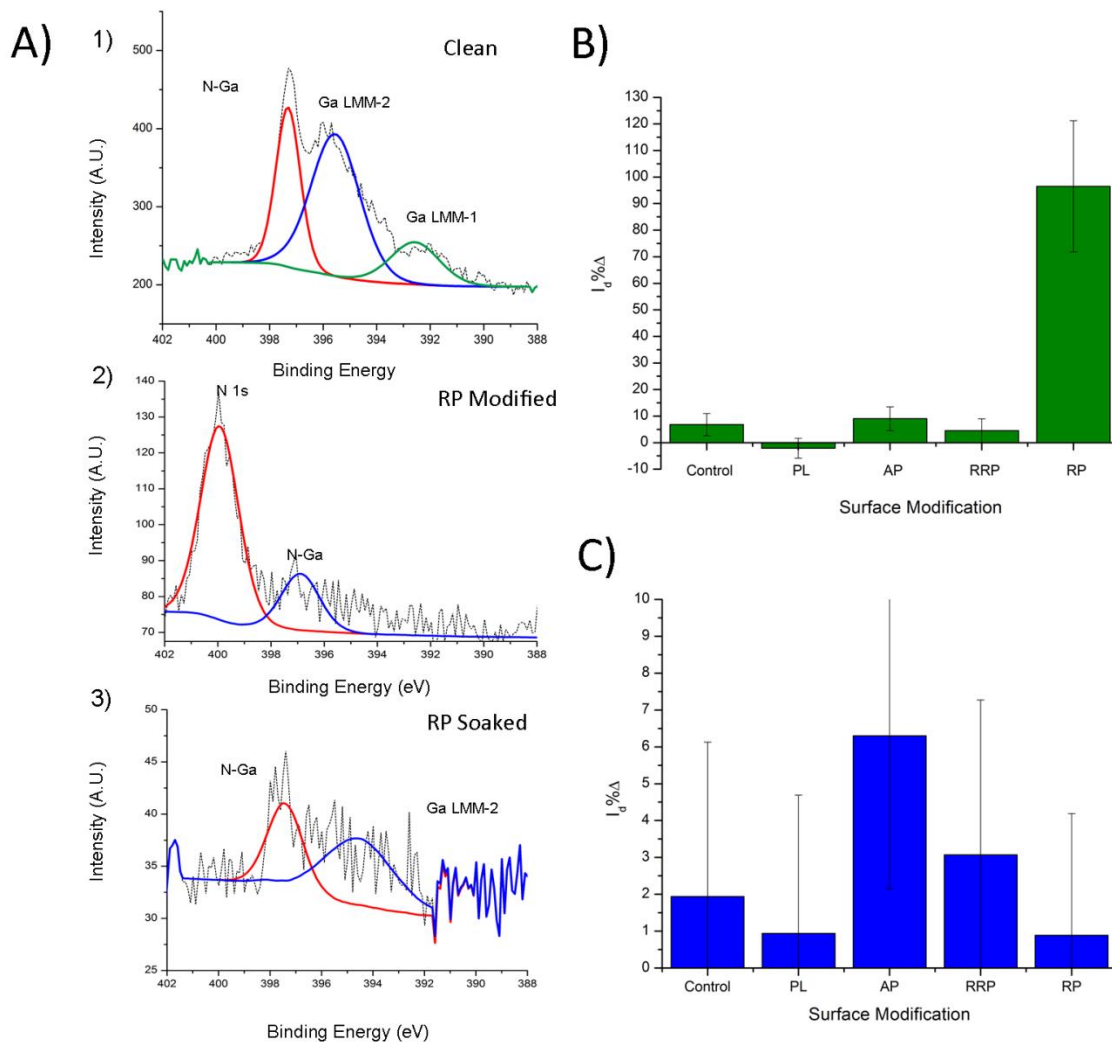


Figure 2.2. (a) X-ray photoelectron spectroscopy analysis of clean devices, RP modified and RP modified devices after soaking in solution. (b) Drain current changes of devices modified with all adsorbates. (c) Drain current changes of devices modified with all adsorbates after soaking in solution.

Data is reported only to the 24 hour soak mark due to the removal of the coated biomolecules. As shown Figure 2.2c the RP signal is reduced to levels that indicate a removal of the amine groups from the surface. Again no significant difference or variance was found within the populations of the individual control groups when comparing groups of

devices that were functionalized and soaked for 24 hours in solution. This observation was confirmed after XPS analysis of the RP group soaking stages. Peaks of interest included N-Ga (397.00 eV), Ga auger peaks (395.33 and 392.39 eV), and a characteristic amine group peak N 1s (399.51 eV).¹⁶⁰ Results were taken as qualitative data and sought as a check for the continued presence of the biomolecule. It is worth noting that XPS data was taken under various apertures to attempt to focus on purely the gate contact area of interest. This effect can be seen in the lower intensity ranges for the descending plots in Figure 2.2**Error!**

Reference source not found.a. Examination of Figure 2.2a clearly shows a strong N 1s peak after incubation in the RP solution, a similar phenomenon was observed in which the N 1s peak occluded the adjacent characteristic GaN peaks.¹⁷⁷ This peak is no longer present following soaking showing that the peptide adlayer desorbed from the surface after 24 hours of soaking in solution. Additionally a signal loss was observed on devices left under air exposure, suggesting the RP layer degrades under ambient conditions.

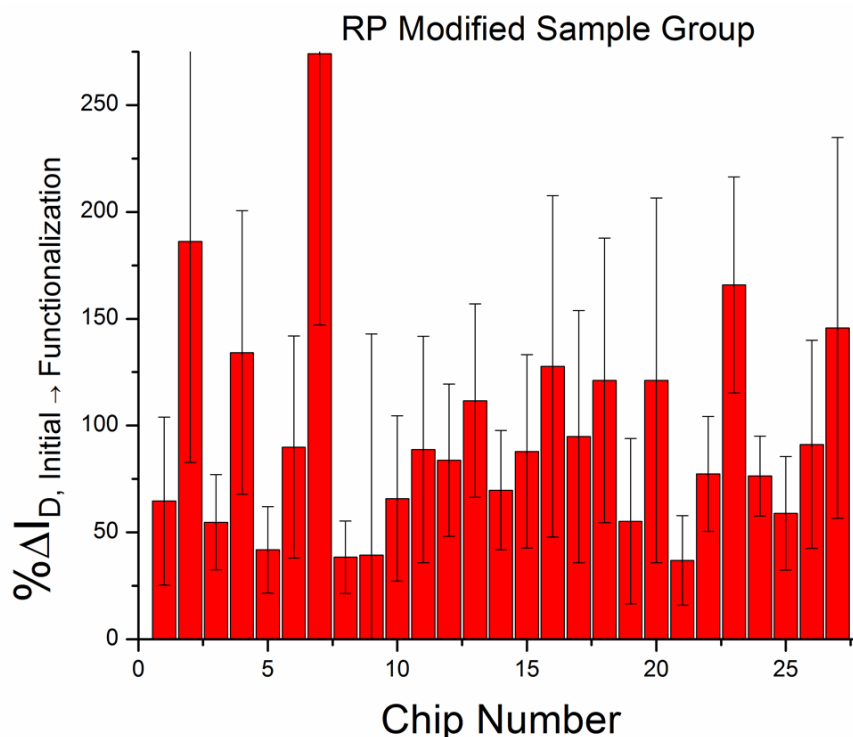


Figure 2.3. Full sample set of percent changes observed for the RP modified FET groups. Three samples were removed for XPS analysis.

Within the RP sample set the average $\% \Delta I_D$ value was 96.43% with a standard deviation of 51.79%. A distribution of functionalization values can be seen in Figure 2.3. The higher standard deviation is attributed to the inclusion of the more anomalous samples in Figure 2.3, including samples 2, 7, and 9. There was additional variability from the wafer itself from both the processing and device position on the wafer as well as different gate widths (50um and 100um). All sample groups demonstrated a positive response to the addition of the RP so further study of these conditions was not necessary for this study. Modified FET groups were incubated with solutions with two different concentrations: 1 mM and 0.1 mM. Statistical analysis showed that the change in the concentration of the adsorbate did not make a difference in the final outcome. A similar observation was made for the three

testing stability conditions: soaking in deionized water, soaking in PBS buffer, and exposure to air. In summary, the large number of devices examined clearly showed that all biomolecules detach from the surface following a 24 hours exposure to water based solutions.

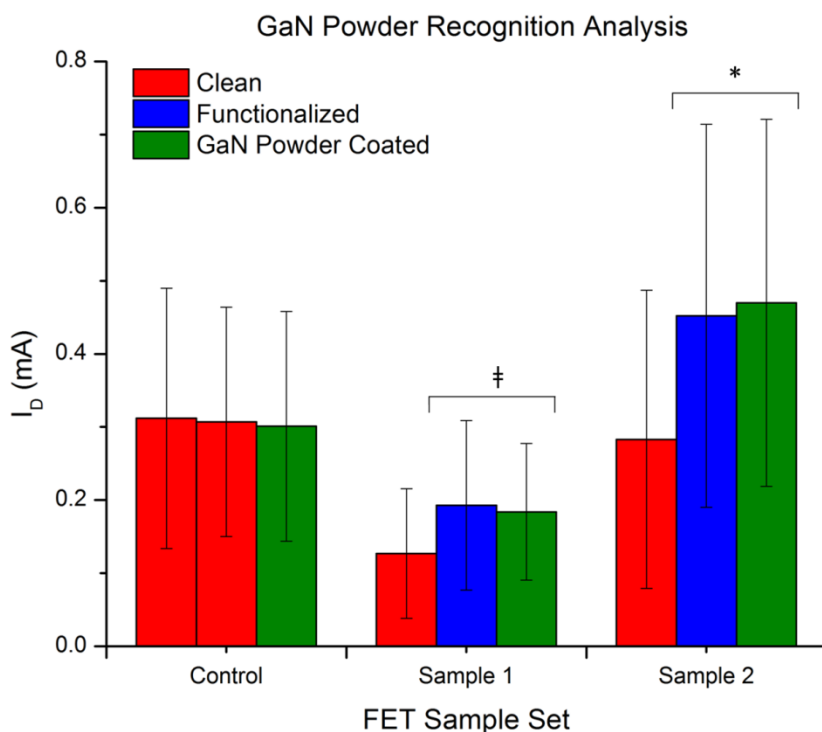


Figure 2.4. Change in drain current of devices modified with RP and exposed to GaN powder slurry.

Additional testing was done to assess the functional behavior of the peptide on the devices using GaN powder, Figure 4. We wanted to assess if the recognition peptide will promote the attachment of larger size matter composed of a material with an affinity for the peptide present on the surface. A slurry consisting of 2 mg GaN powder and 1 mL of DI water was deposited in droplets of 5 μ L onto each diced chip already modified with RP solution. The SEM image on Figure 2.1d clearly shows the powder coating on the device. Three device sets were evaluated using current voltage measurements seen in Figure 2.3.

Results confirmed that the RP, as a charged biomolecule, had a significant effect on the FET conductance. Subsequent measurements of the same devices after powder attachment to the surface showed no significant change compared to either the clean or functionalized surface. This indicates that the AlGa_N/Ga_N biosensors maintain recognition when using charged biomolecules, but shows no response to uncharged particulates. Thus, the Ga_N powder experiments confirm that these FET devices have a preferential response to surface charge changes. This result indicates that such devices can operate in complex solutions containing various analytes including large particulate matter.

In conclusion, four different adsorbates were incubated and dried onto AlGa_N/Ga_N FET surfaces to determine the feasibility of using adsorption of affinity peptides to functionalize biosensors. AlGa_N/Ga_N interfacial effects from the FET structure make it susceptible to alterations in surface charge effects. The study confirmed that a recognition peptide sequence can attach to the active region of the semiconductor device. Current-voltage measurements and XPS analysis demonstrated the presence of the peptide on the device surface and were able to track the stability of the modification through time. The peptide showed enough affinity to initially attach to the surface but the strength of the interaction was weak and therefore exposure to solution resulted in removal of molecules off of the devices. This weak interaction of the recognition peptide to the semiconductor suggests these devices would be suitable for only short-term detection strategies. The easy modification procedure makes it ideal for disposable or single usage devices. The results demonstrate the need for further research into methods to produce more stable attachment of biomolecules to devices using aqueous procedures.

Longer term stability assessment of AlGaN/GaN field effect transistors modified with peptides; a comparison of device characteristics versus surface properties

Summary

AlGaN/GaN Field Effect Transistors (FETs) are promising biosensing devices. Functionalization of these devices is explored in this study using an *in situ* approach with phosphoric acid etchant and a phosphonic acid derivative. Devices are terminated on peptides and soaked in water for up to 168 hrs to examine FETs for both device responses and surface chemistry changes. Measurements demonstrated threshold voltage shifting after the functionalization and soaking processes, but demonstrated stable FET behavior throughout. X-ray photoelectron spectroscopy and atomic force microscopy confirmed peptides attachment to device surfaces before and after water soaking. Results of this work point to the stability of peptide coated functionalized AlGaN/GaN devices in solution and support further research of these devices as disposable, long term, *in situ* biosensors.

Biosensing electronics have made great advances in recent years in both the variety of available materials and the breadth of possible applications.^{178,167} However, there are still challenges facing nanoelectronic devices in terms of long term stability in physiological operating conditions.^{176,162} Research needs to be done to relate both device performance and surface composition of biointerfaces especially for long-term detection or cumulative analyte exposure. Gallium nitride (GaN) is a suitable material for biosensing due to its semiconducting properties, biocompatibility, and adaptability of surface binding sites to a

variety of *in situ* functionalization schemes.^{7,158} Here, an AlGaN/GaN field effect transistor (FET) is used as a biosensor with promising potential for long-term stability. AlGaN/GaN devices are highly sensitive to alterations in surface charge or surface charging effects and have been shown to be biocompatible.^{106,179} In these devices a 2D electron gas layer forms at the AlGaN and GaN interface and is responsible for the high sensitivity due to changes in the surface charges.¹⁸⁰ Here, we are seeking to correlate the device behavior with variations in surface chemistry of the functionalized FETs. We examine the stability of AlGaN/GaN FETs after peptide attachment and exposure to aqueous solutions for a period of 7 days. Previous work has shown AlGaN/GaN field effect transistors as a useful platform for biosensing applications.¹⁸¹ Simple adsorption of recognition peptides directly onto AlGaN/GaN devices successfully functionalized them. However, the incubation step did not provide recognition and stability past 24 hrs of water exposure due to a loss of surface peptide. This indicated a need for stronger bonding of the peptide to the device surface. Recently published work from our group has reported the use of 2-chloroethylphosphonic acid (common name: ethephon) and phosphoric acid for modification of GaN surfaces.⁶¹ This technique was added to fit the goal of maintaining an environmentally friendly scheme that would functionalize device surfaces. Results showed initial success in anchoring peptide to the AlGaN/GaN surfaces.¹⁴¹

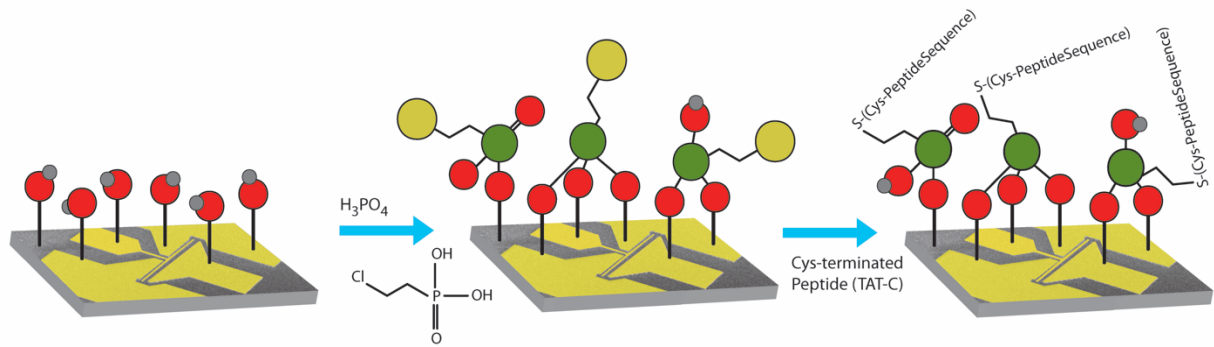


Figure 3.1. Functionalization scheme of AlGaN/GaN FET surfaces through an in-situ functionalization with phosphoric acid and ethephon followed by incubation in a cysteine terminated peptide.

AlGaN/GaN devices were fabricated by using a combination of MOCVD growth, electron beam evaporation, and photolithography as previously described in prior work where we reported the cross-sectional details of the device.^{182, 183} Transmission line measurements were done on various devices from the wafer for a quality check of operable device behavior.¹⁴³ Wafers were diced into 3 mm x 3 mm sections each containing an average of 11 operational FETs. Approximately 450 open channel devices were tested to derive statistically significant conclusions. Diced wafer sections were put through a two-step acetone and methanol sonication. Diced sections were then rinsed in DI water and nitrogen before immediately being moved to a 10 minute HCl etch to remove any remaining surface contaminants. A final DI rinse and nitrogen drying followed. Device surface functionalization was done using a solution of 1:1 (v:v) phosphoric acid and 3 mM ethephon. Samples were modified for 1 hour at 40 degrees Celsius. The ethephon functionalization step attaches the molecule to the –OH sites present on the GaN surface and leaves chlorine groups on the surface as seen in Figure 1. The peptide sequence chosen for the functionalized

devices was CGRKKRRQRRR (more commonly referred to as TAT-C) purchased from Anaspec Inc. The peptide possesses a cysteine residue at the N-terminus of the peptide chain. The end cysteine contains a sulfur group that allows for thioether bonding to take place between the surface bound ethephon and the TAT-C peptide. Ethephon functionalized samples were wetted with 5 μL of 0.01 mM TAT-C and allowed to incubate at 4 degrees Celsius for 48 hours until surfaces were completely dry. Incubated samples were then divided into groups of 5 (approximately 50 FETs per sample group) and each put into wells with 200 μL of DI water to soak. Soaking was done at 24, 48, 72, 96, 120, and 168 (7 days) hour intervals. One group of devices was excluded from soaking for control purposes along with a pristine group, etched group, and a peptide-incubated group all done without the ethephon functionalization. Devices were analyzed for proper FET behavior and for peptide presence over the various tested times using current-voltage measurements, high-resolution X-ray photoelectron spectroscopy (XPS), and atomic force microscopy (AFM). Current-Voltage characteristics were measured using a Keithley 4200-SCS and statistical analysis was done using Origin 8.5. V_{GS} sweeps were from -6 to 0 V at 0.05 step increments with a compliance of 100 mA. All XPS measurements were taken using a Kratos Analytical Axis Ultra X-Ray Photoelectron Spectrometer with a monochromated aluminum source. Analysis was done using CasaXPS software v2.3.16.

Further surface analysis was conducted on the different sample sets via *in-situ* AFM done in DI water solution at ambient conditions. Topographical data was gathered to visualize the peptide attachment on the AlGaIn/GaN FET surface as well as any effects brought on by the long term water exposure and the etch process. Representative scans of

some test groups can be seen in Figure 2. These highlight the effects of both the peptide incubation and the long term soaking on device topography. Pristine etched surfaces showed few signs of particulates and minimal pitting defects over each scan area, those that were found had feature sizes of less than 0.2 μm . Upon addition of the TAT-C peptide, a noticeable presence of clusters can be seen on the surface. Figure 2 c shows the surface topography after soaking in a poly lysine solution to illustrate the expected morphology of a thick biofilm under similar AFM imaging conditions. Following the first soaking session of 24 hrs there appears to be a decrease in the amount of surface clusters of TAT-C peptide. Defects also increased in size as soaking time increased. Surface clusters detected by AFM are consistent with XPS data (see below) showing presence of peptide on the device surfaces even at the longest soaking times.

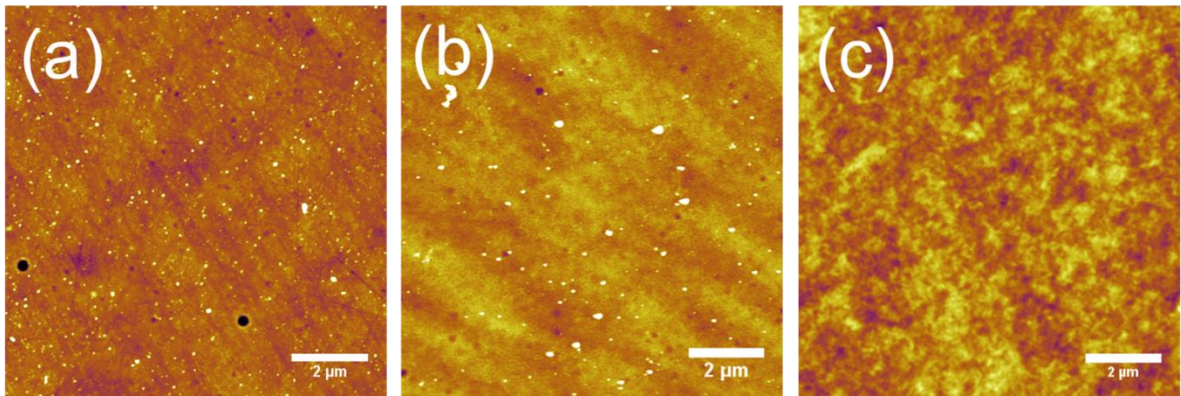


Figure 3.2. Representative AFM images of peptide surfaces at different stages in the solution exposure process. a) peptide terminated device surface prior to soaking in water; peptide agglomerates can be seen as white spots along surface; RMS Roughness of 1.41 ± 0.3 nm, and a maximum surface feature height of 39.3 nm. b) Device surface after 24 hrs of water soaking; fewer particulates and an increase in small defects count are observed; RMS Roughness of 1.89 ± 0.4 nm, and a maximum surface height of 71.2 nm. c) Poly lysine device surfaces demonstrating an

excessively thick and relatively smooth biofilm; RMS Roughness of 3.2 ± 0.4 nm, and a maximum surface feature height of 16.9 nm.

Figure 3 summarizes the mean I_D - V_{GS} current-voltage characteristic curves after each different surface preparation and soaking time. The shaded region corresponds to +/- one standard deviation. The drain current was normalized to the maximum current reached. The I_D - V_{GS} characteristics do not show any significant difference for the soaking times above 72 hrs. Device stability was measured through I_D - V_{GS} current-voltage measurements. FET stability was measured before and after functionalization, and once device groups had soaked for predetermined amounts of time to keep track of any deviations from characteristic FET activity. Figure 3a and Figure 3b shows the IV characteristics of the six groups of soaked devices and four control groups. Previous work has shown that this peptide can be successfully attached to devices.¹⁴¹ The I_D - V_{GS} curves shifted following surface etching due to cleaning and as well as after the subsequent ethephon surface modification. In Figure 3b there is a return to higher threshold voltages as soaking time increases. Shorter soaks of 24 hrs showed peak values in the same range of etched samples (between -3.0 and -3.5 V). This shifted to lower values and finally stabilizing between -1.2 and -1.9 V for soaks longer than 48 hrs. From ANOVA statistical analysis with added Levene tests, ethephon functionalization showed no significant difference in device behavior from the etch and to the variance of the two populations of devices (p values of 0.685 and 0.964 respectively at an α value of 0.05). The shifting of the curves can be attributed to alterations in charged species along the device surfaces. Etching leads to a large number of negatively charged -OH groups along the AlGaIn/GaN surface which are subsequently capped by peptide molecules or

neutralized in solution over time as seen by a shift in threshold voltages in V_g data. The stability of the surface over time in solution is seen as no significant changes in device threshold voltages are found between the 72 hr soaks and 168 hr soaks. ANOVA and Levene testing as seen above showed p values of 0.662 and 0.550 indicating both population means and variances are not significantly different at α of 0.05. A multilayer of charged biomolecules was created on a set of devices through the use of physisorbed poly lysine. The group of devices modified with poly lysine had the largest shift from the control and is expected due to the relatively thick layer of positively charged poly lysine deposited onto the gate region. One would expect that the functionalization process with ethephon would affect the sensitivity of the devices. The degree of change is expected to be dependent on the nature of the surface coverage. We plan to study this effect in future work.

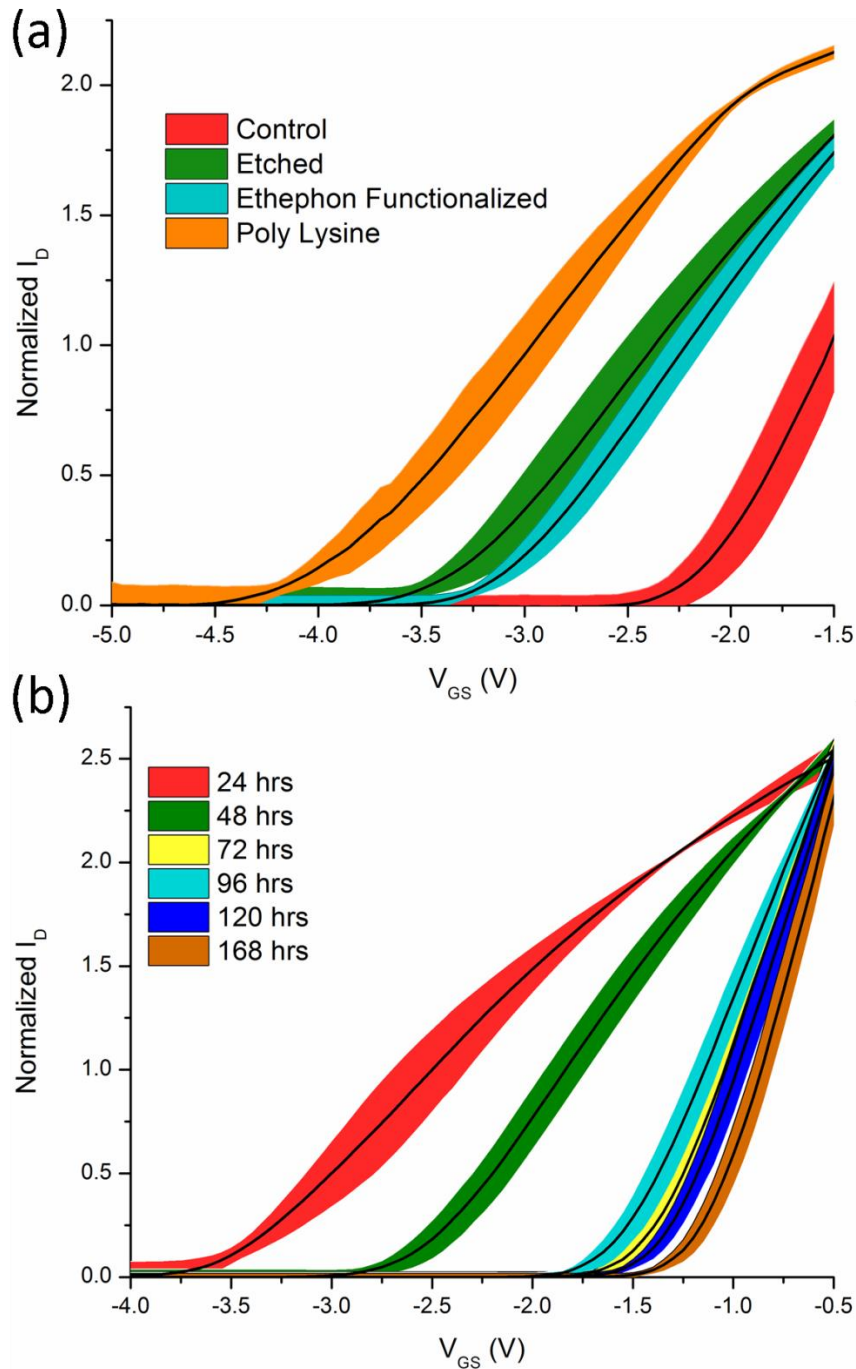


Figure 3.3. a) Gate voltage sweep data for control groups including the etched, pristine, ethephon functionalized and poly lysine sample sets. b) Gate voltage sweep data for soaking stages starting at 24 hrs and going up to 168 hrs. Lines on both parts of the figure represent average value over an entire sample group, and shaded regions represent ± 1 standard deviation.

XPS confirmed the continued presence of peptides on the device surfaces. Three scans were taken per sample with two diced sections being tested from each sample group. Calibration of resulting scans was done using the C 1s peak at 284.8 eV.⁶¹ Regional scans were done for N 1s, C 1s, S 2p, Ga 2p and 3d, and P 2p with N 1s being the primary focus and the data presented here, Figure 4. Representative scans can be seen for a clean (control) device as well as all peptide soaks from 0 hrs (unsoaked) to the maximum of 168 hrs. Other scans served as secondary checks for peptide presence and to monitor the scan area. The strongest indicator for TAT-C on device surfaces was found based on the presence of amines and amide species centered at 399.9 eV in the N 1s spectra. A nitrate presence was also found on freshly functionalized devices and is attributed to oxidation of the excess peptide on the surface. Additional peaks in that regional scan are attributed to N-Ga at 397.3 eV, and Ga LMM peaks at 395.3 eV, 392.4 eV, and 400.8 eV and present in all samples.¹⁶⁰ Results showed no presence of peptide in control groups and clear quantifiable amounts of nitrogen species after peptide modification. Evidence for excess multilayers of peptide can be derived from the dominant N 1s peak that completely occludes the entire N-Ga peak species on modified, unsoaked samples. After the shortest soaking time of 24 hrs a removal of excess peptide is observed. A prominent N 1s amide peak can then be seen for every representative scan up to the 168 hr maximum. Recovery of the N-Ga and Ga LMM peaks can also be seen once the soaking process begins. In addition to the qualitative evidence of peptide presence on the surface, additional information can be gathered from peak area ratios by analyzing the data for soaking times between 24 and 168 hrs. Doing this provides insight into a possible loss of surface bound peptides over time due to soaking in solution. Tabulated data for the

mean and deviation of these ratios can be seen in Table 1. No statistically significant evidence for mean peak area ratios shifting was shown via ANOVA and Tukey population variance tests (p value of 0.1985 at an α of 0.05). This data supports the notion that a negligible amount of peptide is disassociating into solution following the initial solution exposure. XPS peak data provides strong evidence that the functionalization step here was successful in binding the TAT-C onto the AlGaIn/GaN FET surfaces and it demonstrates promising stability up to 168 hrs in water solutions.

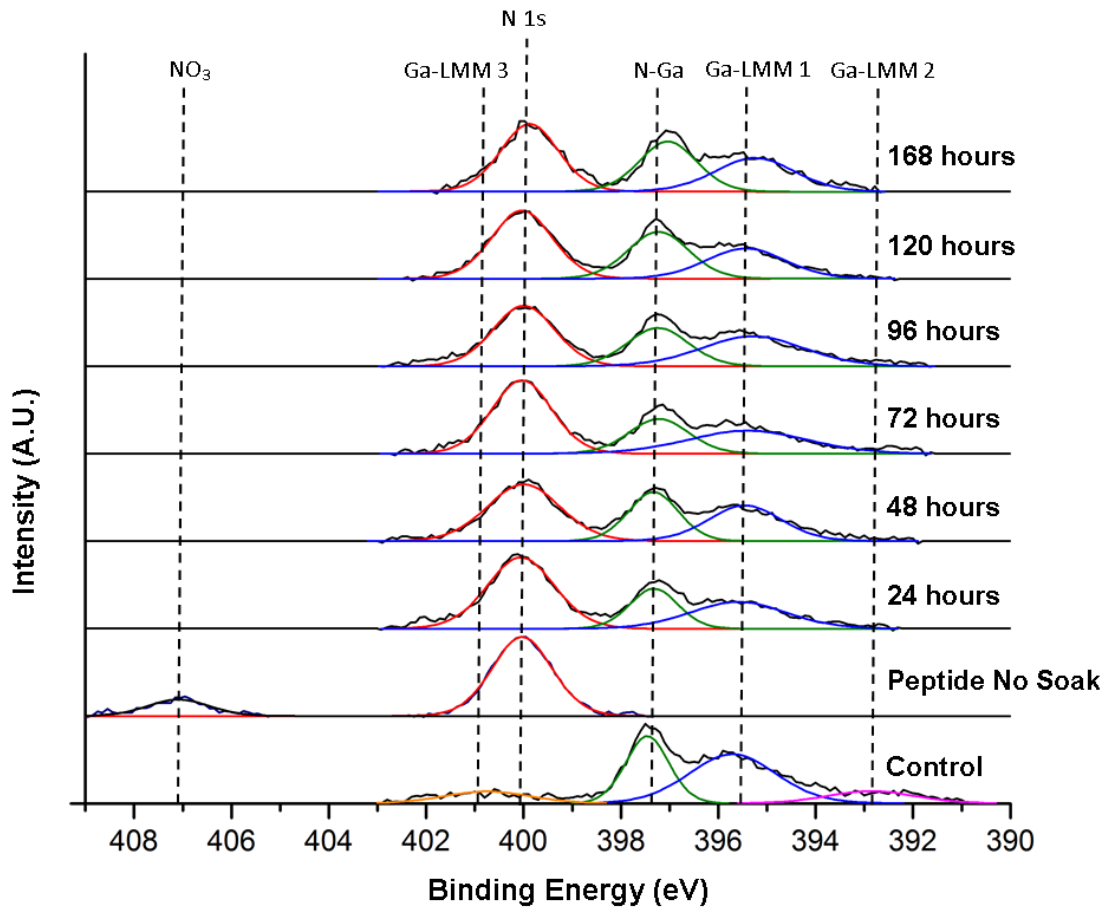


Figure 3.4. Representative high resolution N 1s XPS scans of device surfaces from each soaking group. Data for a peptide terminated device prior to soaking as well as a clean (control) device is also shown.

Table 3.1. Mean peak area ratios for N 1s and N-Ga peaks.

Soaking Time	N 1s : N-Ga	Std. Dev
24 hours	2.25	0.19
48 hours	1.93	0.22
72 hours	2.04	0.13
96 hours	1.98	0.25
120 hours	2.09	0.16
168 hours	1.81	0.14

In summary, following the analysis of the AlGaIn/GaN FETs under soaking conditions, there is evidence that suggests the usefulness of the presented surface functionalization method as a means of covalently bonding peptides to these devices. This covalent attachment was successfully done using a straightforward and environmentally friendly water based solution processing. Electrical measurements demonstrated defined threshold voltages and pinch off points for each test group and changes due to presence of charged species on the device surface. This supports the notion that AlGaIn/GaN FETs can operate after prolonged exposure to solutions following chemical functionalization. Peptide layers added to the surface were also shown to be stable over the tested time period via XPS and AFM measurements. We observed a removal of excess peptide on the onset of soaking and recorded no evidence of peptide disassociation from the device surfaces as soaking continued. Overall this work further advances efforts to develop AlGaIn/GaN FETs as longer term, disposable, *in-situ* biosensing platforms.

HgNO₃ Sensitivity of AlGa_N/Ga_N Field Effect Transistors Functionalized with Phytochelating Peptides

Summary

AlGa_N/Ga_N FETs were examined for environmental stability with a 5 week submersion in solution and incubation in a simulated BSA-biofouling solution. FETs were modified with propyl phosphonic acid and fluorobenzyl phosphonic acid via phosphoric acid etch. Biofouling of controlled samples saw a 35-40% increase in I_D response compared to a 20% increase in control biofouled samples, and no effect was seen in the 5 week FET soaks. When comparing effects to FET gate width it was found that 50 μm gates showed significantly higher response signal and variance with the biofouling than the 150 μm gate width. In conclusion biofouling increased the FET signal and more so in functionalized surfaces, however phosphonic acid modified FETs showed stable signal in aqueous environments after the 5 week period.

There is a growing need for a broader and easily accessible set of sensing modalities that can adjust to the wide variety of environmental factors present in our modern society.^{124,21} Semiconductor devices have shown great promise for these types of applications; in particular III-nitrides are becoming increasingly attractive.¹⁸⁴ AlGa_N/Ga_N field effect transistors (FETs) have channel conductance that can be controlled by the presence of charged surface groups, which opens new possibilities for next generation sensing devices.¹⁰⁵ This behavior arises from a 2-dimensional electron gas (2DEG) present at the interface between the AlGa_N and Ga_N and close to the device surface. Details on the working principle of AlGa_N/Ga_N FETs have been discussed at length in previous

works.^{146,126,123} Successful efforts have been done to capture this behavior using methods such as silanization and functional group termination.^{104,130,127} New surface treatments and functionalization techniques are being studied to further increase the utility of AlGaIn/GaN and elevate them to adaptable sensing platforms.

Peptides provide a versatile choice as a surface modification due to the large variety and abundance of sensing strategies they present. One type in particular is recognition peptides, which are peptides that are highly selective to a specific compound or stimulus.⁶⁰ These are promising for creating detection profiles coupled with FETs for response within complex environmental or biological systems.¹⁸⁵ There will always be a need for active monitoring of pollutants such as Hg in environmental systems, and *in-situ* sensing techniques would be very advantageous.¹⁸⁶ The catalog of chelating and recognition peptides has expanded greatly over the last decade of research such that these sensing systems are well understood.^{187,188}

In this study we utilize AlGaIn/GaN FETs for Hg detection using a phytochelating peptide, Phytochelatin-5 (H- γ -EC- γ -EC- γ -EC- γ -EC- γ -ECG-OH), covalently bound to the AlGaIn surface.¹⁸⁹ Phytochelatin-5 was chosen due to their ability to isolate heavy metal ions, and most commonly seen in various plant species. This behavior comes from the thiol group present on each constituent glutathione group in the peptide chain, and allows for a chelate effect as the phytochelatin changes conformation around the metal ion. Prior publications have covered in depth phytochelatin and associated chelate effect behavior.^{190,191} Devices were tested with varying concentrations of Hg, with results monitoring changes in the device sensitivity and performance. Effects from nitric acid (HNO₃) concentration in solution to

AlGaIn/GaN FETs are reported in this work. HNO₃ is commonly present in Hg standard solutions to better facilitate dissolution of Hg. Functionalization of the sensing devices was done using a phosphoric acid and ethephon:phosphonic acid etching procedure which covalently binds peptide chains to the FET surfaces.^{156,61}

AlGaIn/GaN FETs were fabricated using methods previously described.¹⁷³ Finished wafers were diced into 3mm x 3mm chips each containing up to 13 FETs giving a total of 40 individual chips used in each group of conditions described in this study. Approximately 500 FETs were tested in total. All FETs were tested for current-voltage (IV) characteristics and response after each step in the functionalization and Hg exposure process. The phosphoric acid (H₃PO₄) and ethephon (C₂H₆ClO₃P) functionalization was done following previously discussed procedures.⁶¹ Peptides used in this study were purchased from Anaspec, EGT; 1000 ppm Hg in 9% HgNO₃ standard purchased from LabChem. Functionalized chips were then dried over 48 hours with 10 μL solutions of Hg. The following concentrations were tested: 1000 ppm, 100 ppm, 10 ppm, 1 ppm, and 0 ppm of Hg. Confirmation of surface modification and Hg presence was done using x-ray photoelectron spectroscopy (XPS). IV results were monitored by a percent change in drain current (I_D) at a constant drain voltage (V_D) and were taken using a Keithley 4200-SCS using KITE v8.2 attached to a probe station. XPS measurements were done using a Kratos Analytical Axis Ultra XPS and CasaXPS v2.3. Data analysis, plotting, and statistical calculations were performed using Origin. Figure 1 shows a schematic of the acid surface functionalization (a), the binding between peptide chains and the FET surface (b), and the exposure of the device to Hg solution (c).

Throughout the testing process, samples were removed for XPS analysis in order to confirm the presence of modifications generated during the functionalization process.¹⁶⁰ Peptide functionalized surfaces showed evidence of strong amide peaks as seen in Figure 2 at 399.8 eV.^{112,190} These peaks persisted throughout testing with the addition of the various Hg solutions. This can also be seen in Figure 2 within the 10 and 1000 ppm line scans. This is in agreement with previous work in testing the covalent bonding of peptides to the surface and shows surface peptides remaining intact after exposure to varying solutions of HNO₃.⁶⁰ Diminishing Hg 4f peaks at 104.7 and 101.3 eV were also observed with subsequent steps in the Hg solution used for the various FET test groups, where the peak locations were cross referenced with NIST XPS database.¹⁹¹ HNO₃ within the Hg standard solution can also be observed as a nitrate peak (N 1s at 407.5 eV) present in the 1000 ppm and 10 ppm line scans.¹⁹² With regards to the samples used in this study these XPS scans provided qualitative confirmation of the presence of both TAT-C and Phytocelatin-5 peptides before moving into IV characterization of the devices.

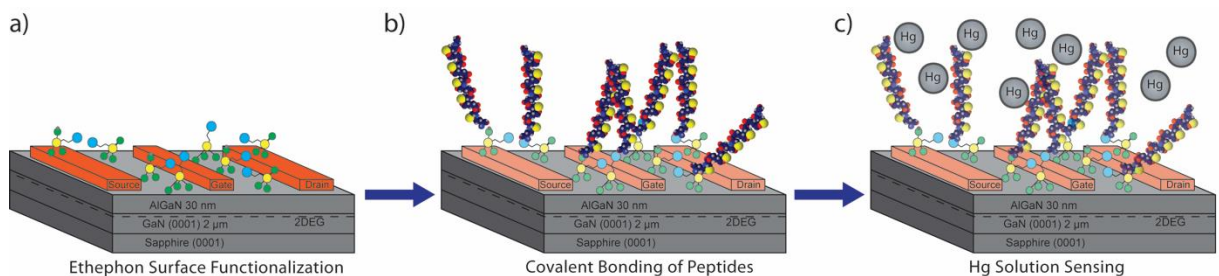


Figure 4.1. a) Ethephon and phosphoric acid surface functionalization, b) Peptide incubation resulting in covalent binding between peptide chains and AlGaIn/GaN FET surfaces, c) Hg standard solution exposure to Hg-sensitive peptide functionalized AlGaIn/GaN FETs.

Initial results from the IV testing revealed solution effects that could not be attributed to Hg-peptide interactions on the AlGaIn/GaN surfaces. Cleaned control samples tested in water showed little change throughout the course of this study and especially when compared to the etch treatments used. Etching of the surface done in the HCl and following phosphonic acid:ethephon etch resulted in a loss of signal or I_D of an average 10-30%, as seen in Figure 3a.⁵⁷ Comparing this to the untreated control in water there is a statistically significant effect of this functionalization effect upon the devices. This is consistent with work previously done by this group which showed a similar effect using only TAT-C functionalization to demonstrate covalent bonding.¹⁵⁶ A similar effect appears to be caused by the Hg solution itself. Testing done with the undiluted Hg standard solution at 1000 ppm resulted in a significant drop in FET activity of an average 60-80% which is shown in Figure 3a. This is attributed to HNO_3 in solution degrading the Au contacts and metal stack that makes up the gate and source/drain features along the FET surfaces. Sensing using phytochelating peptides occurs due to the conformation and charge changes present along the AlGaIn/GaN surface and not the Au contacts, thus this behavior is unaffected.¹⁸⁸ However, any surface or FET contact damage from unwanted etching disrupts the surface charge sensitivity that is created at the AlGaIn/GaN interface and hinders the efficacy of the sensor. By testing for these effects, we isolated and then validated the biomolecular effects observed between the Hg within solution and the Phytochelatin-5 peptide. However, it is believed that these degradation effects can be minimized by directly protecting the contacts during the soaking step or using an optimized FET design with remote contacts. The effect of the Hg standard degrading FET signal can be seen in the ethephon functionalized surfaces in both Figure 3a

and Figure 3b. Further examination of the controls group showed this effect to be unrelated to the addition of the Phytochelatin-5 peptide chain.

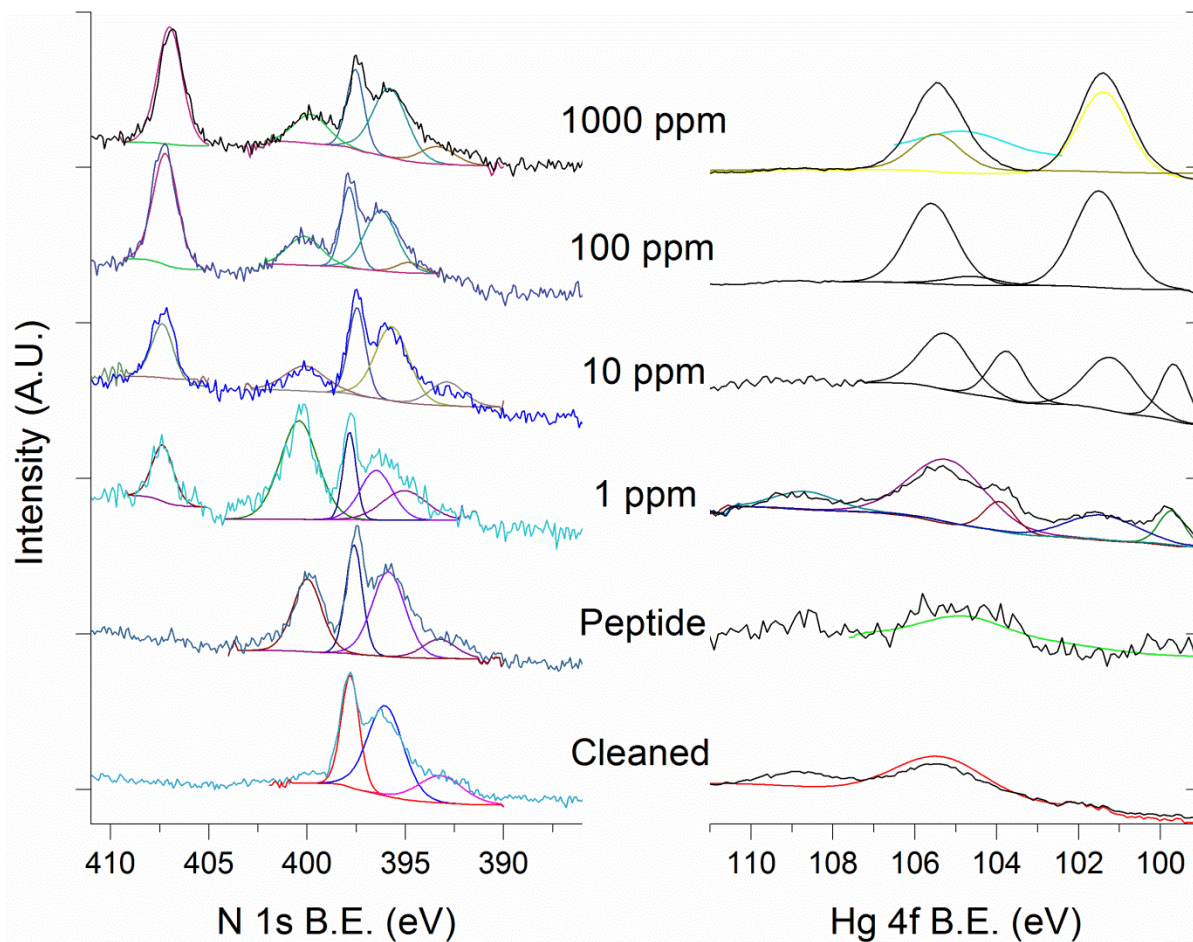


Figure 4.2. XPS spectra of cleaned surfaces, peptide functionalized, 1, 10, 100 and 1000 ppm Hg confirming lack of amide and Hg peaks prior to the functionalization steps and affirming the diminishing Hg peaks as concentration was stepped down.

FETs measuring 10 ppm were also examined in these earlier IV scans in testing for degradation or interaction effects. This data, visible in Figure 3b, did not show any clear effect or statistically significant effect on control or peptide samples. In this figure, 10 ppm controls are compared alongside 1000 ppm and show a lack of the 60-80% degradation seen

in the 1000 ppm samples. Thus IV measurements concluded that the ethephon functionalization and Hg standard solution itself negatively impact FET conductance properties to varying degrees. More so the TAT-C peptide control did not yield any recognition effects as seen later by Phytochelatin-5 treated samples.

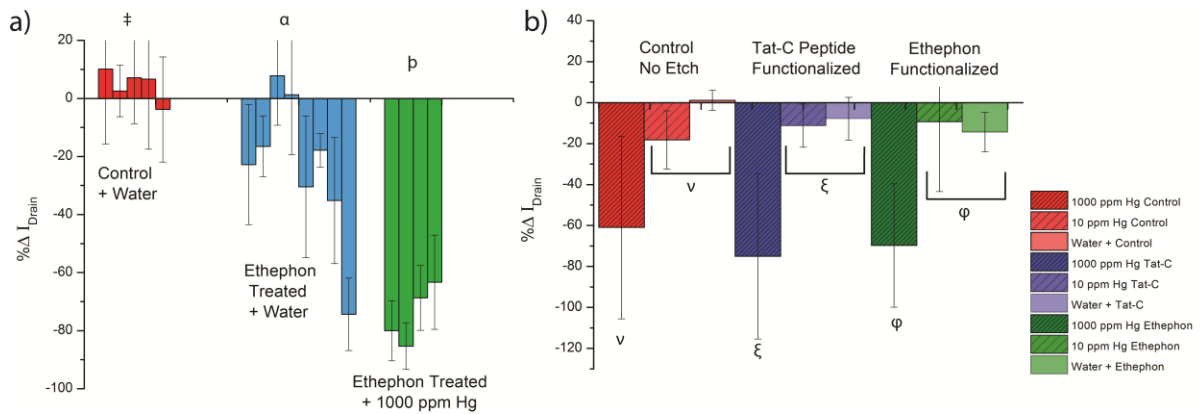


Figure 4.3. a) Three control groups testing the effects of the different solution treatments performed in this experiment including a water control, full ethephon functionalization, and then full functionalization plus the undiluted Hg stock solution. b) Comparison of water, 1000 ppm, and 10 ppm effects on functionalized samples and the negative peptide control using TAT-C.

When testing for the Hg in solution, the Phytochelatin-5 was chosen as a known peptide that is sensitive to Hg.^{193,194} This effect was indeed observed upon our FETs in this experiment as well, and with varying sensitivities. As can be seen in Figure 4 there is a statistically significant difference when moving along the concentration gradient of samples tested from 0 ppm up to 1000 ppm. Immediately visible is that the 1000 ppm coated Phytochelatin-5 sample set does not show the same 60-80% drop off in I_D noted in prior control samples. In fact, as concentration decreases there is a significant increase in the I_D measurements up to a maximum of 10 ppm before dropping once again when approaching 1 ppm. In referencing previous scans shown in Figure 3b the addition of Hg solutions only

reduced FET signal strength and can be seen in the majority of the control samples. However, a large and significant positive percent difference can be observed between those control tests and samples that were incubated in the Phytochelatin-5 peptide. The interaction between Hg in solution and Phytochelatin-5 appears to be occurring and is quantifiable by these FET devices. Varying sensitivities noted in these Phytochelatin-5 samples suggests that this incubation method of peptide based sensing molecules covalently bound to a surface is capable of detecting varying sensitivities of a specific compound or element in solution. One possible explanation for the lack of increasing signal in the 100 ppm and 1000 ppm is the same degradation effect brought on by the HNO_3 as observed in control samples in Figure 3a and Figure 3b.¹⁹⁵ The resulting data then suggests either a passivation or compensation by the peptide adlayer itself. Aside from these two sample sets, which already behaved significantly differently than controls, the recognition events are clearly visible in the remaining two Hg sample sets of 10 ppm and 1 ppm.

AlGaIn/GaN FETs were found to provide concentration sensitive behavior using the ethylenediamine-peptide binding scheme presented here. Hg was selected as a known neurotoxic polluting compound that would be of possible interest to future environmental sensors. Other heavy metal systems, such as Cr, and Pb, with issues of bioaccumulation exist and provide opportunities for testing in the future.¹⁹⁶ The stability of the sensing layer in the presence of aqueous solutions makes this technique viable for future exploration under more representative in-field testing. Data shown here has demonstrated that the covalently bound peptides to AlGaIn/GaN surfaces were still capable of producing a recognition effect in the presence of a 9% solution of HNO_3 .

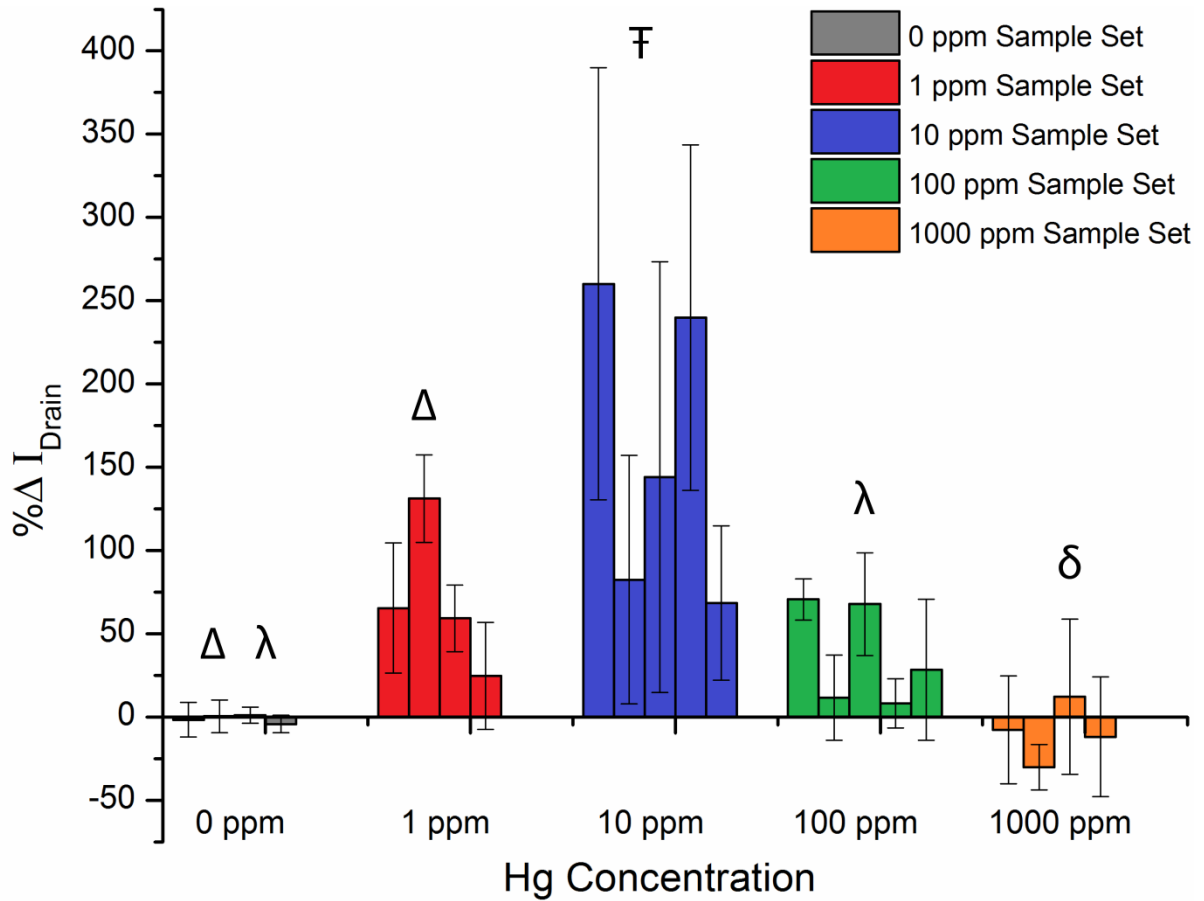


Figure 4.4. I_D response of phytochelatin modified AlGa_N/Ga_N FETs exposed to varying concentrations of Hg in nitric acid solution. Each bar represents a single chip containing a maximum of 13 individual FETs. Significant differences exist between these groups indicating a sensitivity to varying Hg concentration within the solution.

In addition to this stability, surfaces demonstrated sensitivity to varying Hg concentrations. This will eventually allow for highly sensitive heavy metal sensors for future devices that can take advantage of the AlGa_N/Ga_N stability and chemical inertness. Future work in this field would suggest investigation into selectivity of a functionalized AlGa_N/Ga_N FET when exposed to a more complex solution system.

Biofouling and long-term solution exposure stability of phosphonic acid derivative modified AlGa_N/Ga_N Field Effect Transistors.

Summary

AlGa_N/Ga_N FETs were examined for environmental stability with a 5 week submersion in solution and incubation in a simulated BSA-biofouling solution. FETs were modified with propyl phosphonic acid and fluorobenzyl phosphonic acid via phosphoric acid etch. Biofouling of controlled samples saw a 35-40% increase in I_D response compared to a 20% increase in control biofouled samples, and no effect was seen in the 5 week FET soaks. When comparing effects to FET gate width it was found that 50 μm gates showed significantly higher response signal and variance with the biofouling than the 150 μm gate width. In conclusion biofouling increased the FET signal and more so in functionalized surfaces, however phosphonic acid modified FETs showed stable signal in aqueous environments after the 5 week period.

The use of III-nitrides for biological sensing has seen a great deal of attention and progress as research advances the field closer to an industrially viable sensing platform. This is in large part due to the capabilities of III-nitrides to be highly stable under a wide variety of operational conditions and remarkably durable under both etching and prolonged environmental exposure.^{157,3,144} Specifically AlGa_N/Ga_N style field effect transistors (FETs) based devices offer a combination of this high stability, a modifiable and adaptable surface, and are biologically compatible.^{197,160} These devices operate through a surface charge sensitive response via a two dimensional electron gas (2DEG) layer that is present at the

AlGaN and GaN interface.²¹ Multiple studies have been done highlighting the abilities of modified AlGaN/GaN FETs surfaces capable of biological, gas, pH, and pollutant sensing.^{119,118,127} One method of modification or functionalization being explored utilizes phosphoric and phosphonic acid etching techniques to covalently bind biomolecules to the FET surfaces.^{107,61} This method allows for a single step bench top etching process without the use of organic solvents. In work recent work done by I have shown this technique for heavy metal detection for an environmental toxin detection scenario.¹⁹⁸

Examples such as Hg or Cr provide an attractive option for measuring heavy metal content in water supplies, but another useful metric is the monitoring of phosphate compounds in solution. Dissolved phosphates can be related to water/soil quality, microorganism population, and is used in water infrastructure passivation layers.¹⁹⁹ Thus the measurement of shifting concentrations of phosphates may be a worthwhile endeavour, and synergize with recently shown phosphonic acid based functionalization techniques of AlGaN/GaN FETs.¹⁵⁶ High aqueous stability of FET the sensing surface would be required for any such solution based sensing though, and prior testing has only been done to a 7 day timeframe.¹⁵⁶

Work done in this study sought to examine and assess AlGaN/GaN FET behaviour from two key factors of biological aqueous testing. One of these factors is the overall stability of the device following a long term immersion. The second being the effect from a biofouling layer that would likely accumulate during operation. The goal is to understand and the device operability when both of these factors are induced and quantify shifts in the FET conductance properties.

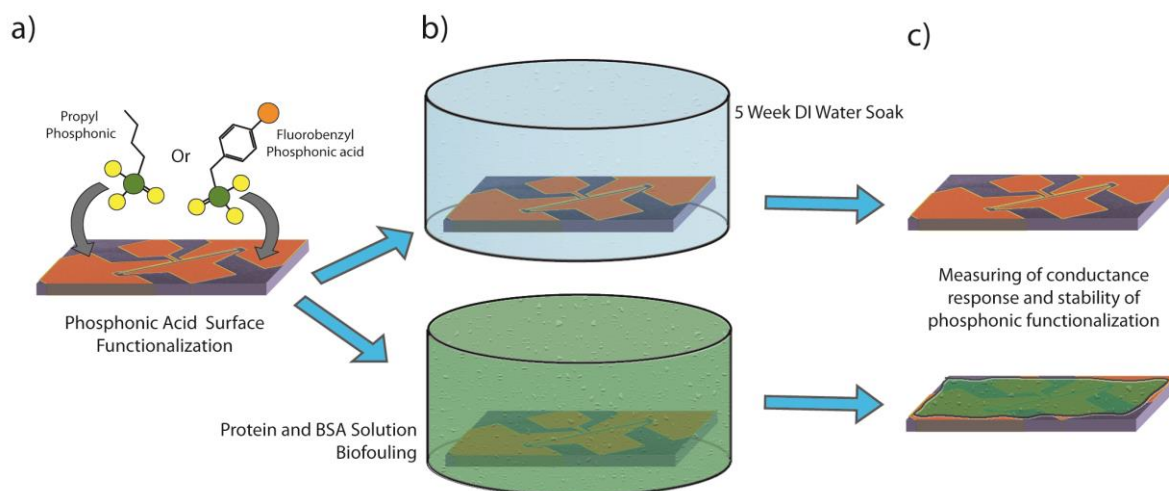


Figure 5.1. Scheme outlining the functionalization and treatment of the AlGaN/GaN FETs throughout the experimentation. a) groups of FETs are functionalized in either PP or PFB. b) FETs are soaked in either a long term DI water solution or biofouling solution. c) FETs are removed, dried, and tested for ID signal response.

AlGaN/GaN FETs were tested for two different effects representative of end use scenarios that future biological sensors may encounter. The first being longer term exposure to solution and the second being the effects of a biofouling of the device surface. In total 72 diced sections of AlGaN/GaN FET printed wafers were tested each containing on average 10 individual FETs. MOCVD Growth and handling of these FETs in this way has been previously discussed in prior work.¹⁷³

Chemical treatments of these devices were completed using a phosphoric acid: 3mM phosphonic acid derivative etch at elevated temperatures. Other examples and more extensive chemistry information can be found in prior work.¹⁰⁷ Selected phosphonic acid derivatives

for this study include propyl phosphonic acid and fluorobenzyl phosphonic acid.

Functionalized FETs were then allowed to soak in DI water for 5 weeks at ambient temperature, or were soaked in a simulated biological fluid for 72 hours. This simulated biological fluid consisted of 50% by volume of 2.5% solution of bovine serum albumin (BSA), 20% phosphate buffered saline (PBS), 20% poly-l-lysine (30,000 MW), and 10% protein standard solutions.

Conductance measurements were divided into three stages: cleaned, functionalized, and BSA fluid soaked. Data is presented as a percent change in drain current (I_D) from either the initial stage to functionalized or the functionalized stage to the BSA soak.¹⁶⁴ Measurements were taken at the peak transconductance of each individual device calculated using methods previously discussed.^{156,144} Statistics and data analysis were done via ANOVA and at a significance level of 0.01 using Origin 8.5.

Several immediate responses were observed in initial testing when transitioning to the functionalized or second stage of the testing. Here etched samples are compared to an unetched control and a control soaked in the BSA fluid. The results of this can be seen in Fig. 2a in which there is approximately 13-14% increase in device signal when undergoing the chemical functionalization procedure. In comparing to the unfunctionalized BSA fluid soaked devices which showed approximately 20% increase in signal. Apart from these two responses there was a lack of statistically significant response between the 5 week soaked functionalized devices and the unsoaked. This suggests that drift of signal from loss of functional layer or oxidation of surface may be minimal in aqueous environments and further

showing the high stability that this method of covalent functionalization offers on the AlGaIn/GaN surfaces.

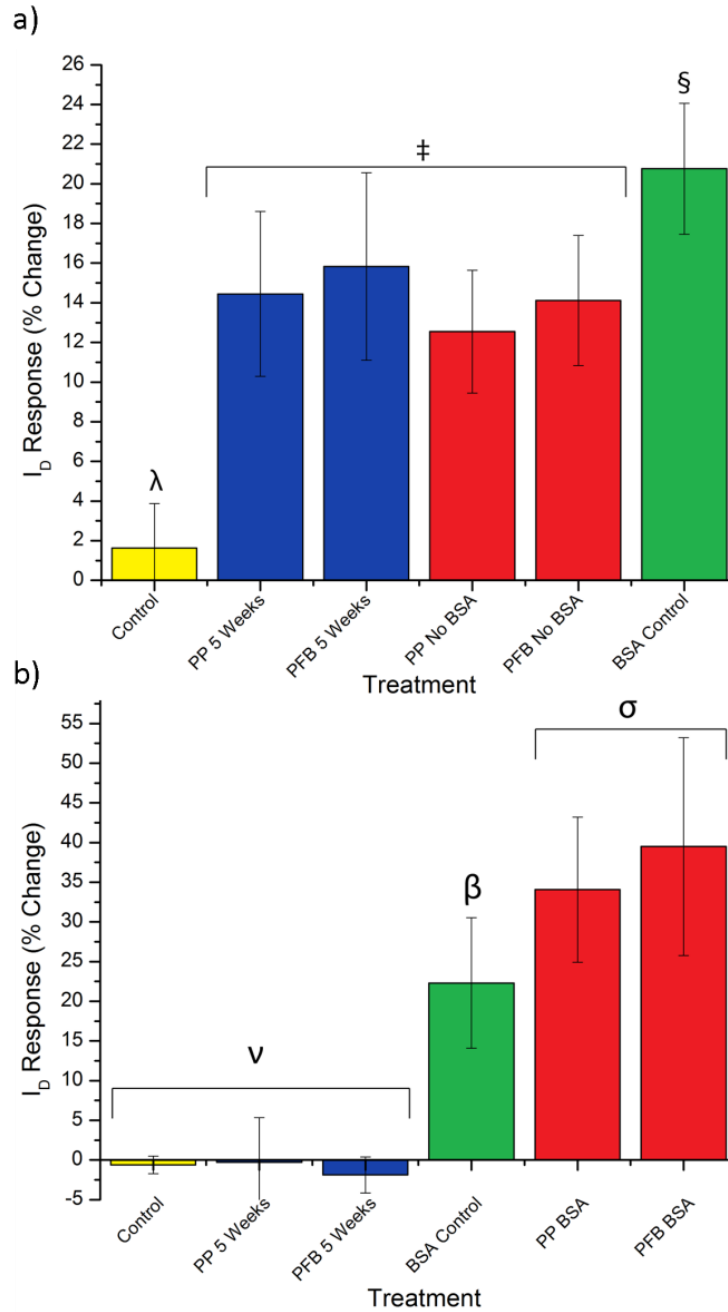


Figure 5.2 Comparison of I_D response at peak transconductance of each sample group. a) Shows shifting I_D signal from the initial untreated phase of the study up to the etched and functionalized

phase including a 5 week soak test and a BSA fluid soak test. b) Shows the shift in ID from the functionalization phase of the study until the final soaking and testing of each sample group, BSA control was tested again from the same setup in part a) for comparison.

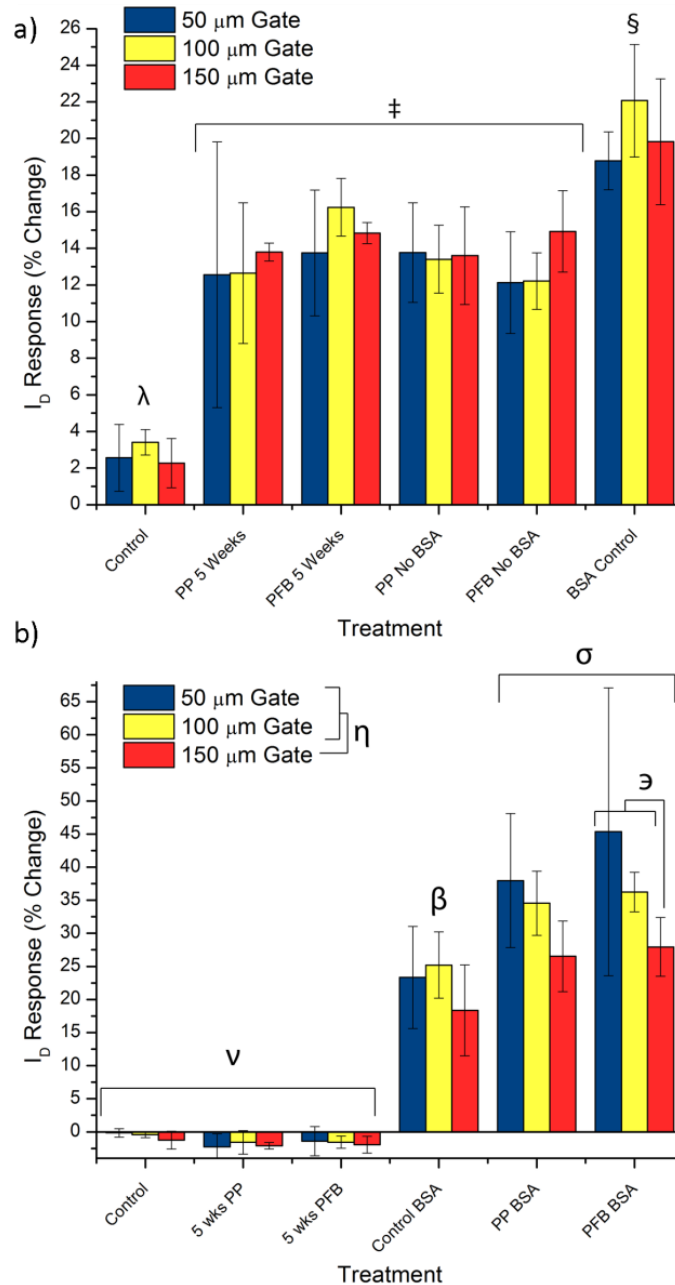


Figure 5.3. Comparison of ID with respect to gate width. a) Comparing initial to functionalization stages of the study showing similar trends as observed in Fig. 2 indicating an effect due to both

functionalization and the BSA Soak, however no significant difference is observed related to gate width. b) Comparing functionalization stage to the final soaking stage showing that there is a gate width dependent effect in the PFB BSA samples.

In Fig. 2b the changes from the functionalized stage of testing to the BSA fluid soak are shown. Within this plot the 5 week samples and control test groups were left unaltered from the previous conductance tests shown in Fig. 2a and left as controls for retesting. Phosphonic derivative functionalized samples however showed approximately a 35-40% increase in I_D from the previous treatments. Fig. 2b shows a retest of the BSA control on unfunctionalized samples for comparison purposes to Fig. 2a. Another important observation was noted that both the BSA fluid samples and the soaked samples did not show any signs of malfunctioning device behaviour, but more so a shift in their conductive properties.

A secondary breakdown of this data was done to examine any effects present from a varied gate width of the different transistor architectures. For the AlGaIn/GaN FETs used in this study three different gate width were used: 50, 100, and 150 μm . The results of this breakdown can be seen in Fig. 3 in which both sets of conductance measurements from Fig. 2 were dissected into their constituent gate architectures. In reducing the data from Fig. 2 to the individual FET structures the overall trends between the sample groups were persistent. In fact no observable difference is observed in sample groups from the initial stage of testing to the functionalized with regard to the variation in gate width, Fig 3a.

However, in analysing the functionalization to soaking stage of the AlGaIn/GaN FETs a gate width effect was observed. As seen in Fig. 2b there is an overall statistically significant difference between the 150 μm gate width and both the 100 and 50 μm gate widths. This

relationship is observed in the functionalized samples soaked in BSA fluid. Additionally the 50 μm gate width showed a statistically significant difference in the variation of their signal responses leading to a much wider range of observed data. This can be seen in Fig. 3b in the 50 μm standard deviations in all BSA soaked samples. The results of this testing suggest that under these circumstances of biofouling in a complex ionic and biological solution the larger gate dimensions tended to yield more consistent results and show a lower response to the added environmental stimuli.

This study sought to identify how one could expect a biofouling solution to affect or not affect the AlGaIn/GaN FETs conductive properties when modified with a phosphonic acid derivative. Findings here confirm that a buffered ionic solution and BSA solution increased the response of AlGaIn/GaN FETs both unfunctionalized and functionalized. Those modified with the phosphonic acids showed response rates approximately 10% higher than control sets. In both cases it was shown that the biofouling had a clear effect on the device performance and presents a factor that would need to be accounted for in a future biosensing situation. A further breakdown of these responses was done against the three different gate widths used in the FETs of this study. From this no significant effect was shown without the functionalization and BSA fluid together on the FET. When both a functionalization and a BSA fluid soak were done a significant increase in both signal and variation were observed in the shorter 50 μm gates when compared to the 150 μm gates. This suggests that the shorter gate widths may be more susceptible to interference from the biofouling.

In looking forward to future works with these AlGaIn/GaN FET type of devices merging stability testing such as this with a sensing scenario will become more important in proving

the worth of this advancing technology. The example of phosphate testing put forth earlier in this work serves a candidate for a larger detection study where multiple dissolved compounds could be tested for. Data presented here suggests that AlGaN/GaN devices would remain stable and operable under such environments and more so that biofouling on these devices may be quantifiable and therefore capable of being accounted for in calibration of the device. Work has been done showing methods of antifouling adlayers using PEG–poly(alkyl phosphonate) compounds that present similar attachment chemistries.²⁰⁰ In moving forward the primary advantages of the covalent attachment of phosphonic acids remain its adaptability and aqueous stability, and make this methodology worthwhile to investigate further to a marketable in-field biological sensor and seeking a coupling of an antifouling component as well.

Conclusions and Future Outlook

6.1 Overall Conclusions From Individual Studies

Listed below is a summary from a chapter by chapter basis of relevant conclusions and findings from within each individual study or body of work. Accompanying these conclusions will be extended comments and details both representing the context of the original work and a retrospective look at the greater goals of the research as a whole.

From the outset of the grander research project detailed in this thesis the goal was to provide a simpler means of functionalizing and modifying the surfaces of FETs. Previously shown in [TABLE] there are a variety of different methods to modify the AlGa_N/Ga_N FETs but most require several steps and require a more complicated surface chemistry approach. Ion and pH sensing has been shown with these FETs by simply drying them to the surface, so the same approach was taken with known charged and responsive peptides and a response of ~96% was seen using the RP group.

Beyond testing for various biomolecule responses on the device surfaces, the devices were soaked in solution for up to 7 days. XPS however, quickly showed that only the first day of soaking yielded any signal of the peptides deposited on the surface. What can be drawn from this is that the interaction between the peptide and surface is too weak to stop the dissolution of the peptide back into the aqueous environment.

This paper concluded that biological molecule sensing in regard to incubation would only be viable in time periods less than 24 hrs, but this dissolution may happen quicker than

this making even short term sensing difficult. In response to this this method is only recommended for disposable or single use type of sensing devices. Overall this study successfully showed biomolecules could draw a response using this simple incubation scheme, but for anything longer term the following studies would need to find a means to create this bond more permanent.

In response to the challenge set out by the previous work the use of phosphonic acid derivative, ethephon, in combination with a heated phosphoric acid etch successfully bound peptide molecules to the AlGa_N surface. This was tested up to a solution immersion time of 7 days and still peptide presence was observed via XPS and the corresponding N 1s peak. In building off of work done by Dr. Stewart Wilkins and Dr. Nora Berg this functionalization can be done in a single step with no organic solvents in a bench top setting. A focus of this paper and other work moving forward was to approach this as both a step forward in chemical modification from both an environmental and cost reduction stand point.

In testing devices for their long term stability (up to a week) two analytical tests were done; XPS and IV/conductance measurements. XPS aided in showing the continued presence of the peptide on the AlGa_N/Ga_N surface, but also showed what could be seen as an excess layer of peptide in the initial scans. Following functionalization and incubation in peptide solution almost a complete occlusion of the other signature Ga_N and P peaks was observed in favor of a dominant amide N 1s peak. This excess biolayer appeared to be removed following soaking but still raised the question as to what kind of effect a biofilm would have on the device properties. This was a question that would not be revisited until the final biofouling study. From the IV measurements however a shift was noted in the threshold voltage and

pinch off points for each different sample groups of the AlGaIn/GaN devices. This shift showed peak a shift toward more lower (-3 V from -1.5 V) voltages immediately following the functionalization process, but also showed a shift back to the original values the longer the device remained in solution. By 72 hours almost all devices had stabilized at a threshold voltage that would remain constant for the remainder of the study. This was also echoed in the I_D signal of the devices themselves which observed a roughly 12% shift in values following the etch, and are documented here.¹⁴¹ In final observations of these effects on the FETs devices operated normally and were not impeded by the etching and incubation steps apart from the shifts in conductive behaviors.

Conductance data from the various sample groups taken in this study culminated in a clear differentiation of signals when placed in environments of varying concentrations of Hg. For the Hg solutions a 1000ppm undiluted stock solution was used to make soaking fluids of 100, 10, and 1 ppm. From these statistically significant responses were noted between 1 and 10 ppm especially and from the 100ppm and control 1000ppm. It is worthwhile to distinguish these two response sets because a secondary effect was created from the HNO_3 used to dissolve the Hg in solution. In control FETs a drop in signal of 60-80% was observed when in contact with the 1000ppm solution and visible degradation of the Au contacts was seen on the FETs. In response to this the phytochelatin modified FETs that were also tested at the 1000ppm solution strength did not observe this same decline in signal strength and in fact remained relatively close to no significant change in signal despite seeing similar contact damage.

This is accounted for as either a compensation or passivation effect largely in part due to the presence of the phytochelatin peptide. As shown in [FIGURE] the 10ppm samples tested with the highest signal compared to the 100 or 1000ppm and the predicted response would be a corresponding increase in signal as you increase concentration leading up to a sensing ceiling of sorts. Instead in the 100ppm samples we see a similarly low change in signal change but again no negative response as noted in controls. Thus, in the conclusions from this portion of the work we determined that these AlGa_N/Ga_N FETs are indeed capable of concentration dependent sensing and can detect interactions between the surface bound receptors and their aqueous counterparts.

XPS analysis played a critical role in this study and provided information regarding the presence of the phytochelatin peptide and the Hg through the variety of concentration testing. One aspect of this study was testing the effects of the acidic HNO₃ based Hg solution on the device itself. As noted above a degradation was observed in the IV measurements in the passivating effects of the higher concentration tested AlGa_N/Ga_N. From XPS data it is clear that under these conditions where up to 80% signal was lost in control samples and visible degradation of Au contacts was observed the peptide layer was persistent on the surface. This gives credence to the strength of the covalent bond generated from the phosphonic acid surface modification method as one that is not only suitable for long term solution exposure but one that can possibly survive a wide range of environmental conditions and pH levels. Without a broader study to investigate this a concise conclusion cannot be given to this phenomena, but this shows promising results for a device that may encounter unwelcoming environments.

This final study sought to address several end environmental factors that a theoretical biological sensor made using AlGaIn/GaN FETs would encounter. The first of which was the long term stability of the functional layer and conductive behavior of the AlGaIn/GaN FETs. In previous work testing was done up to one week, but realistically a sensor may sit in solution for multiple weeks or months in an active sensing environment so a longer time span needed to be confirmed. In this study samples were modified with two different phosphonic acid derivatives and left to soak for 5 weeks' time. Results showed no significant effect on the conductive behaviors of the devices regardless of the gate width effects later discussed in this study. Aqueous stability is a problem that other methods of functionalization cannot fully address, a key example being silane chemistry, and here in the longest test done over the course of this body of work the phosphonic derivative modified FETs show consistent behavior.

The second environmental effect examined in this study is that of a biofilm or biofouling layer that would form on an FET when placed into a solution that is heavy in biomolecules and organics. For this scenario a biofouling solution was made with a mix of BSA, Poly-l-lysine, and PBS. Control samples soaked in the BSA fluid showed ~20% increase in signal in response to the soaking in the ionic biological solution. However, phosphonic acid derivative modified FETs showed significantly higher response to the biofouling. The results of this indicate that is possible for a quantifiable shift in conductance to be measured and accounted for in a biofouling situation but also that there is an effect that can be attributed to it in general. Work done by Zoulalian et al. has shown the use of antifouling adlayers using PEG-poly(alkyl phosphonate) compounds that have similar

attachment chemistries as the phosphonic acid derivatives used here.²⁰⁰ This represents a possible means to address this problem in the future by combining these two techniques.

A final set of statistics and analysis was done on the datasets to assess the effect of gate width on the results of this study. As the same device architecture and growth masks had been used for all devices in these studies performed in this document. The results of this analysis showed what was previously known in that devices behave proportionally to one another and yield signals that are not significantly different from one another under normal circumstance. However, when testing these gate widths after functionalization and exposure to BSA fluid there was a statistically significant difference in the responses between the 50 μm gate widths and the 100 and 150 μm ones. Additionally there was a statistically significant difference in the variation of the 50 μm FETs. This suggests that shorter gate width FETs are more susceptible to environmental interference than the longer gated FETs. This is important because it opens up an opportunity to further optimize the gate structure for environmental sensing. Additionally this may help account for some of the large variations seen in past sets of IV data if the 50 μm FETs in particular have a greater tendency to behave erratically.

6.2 Future Directions

When taking this information into account it has been made clear with contributions by these authors and other corresponding literature that AlGaIn/GaN FETs have a great deal of potential and that research as a whole on the subject is moving towards an industrially produced product. Advancing this end goal new analytes should be explored beyond just the

ones presented or discussed in this work. In referencing Table 1.1 it is clear many different analytes have been examined but these have not been tested using the phosphonic acid method mentioned here. In the future one could see the advantages of a design that could incorporate multiple AlGa_N/Ga_N FETs onto a single PCB that would enable the testing of multiple analytes in solution using some of the analyte-receptor schemes in [table]. An example would be a sensing platform that could be utilized in municipal water supplies to test for levels of heavy metals, dissolved phosphates, pH, and nitrates all at once for an active monitoring setup. This presents more of an industrial design and engineering approach to fabricating a device that could utilize disposable and inexpensively modified FETs. Such set-up will enable multiplexing described here for both medical devices and/or environmental applications.

Lastly work done here has shown preliminary evidence of a stable surface later generated by this functionalization method, but this is not fully representative of an end use application where sensors may be positioned within a soil, bodily fluid, or prolonged harsh environment. It is for this reason that further stability studies should be done in relation to the new analytes being explored. This would allow for the study and incorporation of the PEG derivative adlayers that were discussed in Chapter 5. The use of PEG-based layers could allow for a biofilm resistant surface that may provide some protection to the underlying III-nitride surface from interference seen from the BSA fluid in Chapter 5. Thus for the future of these devices and the technology as a whole we feel it is best to recommend further investigations into AlGa_N/Ga_N biological sensors with special regard to utilizing PEG derivative based protective layering. This would allow for a more controlled biosensor

response. It is projected that this will permit investigation of new analytes and move towards studies that examine the limits of detection using the phosphonic acid modification method detailed over the course of this work.

REFERENCES

- 1 N. Faucheux, R. Schweiss, K. Lützow, C. Werner, and T. Groth, *Biomaterials* **25** (14), 2721 (2004).
- 2 Lauren E. Bain, Ramon Collazo, Shu-han Hsu, Nicole Pfiester Latham, Michael J. Manfra, and Albena Ivanisevic, *Acta Biomaterialia* **10** (6), 2455 (2014).
- 3 S. A. Jewett, M. S. Makowski, B. Andrews, M. J. Manfra, and A. Ivanisevic, *Acta Biomater.* **8** (2), 728 (2012).
- 4 V. M. Bermudez, *Surface Science* **499** (2–3), 109 (2002).
- 5 Edmund Chan, Nathan Jackson, Alan Mathewson, Paul Galvin, Ali B. Alamin Dow, Nazir P. Kherani, Christophe Blaszykowski, and Michael Thompson, *Applied Surface Science* **282** (0), 709 (2013).
- 6 Matthew S. Makowski, Dmitry Y. Zemlyanov, and Albena Ivanisevic, *Applied Surface Science* **257** (10), 4625 (2011).
- 7 B. Baur, G. Steinhoff, J. Hernando, O. Purruicker, M. Tanaka, B. Nickel, M. Stutzmann, and M. Eickhoff, *Applied Physics Letters* **87** (26), 3901 (2005).
- 8 G. Steinhoff, O. Purruicker, M. Tanaka, M. Stutzmann, and M. Eickhoff, *Advanced Functional Materials* **13** (11), 841 (2003).
- 9 Monu Mishra, T. C. Shubin Krishna, Neha Aggarwal, and Govind Gupta, *Applied Surface Science* **345** (0), 440 (2015).
- 10 S. J. Pearton and F. Ren, *IEEE Instrum. Meas. Mag.* **15** (1), 16 (2012).
- 11 O Ambacher, *Journal of Physics D: Applied Physics* **31** (20), 2653 (1998).
- 12 M.E. Levinshtein, in *Scitech Book News* (Ringgold Inc, Portland, 2001), Vol. 25.
- 14 E. Sari, S. Nizamoglu, T. Ozel, H. V. Demir, Ayse Inal, Erkin Ulker, E. Ozbay, Y. Dikme, and M. Heuken, presented at the Lasers and Electro-Optics Society, 2006. LEOS 2006. 19th Annual Meeting of the IEEE, 2006 (unpublished).
- 15 Tevye Kuykendall, Philipp Ulrich, Shaul Aloni, and Peidong Yang, *Nat Mater* **6** (12), 951 (2007).

- 16 K. A. Jones, T. P. Chow, M. Wraback, M. Shatalov, Z. Sitar, F. Shahedipour, K.
Uduary, and G. S. Tompa, *Journal of Materials Science* **50** (9), 3267 (2015).
- 17 B. Kunert, K. Volz, J. Koch, and W. Stolz, *Applied Physics Letters* **88** (18), 182108
(2006).
- 18 C. K. Gan and D. J. Srolovitz, *Physical Review B* **74** (11), 115319 (2006).
- 19 Duanjun Cai and Guang-Yu Guo, *Journal of Physics D-Applied Physics* **42** (18),
185107 (2009).
- 20 F. Bernardini, V. Fiorentini, and D. Vanderbilt, *Physical Review B* **56** (16), 10024
(1997).
- 21 Ronny Kirste, Nathaniel Rohrbaugh, Isaac Bryan, Zachary Bryan, Ramon Collazo,
and Alben Ivanisevic, *Annual Review of Analytical Chemistry* **8**, 149 (2014).
- 22 Jürgen Fritsch, Otto F. Sankey, Kevin E. Schmidt, and John B. Page, *Physical
Review B* **57** (24), 15360 (1998).
- 23 Pyry Kivisaari, Jani Oksanen, and Jukka Tulkki, *Applied Physics Letters* **103** (21),
211118 (2013).
- 24 M. Feneberg, R. A. R. Leute, B. Neuschl, K. Thonke, and M. Bickermann, *Physical
Review B* **82** (7), 075208 (2010).
- 25 C. Guarneros and V. Sánchez, *Materials Science and Engineering: B* **174** (1–3), 263
(2010).
- 26 B. Monemar, P. P. Paskov, G. Pozina, C. Hemmingsson, J. P. Bergman, T.
Kawashima, H. Amano, I. Akasaki, T. Paskova, S. Figge, D. Hommel, and A. Usui,
Physical Review Letters **102** (23), 235501 (2009).
- 27 A. Castiglia, J.-F. Carlin, and N. Grandjean, *Applied Physics Letters* **98** (21), 213505
(2011).
- 28 K. Köhler, T. Stephan, A. Perona, J. Wiegert, M. Maier, M. Kunzer, and J. Wagner,
Journal of Applied Physics **97** (10), 104914 (2005).
- 29 C. J. Eiting, P. A. Grudowski, and R. D. Dupuis, *Journal of Elec Materi* **27** (4), 206
(1998).

- 30 C. G. Van de Walle, J. L. Lyons, and A. Janotti, *physica status solidi (a)* **207** (5), 1024 (2010).
- 31 Chad S. Gallinat, Gregor Koblmüller, and James S. Speck, *Applied Physics Letters* **95** (2), 022103 (2009).
- 32 C. Stampfl, C. G. Van de Walle, D. Vogel, P. Krüger, and J. Pollmann, *Physical Review B* **61** (12), R7846 (2000).
- 33 Chris G Van de Walle, Catherine Stampfl, and Jörg Neugebauer, *J. Cryst. Growth* **189**, 505 (1998).
- 34 Ingrid Wilke, Ricardo Ascazubi, Hai Lu, and William J. Schaff, *Applied Physics Letters* **93** (22), 221113 (2008).
- 35 Wang Ruoxi, Zhang Dongju, Liu Yongjun, and Liu Chengbu, *Nanotechnology* **20** (50), 505704 (2009).
- 36 Chong Zhao, Zhi Xu, Hao Wang, Jiake Wei, Wenlong Wang, Xuedong Bai, and Enge Wang, *Advanced Functional Materials* **24** (38), 5985 (2014).
- 37 V. A. Gubanov, E. A. Pentaleri, C. Y. Fong, and B. M. Klein, *Physical Review B* **56** (20), 13077 (1997).
- 38 Ramón Collazo, Seiji Mita, Jinqiao Xie, Anthony Rice, James Tweedie, Rafael Dalmau, and Zlatko Sitar, *physica status solidi (c)* **8** (7-8), 2031 (2011).
- 39 K. Zhu, M. L. Nakarmi, K. H. Kim, J. Y. Lin, and H. X. Jiang, *Applied Physics Letters* **85** (20), 4669 (2004).
- 40 Robert F. Davis, A. M. Roskowski, Edward A. Preble, James S. Speck, B. Heying, J. A. Freitas, Jr., E. R. Glaser, and W. E. Carlos, *Proceedings of the IEEE* **90** (6), 993 (2002).
- 41 Alexander Y. Polyakov and In-Hwan Lee, *Materials Science and Engineering: R: Reports* **94**, 1 (2015).
- 42 Stephen J. Pearton, Richard Deist, Fan Ren, Lu Liu, Alexander Y. Polyakov, and Jihyun Kim, *Journal of Vacuum Science & Technology A* **31** (5), 050801 (2013).

- 43 A. Y. Polyakov, N. B. Smirnov, A. V. Govorkov, A. V. Markov, E. B. Yakimov, P. S. Vergeles, N. G. Kolin, D. I. Merkurisov, V. M. Boiko, In-Hwan Lee, Cheul-Ro Lee, and S. J. Pearton, *Journal of Elec Materi* **36** (10), 1320 (2007).
- 44 A. Y. Polyakov, N. B. Smirnov, A. V. Govorkov, A. V. Markov, S. J. Pearton, A. M. Dabiran, A. M. Wowchak, B. Cui, A. V. Osinsky, P. P. Chow, N. G. Kolin, V. M. Boiko, and D. I. Merkurisov, *Applied Physics Letters* **93** (15), 152101 (2008).
- 45 A. Y. Polyakov, N. B. Smirnov, A. V. Govorkov, E. A. Kozhukhova, Stephen J. Pearton, Fan Ren, Lu Liu, J. W. Johnson, Wantae Lim, N. G. Kolin, S. S. Veryovkin, and V. S. Ermakov, *Journal of Vacuum Science & Technology B* **30** (6), 061207 (2012).
- 46 B. D. White, M. Bataiev, S. H. Goss, X. Hu, A. Karmarkar, D. M. Fleetwood, R. D. Schrimpf, W. J. Schaff, and L. J. Brillson, *Nuclear Science, IEEE Transactions on* **50** (6), 1934 (2003).
- 47 S. Jha, Emil V. Jelenković, M. M. Pejović, G. S. Ristić, M. Pejović, K. Y. Tong, C. Surya, I. Bello, and W. J. Zhang, *Microelectronic Engineering* **86** (1), 37 (2009).
- 48 A Ionascut-Nedelcescu, C Carlone, A Houdayer, HJ Von Bardeleben, J-L Cantin, and S Raymond, *Nuclear Science, IEEE Transactions on* **49** (6), 2733 (2002).
- 49 Samuel Gissot, Ali BenMoussa, Boris Giordanengo, Ali Soltani, Takashi Saito, Udo Schuhle, Udo Kroth, and Alexander Gottwald, presented at the Radiation Effects Data Workshop (REDW), 2014 IEEE, 2014 (unpublished).
- 50 D. Parks and B. Tittmann, *Ultrasonics, Ferroelectrics, and Frequency Control, IEEE Transactions on* **61** (7), 1216 (2014).
- 51 BR Tittmann, B Reinhardt, and Daniel Parks, presented at the Ultrasonics Symposium (IUS), 2014 IEEE International, 2014 (unpublished).
- 52 J. Wu, W. Walukiewicz, K. M. Yu, W. Shan, J. W. Ager, E. E. Haller, Hai Lu, William J. Schaff, W. K. Metzger, and Sarah Kurtz, *Journal of Applied Physics* **94** (10), 6477 (2003).
- 53 V. V. Emtsev, V. Yu Davydov, E. E. Haller, A. A. Klochikhin, V. V. Kozlovskii, G. A. Oganessian, D. S. Poloskin, N. M. Shmidt, V. A. Vekshin, and A. S. Usikov, *Physica B: Condensed Matter* **308–310**, 58 (2001).
- 54 S. Zhao, S. Fatholouloumi, K. H. Bevan, D. P. Liu, M. G. Kibria, Q. Li, G. T. Wang, Hong Guo, and Z. Mi, *Nano Letters* **12** (6), 2877 (2012).

- 55 D. Zhuang and J. H. Edgar, *Materials Science and Engineering: R: Reports* **48** (1), 1 (2005).
- 56 I. Adesida, C. Youtsey, A. T. Ping, F. Khan, L. T. Romano, and G. Bulman, *MRS Proceedings* **537** (G1.4) (1999).
- 57 Maria Reiner, Marcus Reiss, Thorge Brünig, Lauri Knuuttila, Rudolf Pietschnig, and Clemens Ostermaier, *Phys. Status Solidi B* **252** (5), 1121 (2015).
- 58 Steve Pearton, W Lim, Fan Ren, and David Norton, *ECS Transactions* **6** (2), 501 (2007).
- 59 Hadis Morkoc, *Handbook of Nitride Semiconductors and Devices, GaN-based Optical and Electronic Devices*. (Wiley-VCH, Hoboken, NJ, USA, 2009).
- 60 N. Rohrbaugh, I. Bryan, Z. Bryan, C. Arellano, R. Collazo, and A. Ivanisevic, *Applied Physics Letters* **105** (13) (2014).
- 61 N. G. Berg, M. W. Nolan, T. Paskova, and A. Ivanisevic, *Langmuir* **30** (51), 15477 (2014).
- 62 Y. Gao, M. D. Craven, J. S. Speck, S. P. Den Baars, and E. L. Hu, *Applied Physics Letters* **84** (17), 3322 (2004).
- 63 Xiuling Li, Young-Woon Kim, Paul W. Bohn, and Ilesanmi Adesida, *Applied Physics Letters* **80** (6), 980 (2002).
- 64 A. Ababneh, H. Kreher, and U. Schmid, *Microsyst Technol* **14** (4-5), 567 (2008).
- 65 M. Bickermann, S. Schmidt, B. M. Epelbaum, P. Heimann, S. Nagata, and A. Winnacker, *J. Cryst. Growth* **300** (2), 299 (2007).
- 66 Jinwang Li, Masaru Nakamura, Takashi Shirai, Koji Matsumaru, Chanel Ishizaki, and Kozo Ishizaki, *Journal of the American Ceramic Society* **89** (3), 937 (2006).
- 67 S. Fukumoto, T. Hookabe, and H. Tsubakino, *Journal of Materials Science* **35** (11), 2743 (2000).
- 68 SM Olhero, FL Alves, and JMF Ferreira, *Last Advances in Aqueous Processing of Aluminium Nitride (AlN)-A Review*. (INTECH Open Access Publisher, 2011).

- 69 Zheng Liu, Yongji Gong, Wu Zhou, Lulu Ma, Jingjiang Yu, Juan Carlos Idrobo, Jeil Jung, Allan H. MacDonald, Robert Vajtai, Jun Lou, and Pulickel M. Ajayan, *Nat Commun* **4** (2013).
- 70 Cameron G. Cofer and James Economy, *Carbon* **33** (4), 389 (1995).
- 71 Amir Pakdel, Chunyi Zhi, Yoshio Bando, Tomonobu Nakayama, and Dmitri Golberg, *ACS Nano* **5** (8), 6507 (2011).
- 72 Weiwei Lei, David Portehault, Dan Liu, Si Qin, and Ying Chen, *Nat Commun* **4**, 1777 (2013).
- 73 Jun Dai, Xiaojun Wu, Jinlong Yang, and Xiao Cheng Zeng, *The Journal of Physical Chemistry Letters* **4** (20), 3484 (2013).
- 74 K. S. A. Butcher, A. J. Fernandes, P. P.-T. Chen, M. Wintrebert-Fouquet, H. Timmers, S. K. Shrestha, H. Hirshy, R. M. Perks, and Brian F. Usher, *Journal of Applied Physics* **101** (12), 123702 (2007).
- 75 Yen-Sheng Lu, Chi-Cheng Huang, J. Andrew Yeh, Chi-Fan Chen, and Shangjr Gwo, *Applied Physics Letters* **91** (20), 202109 (2007).
- 76 Torbjörn Lindgren, Magnus Larsson, and Sten-Eric Lindquist, *Solar Energy Materials and Solar Cells* **73** (4), 377 (2002).
- 77 Q. X. Guo, O. Kato, and A. Yoshida, *Journal of The Electrochemical Society* **139** (7), 2008 (1992).
- 78 Christopher R Chitambar, *International journal of environmental research and public health* **7** (5), 2337 (2010).
- 79 Ayadi Ahlem, Maghraoui Samira, El Hili Ali, Galle Pierre, and Tekaya Leila, *Microscopy Research and Technique* **71** (12), 849 (2008).
- 80 S. Millour, L. Noel, R. Chekri, C. Vastel, A. Kadar, V. Sirot, J. C. Leblanc, and T. Guerin, *J. Food Compos. Anal.* **25** (2), 108 (2012).
- 81 Ahlem Ayadi, Samira Maghraoui, Sayda Kammoun, and Leila Tekaya, *Microscopy* **63** (5), 383 (2014).
- 82 Maghraoui Samira, Ayadi Ahlem, Ben Ammar Aouatef, Jaafoura Mohamed Habib, and Tekaya Leila, *Microscopy Research and Technique* **74** (6), 546 (2011).

- 83 Samira Maghraoui, Ahlem Ayadi, Aouatef Ben Ammar, Mohamed-Habib Jaafoura, Ali El Hili, Pierre Galle, and Leila Tekaya, *Journal of Electron Microscopy* **60** (2), 183 (2011).
- 84 F. P. Castronovo and H. N. Wagner, *British Journal of Experimental Pathology* **52** (5), 543 (1971).
- 85 Akiyo Tanaka, Miyuki Hirata, Yutaka Kiyohara, Makiko Nakano, Kazuyuki Omae, Masaharu Shiratani, and Kazunori Koga, *Thin Solid Films* **518** (11), 2934 (2010).
- 86 Cheol Hong Lim, Jeong-Hee Han, Hae-Won Cho, and Mingu Kang, *Toxicological Research* **30** (1), 55 (2014).
- 87 David P. Kelsen, Nancy Alcock, Samuel Yeh, John Brown, and Charles Young, *Cancer* **46** (9), 2009 (1980).
- 88 Shannon Reagan-Shaw, Minakshi Nihal, and Nihal Ahmad, *The FASEB Journal* **22** (3), 659 (2008).
- 89 Christopher R. Chitambar, David P. Purpi, Jeffrey Woodliff, Meiyong Yang, and Janine P. Wereley, *Journal of Pharmacology and Experimental Therapeutics* **322** (3), 1228 (2007).
- 90 S. R. Vallabhajosula, J. F. Harwig, and W. Wolf, *International Journal of Nuclear Medicine and Biology* **8** (4), 363 (1981).
- 91 E Salloum, D S Brandt, V J Caride, E Cornelius, D Zeltermann, W Schubert, T Mannino, and D L Cooper, *Journal of Clinical Oncology* **15** (2), 518 (1997).
- 92 N. V. Boshitskaya, V. A. Lavrenko, T. S. Bartnitskaya, G. N. Makarenko, G. A. Shkurko, and N. V. Danilenko, *Powder Metall Met Ceram* **39** (3-4), 157 (2000).
- 93 Kang Yu-Ting and Yen Ta-Jen, presented at the Nanoelectronics Conference (INEC), 2010 3rd International, 2010 (unpublished).
- 94 Lauren E. Bain and Albena Ivanisevic, *Small* **11** (7), 768 (2015).
- 95 Derick C. Miller, Anil Thapa, Karen M. Haberstroh, and Thomas J. Webster, *Biomaterials* **25** (1), 53 (2004).
- 96 Jingying Li, Qiusen Han, Xinhuan Wang, Rong Yang, and Chen Wang, *Colloids and Surfaces B: Biointerfaces* **123**, 293 (2014).

- 97 J. P. McAllister, J. Li, K. Deren, P. G. Finlayson, C. Jaboro, G. A. Auner, R. Baird, A. Lagman, R. Iezzi, and G. W. Abrams, presented at the Investigative Ophthalmology & Visual Science, 2004 (unpublished).
- 98 Anna Podolska, Stephanie Tham, Robert D. Hart, Ruth M. Seeber, Martin Kocan, Martina Kocan, Umesh K. Mishra, Kevin D. G. Pflieger, Gia Parish, and Brett D. Nener, *Sensors and Actuators B: Chemical* **169**, 401 (2012).
- 99 A. Podolska, R. M. Seeber, M. Kocan, K. D. G. Pflieger, G. Parish, and B. D. Nener, presented at the Nanoscience and Nanotechnology (ICONN), 2010 International Conference on, 2010 (unpublished).
- 100 Gayoung Park, Hyun-Joong Chung, Kwanghee Kim, Seon Ah Lim, Jiyoung Kim, Yun-Soung Kim, Yuhao Liu, Woon-Hong Yeo, Rak-Hwan Kim, and Stanley S Kim, *Advanced healthcare materials* **3** (4), 515 (2014).
- 101 Chi-Shun Chiu, Hong-Mao Lee, and Shangjr Gwo, *Langmuir* **26** (4), 2969 (2010).
- 102 Christophe Blaszykowski, Sonia Sheikh, Pasquale Benvenuto, and Michael Thompson, *Langmuir* **28** (5), 2318 (2012).
- 103 Hsien Tang Chiu, Tanapon Sukachonmakul, Ming Tai Kuo, Yu Hsiang Wang, and Karnthidaporn Wattanakul, *Applied Surface Science* **292** (0), 928 (2014).
- 104 Byung Hwan Chu, C. Y. Chang, Kevin Kroll, Nancy Denslow, Yu-Lin Wang, S. J. Pearton, A. M. Dabiran, A. M. Wowchak, B. Cui, P. P. Chow, and Fan Ren, *Applied Physics Letters* **96** (1), 013701 (2010).
- 105 B. Baur, J. Howgate, H. G. von Ribbeck, Y. Gawlina, V. Bandalo, G. Steinhoff, M. Stutzmann, and M. Eickhoff, *Applied Physics Letters* **89** (18), 3901 (2006).
- 106 Y. L. Wang, B. H. Chu, C. Y. Chang, C. F. Lo, S. J. Pearton, A. Dabiran, P. P. Chow, and F. Ren, *Sens. Actuator B-Chem.* **146** (1), 349 (2010).
- 107 S. J. Wilkins, M. Greenough, C. Arellano, T. Paskova, and A. Ivanisevic, *Langmuir* **30** (8), 2038 (2014).
- 108 Heesuk Kim, Paula E. Colavita, Peerasak Paoprasert, Padma Gopalan, T. F. Kuech, and Robert J. Hamers, *Surface Science* **602** (14), 2382 (2008).
- 109 E. L. Hanson, J. Schwartz, B. Nickel, N. Koch, and M. F. Danisman, *J. Am. Chem. Soc.* **125** (51), 16074 (2003).

- 110 Heesuk Kim, Paula E. Colavita, Kevin M. Metz, Beth M. Nichols, Bin Sun, John Uhlrich, Xiaoyu Wang, Thomas F. Kuech, and Robert J. Hamers, *Langmuir* **22** (19), 8121 (2006).
- 111 S. U. Schwarz, V. Cimalla, G. Eichapfel, M. Himmerlich, S. Krischok, and O. Ambacher, *Langmuir* **29** (21), 6296 (2013).
- 112 Matthew S. Makowski, Dmitry Y. Zemlyanov, Jason A. Lindsey, Jonathan C. Bernhard, Evan M. Hagen, Burke K. Chan, Adam A. Petersohn, Matthew R. Medow, Lindsay E. Wendel, Dafang Chen, Jamie M. Canter, and Albena Ivanisevic, *Surface Science* **605** (15–16), 1466 (2011).
- 113 Jhindan Mukherjee, Sabrina Peczonczyk, and Stephen Maldonado, *Langmuir* **26** (13), 10890 (2010).
- 114 Sabrina L. Peczonczyk, Jhindan Mukherjee, Azhar I. Carim, and Stephen Maldonado, *Langmuir* **28** (10), 4672 (2012).
- 115 V. M. Bermudez, *Surface Science* **519** (3), 173 (2002).
- 116 Huaiguo Xue, Zhiquan Shen, and Chunmei Li, *Biosensors and Bioelectronics* **20** (11), 2330 (2005).
- 117 Nicholas M. Fahrenkopf, Fatemeh Shahedipour-Sandvik, Natalya Tokranova, Magnus Bergkvist, and Nathaniel C. Cady, *Journal of Biotechnology* **150** (3), 312 (2010).
- 118 Li Jia-dong, Cheng Jun-jie, Miao Bin, Wei Xiao-wei, Xie Jie, Zhang Jin-cheng, Zhang Zhi-qiang, and Wu Dong-min, *Journal of Micromechanics and Microengineering* **24** (7), 075023 (2014).
- 119 S. J. Pearton, B. S. Kang, S. K. Kim, F. Ren, B. P. Gila, C. R. Abernathy, J. S. Lin, and S. N. G. Chu, *J. Phys.-Condes. Matter* **16** (29), R961 (2004).
- 120 Chun-Chia Chen, Huey-Ing Chen, Hao-Yeh Liu, Po-Cheng Chou, Jian-Kai Liou, and Wen-Chau Liu, *Sensors and Actuators B: Chemical* **209**, 658 (2015).
- 121 G. Auner, G. Shreve, H. Ying, G. Newaz, C. Hughes, and J. Z. Xu, in *Bioengineered and Bioinspired Systems*, edited by A. RodriguezVazquez, D. Abbott, and R. Carmona (Spie-Int Soc Optical Engineering, Bellingham, 2003), Vol. 5119, pp. 129.
- 122 K. Lange, B. E. Rapp, and M. Rapp, *Anal. Bioanal. Chem.* **391** (5), 1509 (2008).

- 123 O. Ambacher, B. Foutz, J. Smart, J. R. Shealy, N. G. Weimann, K. Chu, M. Murphy, A. J. Sierakowski, W. J. Schaff, L. F. Eastman, R. Dimitrov, A. Mitchell, and M. Stutzmann, *Journal of Applied Physics* **87** (1), 334 (2000).
- 124 M. Stutzmann, G. Steinhoff, M. Eickhoff, O. Ambacher, C. E. Nebel, J. Schalwig, R. Neuberger, and G. Müller, *Diamond and Related Materials* **11** (3–6), 886 (2002).
- 125 J. P. Ibbetson, P. T. Fini, K. D. Ness, S. P. DenBaars, J. S. Speck, and U. K. Mishra, *Applied Physics Letters* **77** (2), 250 (2000).
- 126 T. R. Lenka and A. K. Panda, *Semiconductors* **45** (5), 650 (2011).
- 127 Matthew Myers, Farah Liyana Muhammad Khir, Anna Podolska, Gilberto A. Umana-Membreno, Brett Nener, Murray Baker, and Giacinta Parish, *Sensors and Actuators B: Chemical* **181**, 301 (2013).
- 128 Wen Xuejin, Michael L. Schuette, S. K. Gupta, T. R. Nicholson, S. C. Lee, and Wu Lu, *Sensors Journal, IEEE* **11** (8), 1726 (2011).
- 129 F. L. M. Khir, M. Myers, A. Podolska, T. M. Sanders, M. V. Baker, B. D. Nener, and G. Parish, *Applied Surface Science* **314**, 850 (2014).
- 130 Anna Podolska, Martin Kocan, Alex M. Garces Cabezas, Timothy D. Wilson, Gilberto A. Umana-Membreno, Brett D. Nener, Giacinta Parish, Stacia Keller, and Umesh K. Mishra, *Applied Physics Letters* **97** (1), 012108 (2010).
- 131 N. A. Chaniotakis, Y. Alifragis, G. Konstantinidis, and A. Georgakilas, *Anal. Chem.* **76** (18), 5552 (2004).
- 132 Hung-Ta Wang, BS Kang, TF Chancellor, TP Lele, Y Tseng, F Ren, SJ Pearton, WJ Johnson, P Rajagopal, and JC Roberts, *Applied Physics Letters* **91** (4), 42114 (2007).
- 133 K. H. Chen, H. W. Wang, B. S. Kang, C. Y. Chang, Y. L. Wang, T. P. Lele, F. Ren, S. J. Pearton, A. Dabiran, A. Osinsky, and P. P. Chow, *Sensors and Actuators B: Chemical* **134** (2), 386 (2008).
- 134 Byung-Hwan Chu, Hon-Way Lin, Shangjr Gwo, Yu-Lin Wang, S. J. Pearton, J. W. Johnson, P. Rajagopal, J. C. Roberts, E. L. Piner, K. J. Linthicuni, and Fan Ren, *Journal of Vacuum Science Technology B* **28** (1), L5 (2010).
- 135 Kun-Wei Kao, Yun-Wen Su, Yen-Sheng Lu, Shangjr Gwo, and J Andrew Yeh, *International Journal of Automation and Smart Technology* **2** (1), 49 (2012).

- 136 P. D. C. King, T. D. Veal, C. F. McConville, F. Fuchs, J. Furthmüller, F. Bechstedt, P. Schley, R. Goldhahn, J. Schörmann, D. J. As, K. Lischka, D. Muto, H. Naoi, Y. Nanishi, Hai Lu, and W. J. Schaff, *Applied Physics Letters* **91** (9), 092101 (2007).
- 137 Ching-Ting Lee, Ying-Shuo Chiu, and Xin-Qiang Wang, *Sensors and Actuators B: Chemical* **181**, 810 (2013).
- 138 Y. H. Chang, K. K. Chang, S. Gwo, and J. A. Yeh, *Appl. Phys. Express* **3** (11), 114101 (2010).
- 139 Kun-Wei Kao, Ming-Che Hsu, Yuh-Hwa Chang, Shangjr Gwo, and J. Andrew Yeh, *Sensors (Basel, Switzerland)* **12** (6), 7157 (2012).
- 140 Hai Lu, William J. Schaff, Lester F. Eastman, and C. E. Stutz, *Applied Physics Letters* **82** (11), 1736 (2003).
- 141 R. Kirste, N. Rohrbaugh, I. Bryan, Z. Bryan, R. Collazo, and A. Ivanisevic, *Annual Review of Analytical Chemistry* **8** (1), DOI: 10.1146/annurev (2015).
- 142 F. S. Tulip, E. Eteshola, S. Desai, S. Mostafa, S. Roopa, B. Evans, and S. K. Islam, *NanoBioscience, IEEE Transactions on* **13** (2), 138 (2014).
- 143 Dieter Schroder, in *Semiconductor Material and Device Characterisation* (John Wiley & Sons, 2006).
- 144 M. S. Makowski and A. Ivanisevic, *Small* **7** (14), 1863 (2011).
- 145 Masanori Yamada, Yuichi Kadoya, Shingo Kasai, Kozue Kato, Mayumi Mochizuki, Norio Nishi, Nobuhisa Watanabe, Hynda K. Kleinman, Yoshihiko Yamada, and Motoyoshi Nomizu, *FEBS Letters* **530** (1–3), 48 (2002).
- 146 M. S. Makowski, S. Kim, M. Gaillard, D. Janes, M. J. Manfra, I. Bryan, Z. Sitar, C. Arellano, J. Xie, R. Collazo, and A. Ivanisevic, *Applied Physics Letters* **102** (7), 074102 (2013).
- 147 Elias Estephan, Marie-Belle Saab, Marta Martin, Christian Larroque, Frédéric J. G. Cuisinier, Olivier Briot, Sandra Ruffenach, Matthieu Moret, and Csilla Gergely, *Journal of Peptide Science* **17** (2), 143 (2011).
- 148 Byung Hwan Chu, CY Chang, YL Wang, SJ Pearton, and Fan Ren, *ECS Transactions* **33** (13), 3 (2010).

- 149 Q. Huang, Y. Bando, L. Zhao, C. Y. Zhi, and D. Golberg, *Nanotechnology* **20** (41), 415501 (2009).
- 150 Dmitri Golberg, Yoshio Bando, Yang Huang, Takeshi Terao, Masanori Mitome, Chengchun Tang, and Chunyi Zhi, *ACS Nano* **4** (6), 2979 (2010).
- 151 Eric Stern, Robin Wagner, Fred J. Sigworth, Ronald Breaker, Tarek M. Fahmy, and Mark A. Reed, *Nano Letters* **7** (11), 3405 (2007).
- 152 Jun Pyo Kim, Byung Yang Lee, Joohyung Lee, Seunghun Hong, and Sang Jun Sim, *Biosensors and Bioelectronics* **24** (11), 3372 (2009).
- 153 A. V. Rebriv and N. F. Starodub, *Electroanalysis* **16** (22), 1891 (2004).
- 154 XueJin Wen, ShengNian Wang, YuJi Wang, LyJames Lee, and Wu Lu, *Chin. Sci. Bull.* **58** (21), 2601 (2013).
- 155 Matthew S Makowski, Purdue University, 2013.
- 156 Nathaniel Rohrbaugh, Isaac Bryan, Zachary Bryan, Ramon Collazo, and Albena Ivanisevic, *AIP Advances* **5** (9), 097102 (2015).
- 157 C. M. Foster, R. Collazo, Z. Sitar, and A. Ivanisevic, *Langmuir* **29** (1), 216 (2013).
- 158 V. C. Ayala, K. Moosmann, O. Prucker, J. Ruhe, and L. M. Reindl, in *Micro-and Nanosystems in Medicine, Active Implants, Biosensors*, edited by O. Dissel and W. C. Schlegel (Springer, New York, 2009), Vol. 25, pp. 339.
- 159 A. Ramesh, F. Ren, P. R. Berger, P. Casal, A. Theiss, S. Gupta, and S. C. Lee, *Electron. Lett.* **49** (7), 450 (2013).
- 160 Corey M. Foster, Ramon Collazo, Zlatko Sitar, and Albena Ivanisevic, *Langmuir* **29** (26), 8377 (2013).
- 161 B. Baur, J. Howgate, H. G. von Ribbeck, Y. Gawlina, V. Bandalo, G. Steinhoff, M. Stutzmann, and M. Eickhoff, *Appl. Phys. Lett.* **89** (18) (2006).
- 162 A. Das, L. B. Chang, C. S. Lai, R. M. Lin, F. C. Chu, Y. H. Lin, L. Chow, and M. J. Jeng, *Appl. Phys. Express* **6** (3) (2013).
- 163 B. Baur, G. Steinhoff, J. Hernando, O. Purrucker, M. Tanaka, B. Nickel, M. Stutzmann, and M. Eickhoff, *Applied Physics Letters* **87** (26) (2005).

- 164 M. S. Makowski, S. Kim, M. Gaillard, D. Janes, M. J. Manfra, I. Bryan, Z. Sitar, C. Arellano, J. Xie, R. Collazo, and A. Ivanisevic, *Applied Physics Letters* **102** (7) (2013).
- 165 B. S. Kang, H. T. Wang, F. Ren, and S. J. Pearton, *Journal of Applied Physics* **104** (3) (2008); C. C. Huang, C. P. Hsu, Y. R. Hsu, Y. L. Wang, G. Y. Lee, J. I. Chyi, H. T. Cheng, F. Ren, and Ieee, in *2012 Ieee Sensors Proceedings* (Ieee, New York, 2012), pp. 805.
- 166 Matthew S. Makowski, Isaac Bryan, Zlatko Sitar, Consuelo Arellano, Jinqiao Xie, Ramon Collazo, and Albena Ivanisevic, *Applied Physics Letters* **103** (1) (2013).
- 167 Nikos Chaniotakis and Nikoletta Sofikiti, *Analytica Chimica Acta* **615** (1), 1 (2008).
- 168 Ryan Coppage, Joseph M. Slocik, Hadi Ramezani-Dakhel, Nicholas M. Bedford, Hendrik Heinz, Rajesh R. Naik, and Marc R. Knecht, *Journal of the American Chemical Society* **135** (30), 11048 (2013).
- 169 E. Estephan, J. Dao, M. B. Saab, I. Panayotov, M. Martin, C. Larroque, C. Gergely, F. J. G. Cuisinier, and B. Levallois, *Biomedical Engineering-Biomedizinische Technik* **57** (6), 481 (2012).
- 170 Elias Estephan, Christian Larroque, Nicole Bec, Pierre Martineau, Frédéric J. G. Cuisinier, Thierry Cloitre, and Csilla Gergely, - **104** (- 6) (2009).
- 171 Karsten Goede, Peter Busch, and Marius Grundmann, *Nano Letters* **4** (11), 2115 (2004).
- 172 C. C. Huang, G. Y. Lee, J. I. Chyi, H. T. Cheng, C. P. Hsu, Y. R. Hsu, C. H. Hsu, Y. F. Huang, Y. C. Sun, C. C. Chen, S. S. Li, J. A. Yeh, D. J. Yao, F. Ren, and Y. L. Wang, *Biosens. Bioelectron.* **41**, 717 (2013).
- 173 S. Mita, R. Collazo, A. Rice, R. F. Dalmau, and Z. Sitar, *Journal of Applied Physics* **104** (1) (2008).
- 174 D. J. Cheney, E. A. Douglas, L. Liu, C. F. Lo, Y. Y. Xi, B. P. Gila, F. Ren, D. Horton, M. E. Law, D. J. Smith, and S. J. Pearton, *Semicond. Sci. Technol.* **28** (7) (2013).
- 175 Patricia Casal, Xuejin Wen, Samit Gupta, Theodore Nicholson, Yuji Wang, Andrew Theiss, Bharat Bhushan, Leonard Brillson, Wu Lu, and Stephen C. Lee, *Philosophical Transactions of the Royal Society A: Mathematical, Physical and Engineering Sciences* **370** (1967), 2474 (2012).

- 176 Wei Zhou, Xiaochuan Dai, Tian-Ming Fu, Chong Xie, Jia Liu, and Charles M. Lieber, *Nano Letters* **14** (3), 1614 (2014).
- 177 Lauren E. Bain, Scott A. Jewett, Aadithya Hosalli Mukund, Salah M. Bedair, Tania M. Paskova, and Albena Ivanisevic, *ACS Applied Materials & Interfaces* **5** (15), 7236 (2013).
- 178 Y. Zhao, P. Deng, Y. Nie, P. Wang, Y. Zhang, L. Xing, and X. Xue, *Biosensors and Bioelectronics* **57** (0), 269 (2014).
- 179 X. Wen, S. Gupta, T. R. Nicholson, S.C. Lee, and W. Lu, *physica status solidi (c)* **8** (7-8), 2489 (2011).
- 180 D. J. Cheney, E. A. Douglas, L. Liu, C. F. Lo, Y. Y. Xi, B. P. Gila, F. Ren, D. Horton, M. E. Law, D. J. Smith, and S. J. Pearton, *Semicond. Sci. Technol.* **28** (7), 4019 (2013).
- 181 N. Rohrbaugh, I. Bryan, Z. Bryan, R. Collazo, and A. Ivanisevic, *Appl. Phys. Lett.* **105**, 134103 (2014).
- 182 S. Mita, R. Collazo, A. Rice, J. Tweedie, J. Q. Xie, R. Dalmau, and Z. Sitar, *Physica Status Solidi C: Current Topics in Solid State Physics, Vol 8, No 7-8* **8** (7-8) (2011).
- 183 N. Rohrbaugh, I. Bryan, Z. Bryan, C. Arellano, R. Collazo, and A. Ivanisevic, *Applied Physics Letters* **105** (13), 134103 (2014).
- 184 Elias Estephan, Christian Larroque, Frédéric J. G. Cuisinier, Zoltán Bálint, and Csilla Gergely, *The Journal of Physical Chemistry B* **112** (29), 8799 (2008).
- 185 Patricia Casal, Xuejin Wen, Samit Gupta, Theodore Nicholson, Yuji Wang, Andrew Theiss, Bharat Bhushan, Leonard Brillson, Wu Lu, and Stephen C. Lee, *Philosophical Transactions of the Royal Society of London A: Mathematical, Physical and Engineering Sciences* **370** (1967), 2474 (2012).
- 186 Feng He, Jie Gao, Eric Pierce, P. J. Strong, Hailong Wang, and Liyuan Liang, *Environmental Science and Pollution Research* **22** (11), 8124 (2015).
- 187 Vinay Shankar, Veena Thekkeetil, Gaurav Sharma, and Veena Agrawal, *In Vitro Cellular & Developmental Biology - Plant* **48** (1), 113 (2011).
- 188 W. Ben Ammar, C. Mediouni, B. Tray, M. H. Ghorbel, and F. Jemal, *Biologia Plantarum* **52** (2), 314.

- 189 Vaclav Diopan, Violetta Shestivska, Ondrej Zitka, Michaela Galiova, Vojtech Adam,
Jozef Kaiser, Ales Horna, Karel Novotny, Miroslav Liska, Ladislav Havel, Josef
Zehnalek, and Rene Kizek, - **22** (- 11) (2010).
- 190 G. Iucci, C. Battocchio, M. Dettin, F. Ghezzi, and G. Polzonetti, *Solid State
Sciences* **12** (11), 1861 (2010).
- 191 Bobby Pejicic and Roland De Marco, *Applied Surface Science* **228** (1–4), 378 (2004).
- 192 Brady L. Pearce, Nora G. Berg, Matthew S. Rahn, and Albena Ivanisevic, (2016).
- 193 Liqin Chen, Limin Yang, and Qiuquan Wang, *Metallomics* **1** (1), 101 (2009).
- 194 A. Dago, C. Arino, J. M. Diaz-Cruz, and M. Esteban, *Int. J. Environ. Anal. Chem.* **94**
(7), 668 (2014).
- 195 Elias Estephan, Christian Larroque, Frédéric J. G. Cuisinier, Zoltán Bálint, and Csilla
Gergely, *The Journal of Physical Chemistry B* **112** (29), 8799 (2008).
- 196 H. P. Jambhulkar and A. A. Juwarkar, *Ecotox. Environ. Safe.* **72** (4), 1122 (2009).
- 197 Byung Hwan Chu, C. Y. Chang, Kevin Kroll, Nancy Denslow, Yu-Lin Wang, S. J.
Pearson, A. M. Dabiran, A. M. Wowchak, B. Cui, P. P. Chow, and Fan Ren, *Applied
Physics Letters* **96** (1) (2010).
- 198 Nathaniel Rohrbaugh, Luis Hernandez-Balderrama, Felix Kaess, Ronny Kirste,
Ramon Collazo, and Albena Ivanisevic, *AIP Advances* **6** (6), 065105 (2016).
- 199 Zhongmin Feng, Peng Zhu, Hongtao Fan, Shanshan Piao, Liang Xu, and Ting Sun,
Anal. Chem. **88** (13), 6836 (2016).
- 200 Vincent Zoulalian, Stefan Zürcher, Samuele Tosatti, Marcus Textor, Sophie Monge,
and Jean-Jacques Robin, *Langmuir* **26** (1), 74 (2010).